Antibacterial and Biocompatible Coating for Cardiovascular Grafts

Dissertation

zur Erlangung des Doktorgrades der Naturwissenschaften (Dr.rer.nat)

der

Fachbereich Pharmazie der Philipps-Universität Marburg

Vorgelegt von

Bassam Al Meslmani

Aus Syrien

Die vorliegende Arbeit entstand auf Anregung und unter Leitung von

Herrn Prof. Dr. Udo Bakowsky

Am Institut für Pharmazeutische Technologie und Biopharmazie der Philipps Universität Marburg

Vom Fachbereich Pharmazie

der Philipps-Universität Marburg als Publikation am angenommen.

Erstgutachter: Prof Dr. Udo Bakowsky

Zweitgutachter: Prof. Dr. Michael Keusgen

Tag der mündlichen Prüfung am 29. Januar. 2014

Content

Chapter 1

General introduction

1. Introduction

Cardiovascular diseases are considered as the major health problem responsible for about 30% of the global death [1,2,3]. The high prevalence rate of cardiac diseases and the associated critical case of the patient entailed innovative treatment. Using cardiovascular prostheses, the damaged functions and consequently the patient`s life quality were significantly improved. The surgeons have turned to prosthetic grafts mostly made from polymeric or metallic materials to hold the graft long-term patency because of lack of suitable autologous grafts, while the biodegradable implantable grafts are applied to disappear after performing their purposed function [1-3]. However, polyethylene terephthalate, PET (Dacron®) textiles are preferably utilized to replace the damaged blood vessels and for artificial heart valves in order to restore the normal blood flow and cardiac output.

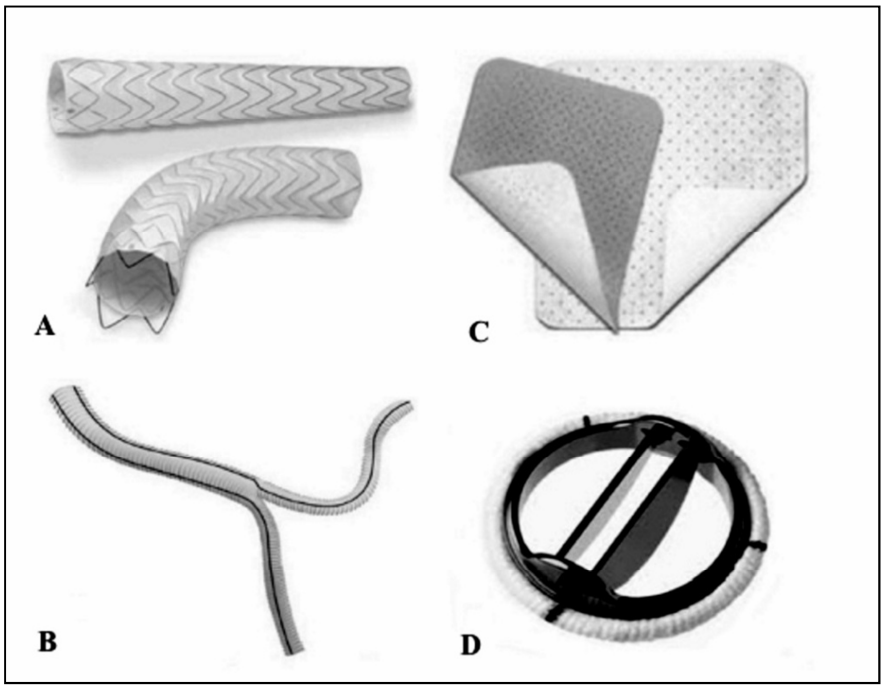

Fig. 1. Cardiovascular devices of PET textile. Covering the stent graft (A), branched vascular graft (B), surgical meshes(C), and covering the sewing rings of artificial heart valves (D).

Utilization of PET graft was historically of the most interest as DeBakey and Julian firstly in 1957 employed it to repair different vascular defects [3,4], followed by implantation of artificial heart valve in 1960 which increased into approximately 325,000 valve replacements worldwide every year, with a reported market sales of about 1.45 $ billion [5].

Currently, PET textiles with various configurations are available for many medical devices to support and ensure the desired performance and stability (Fig.1). Nonetheless, a grafts failure is also associated although most medical PET grafts satisfactorily work. Individually, this may be dependent on the age of the patient, lifestyle, medical history, body chemistry, and the graft properties. Importantly, the graft-associated infection, in addition to the thrombogenic properties of PET trigger a variety of adverse reactions in the host, and activate a number of biological cascades that display various complications mainly; tissue inflammation, and formation of fibrotic tissue around the graft which are the leading case for grafts failure and reoperation, increasing both the risk to patients and the cost of health care [3,6,7]. Accordingly, the necessity to biocompatible and infection-resistant graft is still one of the most challenges that encouraged us to improve the properties of cardiovascular PET grafts in objective to enhance the grafts long-term patency and patient`s life quality.

2. Synthetic polymeric prostheses are the gold standard for cardiovascular grafts

The auto natural bypasses grafts (patient`s own) such as saphenous veins or mammary arteries were used to treat the damaged vessels. However, about one-third of the patients don`t have veins suitable for grafting owing to previous vascular disease or vein stripping. Additionally, limited success was reported with patency rates generally ranging between 50-70% due to dimension restrictions, mechanical property mismatch, and disjunction at the anastomosis associated with significant morbidity and surgical costs [8-11]. Hence, the

synthetic polymeric grafts have been investigated and demonstrated a superior success. Mostly PET textiles are become gold standard for cardiovascular grafts in clinical practice due to its excellent mechanical properties, good healing features, nontoxic, strong with sufficient flex and tensile strength. In addition, the PET tendency to dilate over time makes it the best choice for long-term use *in-vivo*. The most permanent PET grafts are applied to replace the large diameter arterial vessels and covering the sewing rings of heart valves and vascular stent, based on its highly flexible mechanical feature, and its micro-porous wall structure which hold promise for enhanced healing, suture retention, and compression resistance [5,12].

3. Woven and knitted forms of Crimped PET are the most successful cardiovascular grafts

Firstly in 1950, DuPont developed PET and patented its widely known name Dacron® fibers. Currently, ten PET configurations are available in clinical use with high reported rates of success for woven and knitted configurations [2,4] (Fig.2). The multifilament PET threads in woven form are fabricated in an over-and-under pattern resulting in very limited porosity and minimal creep of the finished graft. While PET threads in knitted form are looped to create greater porosity and radial distensibility. The velour technique that extends the loops of yarn on the surfaces of the fabrics has been used in an attempt to increase tissue incorporation. Moreover a crimping technique is utilized to increase the flexibility, distensibility, and kink-resistance of textile grafts. Finally, prosthetic rings or coils are applied to the external surface of the grafts as external support to resist kinking and possible mechanical compression [2,4].

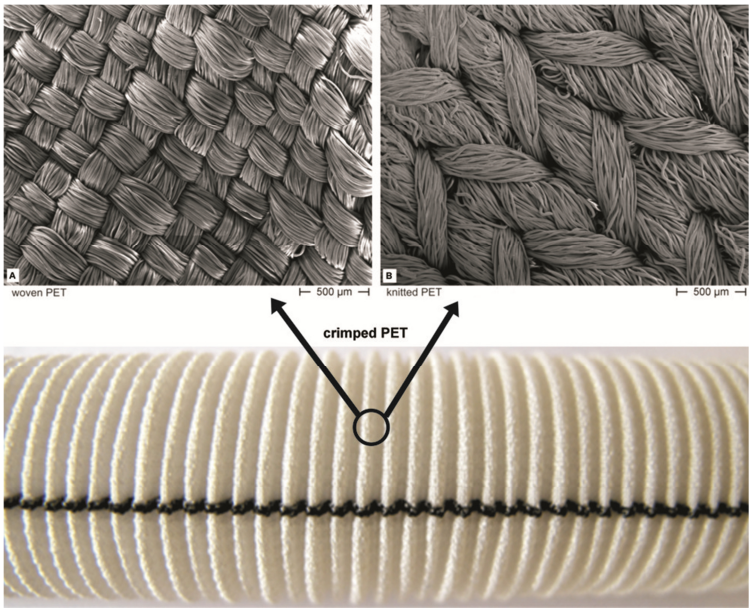

Fig. 2. SEM micrographs of woven (A) and knitted (B) forms of crimped PET grafts. The multifilament PET threads in woven form are fabricated in an over-and-under pattern, while they are looped in knitted form. The crimped technique, shown in picture, is utilized to increase the flexibility, distensibility, and kink-resistance of grafts.

4. The thrombogenic property of PET restricted the grafts patency

The extended stability of PET over 10 years without significant deterioration offers advantages to medical applications as non-degradable implantable graft [14]. Nevertheless, one of the prominent shortcomings of PET is the intrinsic thrombogenic property that impaired ultimately the long-term patency of the graft and hence, the patient`s life quality. However, the development of the host response depends on the intrinsic properties of the graft itself and the hemodynamic environment in which the graft is placed [15].

5. Host response

5.1. Initial tissue damage leads to thrombin formation and platelets aggregation

It is unavoidable to damage the tissue during implantation of medical graft. The initial injury of surrounding tissue initiates complex series of biological and biochemical cascades [16,17] (Fig.3). The coagulation cascade and platelets aggregation are triggered by blood contact with collagen in the sub-endothelial tissue. The coagulation cascade submits ultimately thrombin which hydrolyses fibrinogen and forms the fibrin network. Likewise, activation of platelets contributes to coagulation by secretion of pro coagulant factors. This event is essential for the healing of damaged tissue, because the activated platelets also release many proteins participate in the healing. Moreover, the release of interleukin 8 (IL8), and macrophage inflammatory protein 1 alpha (MIP1α) from the activated platelets attracts and activates the macrophages leading to initiation of the inflammatory response [16-18].

5.2. The host recognizes the graft as being foreign after fibrinogen adsorption on grafts surface

Upon implantation of a graft, serum proteins such as IgG and the complement factors adsorb physically on the grafts surface (Fig.3). The adsorbed proteins act as chemo attractants and hence accelerate the migration of neutrophils and monocytes towards the implanted graft [16-18]. Furthermore, the interaction of fibrinogen with grafts surface leads to conformation of fibrinogen into more energetically favorable form, thereby exposing the occult epitopes P1 (γ 190-202) and P2 (γ3727-395). Presence of these epitopes on the grafts surface displays an essential role in the development of the inflammatory response as they will be recognized by the neutrophils. Through this mechanism, the body will recognize the graft as being foreign and will subsequently attempt to remove it. In the case of non-degradable graft, the body cannot digest the graft instead a chronic inflammatory response and a fibrous capsule are developed around the graft (Opsonization) [16-18].

5.3. The activated neutrophils excrete chemo attractants and accelerate the monocytes migration towards the implantation site

Neutrophils are the predominant cell type during the acute inflammatory response. The soluble complement factors formed on the grafts surface along with fibrinogen and fibrin attract and accelerate the migration of neutrophils towards the implantation site initiating the acute inflammation (Fig.3). Subsequently, the activated neutrophils secrete the most important chemo attractant IL8 that enhances their own recruitment, In addition to macrophage inflammatory protein 1 (MIP-1α) which accelerates the monocytes migration towards the implantation site. Moreover, the released histamine from mast cell increases the vascular permeability in the surrounding tissue and attracting monocytes [16-18]. Consequently the attracted monocytes adhere and differentiate into macrophages, and secrete many factors which contribute in the inflammatory progresses [16-18].

5.4. Foreign body giant cells are formed as a response to non-biodegradable graft

The macrophages attempt to remove the foreign graft from the body. Differently, depression of macrophages is developed due to resistance of the non-biodegradable graft that triggers the formation of foreign body giant cells (FBGCs) (Fig.3). Although the exact mechanism of FBGCs formation has not yet been completely explained, macrophage fusion on grafts surface depends on the material itself and the absorbed proteins as vitronectin, in addition to IL4 and IL13 from mast cells and T-cells. The resulting multinuclear phagocytes (FBGCs) secrete reactive oxygen and degradative enzymes and acids in attempt to degrade the implanted graft [16-18].

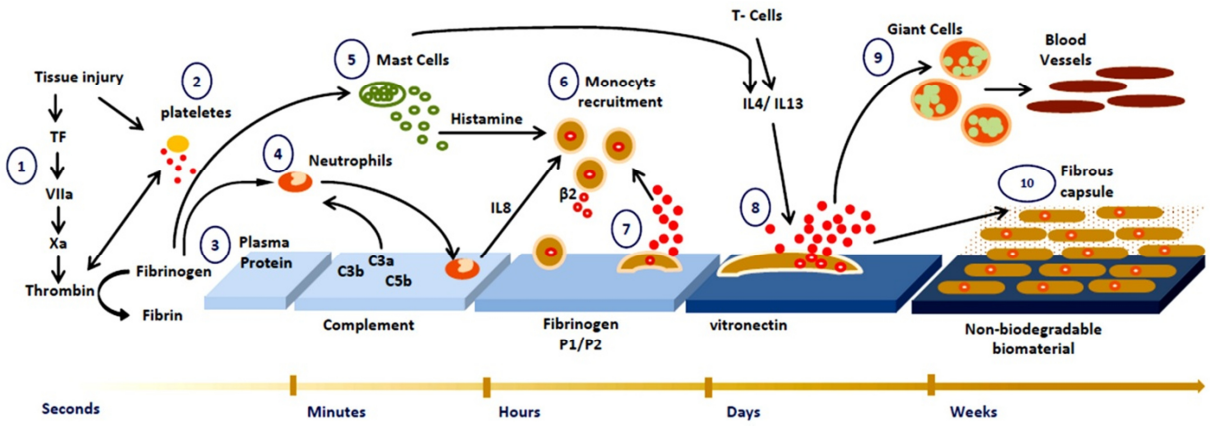

Fig. 3. Host response after graft implantation

1) Upon implantation, tissue injury initiates the release of tissue factor (TF) from sub endothelial tissue that triggers the extrinsic coagulation pathway leading to activation of thrombin. Consequently, fibrin is formed and starts the blood clot.

2) Platelets are activated after contact with extracellular matrix proteins and release healing factor as soon as thrombin that enhance the coagulation cascade and the recovery process.

3) Plasma proteins and complement factors adsorb on the grafts surface directly after implantation, and activate the alternative complement pathway leading to formation of C3a and C5b responsible for monocytes migration towards the implanted graft. Other adsorbed plasma proteins; fibrinogen and vitronectin, facilitate neutrophils recognition and adherence.

4) The presence of the complement factors along with fibrinogen and fibrin at the implant site attract and activate neutrophils. The activated neutrophils recognize and adhere onto implanted surface by interaction with the adsorbed fibrinogen. Subsequently IL8 is released from the neutrophils.

5) Mast cells are activated and release histamine after degranulation leading to increase in the vascular permeability and attract monocytes.

6) Monocytes are attracted by histamine and IL8.

7) Monocytes express the β2 integrin that recognize P1/P2 epitopes on the fibrinogen surface after conformational change. The monocytes adhere to the implant graft and differentiate into macrophages. Subsequently, the release of tumor necrosis factor (TNF-α), IL6, granulocyte-colony stimulating factor (G-CSF), and granulocyte-macrophage colony stimulating factor (GM-CSF) contribute to the amplification of the inflammatory response.

8) Macrophages interact with vitronectin on the grafts surface. The released IL4 and IL13 accelerate the macrophage fusion leading to formation of foreign body giant cells.

9) The cytokines and growth factor released from macrophages and giant cells initiate blood vessel formation.

10) The released proteins from the macrophages and giant cells attract connective tissue cells (fibroblast) and activate the tissue remodeling. Over time, the fibroblast forms a fibrous capsule around the graft.

5.5. Host response is completed by formation of fibrous capsule around the graft

As a result of the previously described complex events, the tissue surrounding the implanted graft will remodel. Fibroblasts become activated by inflammatory proteins and produce new extracellular matrix (ECM) proteins contain different subtypes of collagen. The newly formed ECM has much more stable cross-linked proteins, resulting in the formation of a fibrous capsule around the graft [16-18] (Fig.3).

6. Graft-associated infection is the most substantial challenge after graft implantation

Graft-associated infection is still the substantial complication after implantation. Infections of medical grafts occur despite full sterility during surgical operation and regardless of perioperative parenteral antibiotic prophylaxis [19]. Such infections increase the risk of graft failure and patient's death. The morbidity as high as 75% has been reported to graft infection related to; *Staphylococcus aureus, Staphylococcus epidermidis, Escherichia coli, Pseudomonas aeruginosa,* and *Proteus* bacterial strains, which can be introduced into the graft site at the time of implantation by preoperative contamination, postoperative wound infection or systemic bacteraemia. However, bacteria frequently present in the circulation are in sufficient quantities to cause graft infection [20,21].

7. Bacterial adhesion is the first step of biofilm formation and subsequent infection

The infection initiates by successful attachment of free, floating bacteria into grafts surface. The first colonist adheres to the surface through weak, reversible physical forces (Fig.4), subsequently they anchor themselves more permanently using cellular adhesive structures such as pili, and start to produce exo-polysaccharides substance (EPS). Afterwards, the cell-cell bridges are developed upon stimulation of signal proteins in the bacterial wall to hold irreversibly the bacteria on the

grafts surface [22]. The attached bacteria proliferate forming the basic organizational units of biofilm. The primary colony accelerates the attachment of other bacterial cells to the EPS, resulting in bacterial aggregation and increased production of EPS which forms finally the bacterial biofilm. Occupied volume occurs during biofilm maturation due to cell proliferation and recruitment associated with formation of water channels and changes in shape and size, before the bacterial dissemination occurs and colonize new surfaces [23,24]. The five main steps in biofilm formation are schematically illustrated in figure 4.

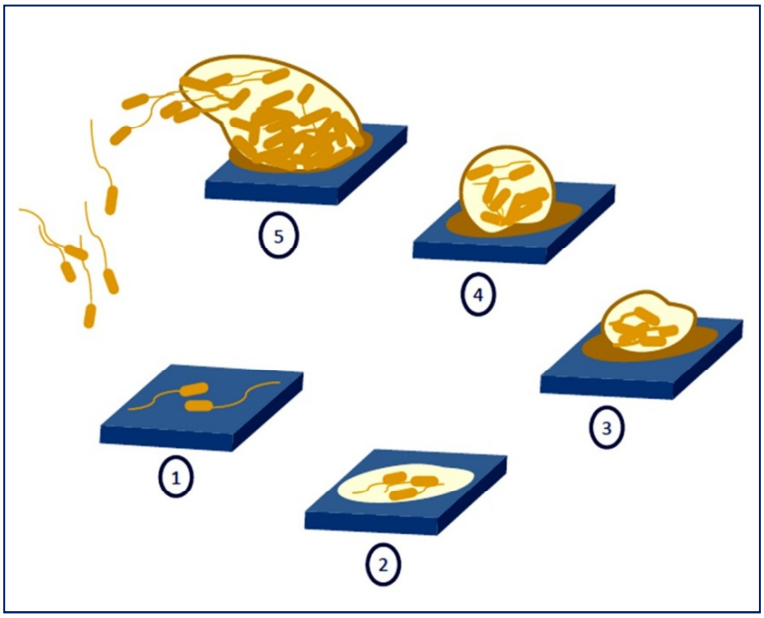

Fig. 4. Systematic steps of biofilm formation. Initial bacterial attachment (1), bacterial irreversible attachment (2), colonization (3), maturation (4), and dispersion (5).

8. Tissue engineering of cardiovascular grafts

One approach that addresses the problems associated with cardiovascular prostheses is the tissue engineering because it offers the possibility of designing a biocompatible graft appropriate for long-term patency [25,26]. Tissue engineering has been defined as the persuasion of the body to accept the graft by introduction of biomolecules, cells and supporting structures to the proper sites of graft [27]. Particularly, tissue engineering of the cardiovascular grafts involves the

development of biological substitutes with inherent mechanical, chemical, and morphological properties meet the cardiovascular system requirements. The potential biocompatibility and bacterial infection resistance properties of tissue-engineered cardiovascular graft hold promise to decrease the risk of grafts rejection.

9. Conclusion and scope of thesis

PET textile is the gold standard graft mainly employed to cardiovascular applications due to its preferable advantages. However, implantation of PET graft is associated with bacterial infections and triggers a chronic host response that essentially decreased the grafts patency and necessities its replacement. These complications are standing as a tough challenge for many researchers. In this thesis, two different crimped configurations of PET cardiovascular grafts, woven and knitted, were modified to minimize the bacterial adhesion and to enhance the biocompatibility. Using various ideas and strategies along with different standard methods supported with *in-vitro* studies and statistical data analysis, we present effective approaches to treat the most common complications after PET graft implantation in aim to potentially improvement of grafts patency and patient`s life quality:

In chapter 2: A multifunctional network-structured film coat was developed using newly synthesized polymer that manifested paramount properties, mostly the bacterial anti-adhesion efficiency and biocompatibility. The developed coat maintained the grafts flexibility and folding ability.

In chapter 3: The initial bacterial adhesion was enzymatically inhibited using covalently immobilized lysozyme on PET graft to eradicate predominantly Gram-positive bacteria and to maintain the biocompatibility of the modified graft.

In chapter 4: PLGA nanoparticles were covalently immobilized onto two different cardiovascular prostheses namely; woven crimped polyethylene terephthalate (PET, Dacron®) and expanded polytetrafluoroethylene (ePTFE, Teflon®) using FITC-dextran as hydrophilic model.

In chapter 5: Heparin was covalently immobilized to develop thrombus resistant grafts. Additionally, collagen was co-immobilized to enhance the host cell compatibility and the long-term patency of PET grafts.

10. References

[1] Elliott M. Antman, Marc S. Sabatine. Cardiovascular therapeutics: a companion to Braunwald`s heart disease. 4th Elsevier 2013.

[2] Paul A. laizza. Handbook of Cardiac Anatomy, Physiology and Devices. 2th Springer. 2009

[3] Sanjay Shrivastava. Medical Device Materials. 1th. ASM international. 2004

[4] Clagett GP. What's new in vascular surgery. J Am Coll Surg 2002;194:165-201

[5] Worldwide Heart Valve Market Report: 2009 Edition. Koncept Analytics 2009.

[6] Roald HE, Barstad RM, Bakken IJ, Roald B, Lyberg T, Sakariassen KS. Initial interactions of platelets and plasma proteins in flowing non-anticoagulated blood with the artificial surfaces Dacron and PTFE. Blood Coagul Fibrinolysis. 1994;5:355-63

[7] Luttikhuizen DT, van Amerongen MJ, de Feijter PC, Petersen AH, Harmsen MC, van Luyn MJ.The correlation between difference in foreign body reaction between implant locations and cytokine and MMP expression. Biomaterials 2006;34:5763-70

[8] Xinwen Wang, Peter Lin, Qizhi Yao, Changyi Chen. Development of Small-Diameter Vascular Grafts. World J Surg. 2007;31: 682-9

[9] Campbell J, Efendy L, and Campbell R. Novel vascular graft grown within recipient's own peritoneal cavity. Circ. Res. 1999;12:1173-78

[10] Mann K, and West L. Tissue engineering in the cardiovascular system: Progress toward a tissue engineered heart. Anat. Rec. 2001;4:367-71

[11] Xue L, and Griesler P. Blood vessels. In: Vacanti P editor. Principles of Tissue Engineering. San Diego, CA, Academic, 2000, pp. 427-46

[12] Boss A, Stierli P. Dacron prosthesis dilatation. Case report and review of the literature. Helv Chir Acta.1993;60:153-56

[13] Dumitriu S. Polymeric biomaterials. Polymer International. 1994;35: 299-300

[14] Alimi Y, Juhan C, Morati N, Girard N, Cohen S. Dilation of woven and knitted aortic prosthetic grafts: CT scan evaluation. Ann Vasc Surg. 1994;8:238-42

[15] Luke Brewster, Eric M. Brey, Howard P.Greisler. Blood vessels. in Robert Lanza, Robert Langer, Joseph Vacanti editors. Principles of tissue engineering . 3th ed. Elsevier 2007,p. 569-84.

[16] Anitua E, Andia I, Ardanza B, Nurden P, Nurden AT. Autologous platelets as a source of proteins for healing and tissue regeneration. Thromb Haemost 2004;91:4-15

[17] Rinder C, Fitch J. Amplification of the inflammatory response: adhesion molecules associated with platelet/white cell responses. J Cardiovasc Pharmacol 1996;27:6-12

[18] Hu WJ, Eaton JW, Ugarova TP, Tang L. Molecular basis of biomaterial-mediated foreign body reactions. Blood 2001;98:1231-8

[19] Darouiche RO. Device-associated infections: a macroproblem that starts with microadherence. Clin Infect Dis 2001;33:1567-72

[20] Bunt TJ. Synthetic vascular graft infections. Surger 1983;93:733-46

[21] Hernandez-Richter H,Schardey F, Lohlein M. The prevention and treatment of vascular graft infection with triclosan(Irgasan®)-bonded Dacron graft: an experimental study in the pig. Eur. J. Vasc. Endovasc. Surg 2000; 20:413-8

[22] Stoodley P, Sauer K, Davies DG, and Costerton JW. Biofilms as complex differentiated communities. Ann. Rev. Microbiol 2002; 56:187- 209

[23] Davies DG. Understanding biofilm resistance to antibacterial agents. Nature 2003;2:114-122

[24] Sauer K, Camper AK, Ehrlich GD, Costerton JW, and Davies DG. Pseudomonas aeruginosa displays multiple phenotypes during development as a biofilm. J.Bacteriol 2002;184:1140- 54

[25] Godbey, W. T., and A. Atala. In vitro systems for tissue engineering. Ann. N.Y. Acad. Sci. 961:10–26, 2002.

[26] Griffith, L. G. Emerging design principles in biomaterials and scaffolds for tissue engineering. Ann. N.Y. Acad. Sci. 961:83– 95, 2002.

[27] Williams, D. F. The Williams Dictionary of Biomaterials. Liverpool: Liverpool University Press, 1999.

Chapter 2

Multifunctional Network-structured Film Coating for Woven and Knitted Polyethylene Terephthalate against Cardiovascular Graft-associated Infections

Al Meslmani B, Mahmoud G, Sommer F, Lohoff M, Bakowsky U

Prepared to submit to *Biomaterials* Journal

Abstract

A multifunctional network- structured film coating of woven and knitted forms of crimped polyethylene terephthalate PET graft was developed to hinder graft-associated infections. Sulfadimethoxine polyhexylene adipate-b-methoxy polyethylene oxide (SD-PHA-b-MPEO) diblock copolymer was employed for coating of previously oxidized PET to acquire negative charge to the surface as confirmed by Fourier transform infrared spectroscopy. The network-structured topography of the coat was visualized by scanning electron microscopy. The biocompatibility of the prepared coat was evaluated by mouse L929 fibroblast cell, in addition to the bacterial anti-adhesion efficiency against three different broad-spectrum pathogens. Our figures of merit revealed that the formed coat showed a porous topographic architecture which manifested paramount properties, mostly bacterial anti-adhesion efficiency, biocompatibility with host cells as well as maintenance of grafts flexibility and folding ability. Compared to untreated control grafts, the number of adhered Gram-positive *Staphylococcus epidermidis* previously isolated from a patient's vein catheter was decreased by 2.6 and 2.3 folds and of adhered *Staphylococcus aureus* by 2.3 and 2.4 folds for woven and knitted grafts, respectively. Gram-negative *Escherichia coli* demonstrated a reduction by 2.9 and 2.7 folds for woven and knitted grafts, respectively. In addition, the adhesion and growth characteristics of L929 cells revealed no significant effect of the grafts modification on the biocompatibility. In conclusion, our data suggests that coating of PET with (SD-PHA-b-MPEO) is a versatile approach switches the surface into higher hydrophobic and negatively charged to offer a synergistic antibacterial effect with improved efficacy.

Keywords: Network-structured coat; Crimped polyethylene terephthalate; Bacterial anti-adhesion.

1. Introduction

Damaged blood vessels or heart valves are usually replaced using polyethylene terephthalate PET (Dacron®) grafts due to various advantages mainly; tensile ability, strength, stability, and low production cost [1,2,3]. Particularly, woven and knitted forms of crimped PET (Fig.1) are mostly used to replace the large diameter blood vessels and cover the heart valve swing ring and vascular stent [1,2].

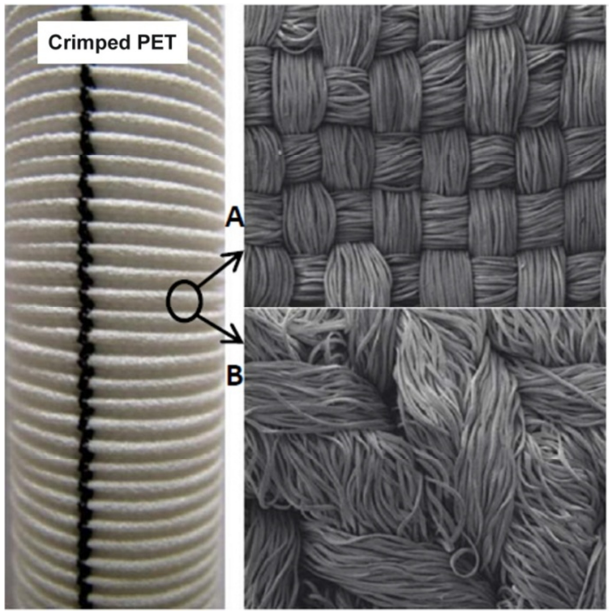

Figure 1. SEM micrographs of woven (A) and knitted (B) forms of crimped PET grafts. The multifilaments PET threads in woven form are fabricated in an over-and-under pattern, while PET threads in the knitted form are looped. The crimped technique, shown in the picture, is utilized to increase the flexibility, distensibility, and kink-resistance of grafts.

However, so far prosthetic valve endocarditis (PVE) or prosthetic vascular graft infection (PVGI) are the leading cause of short-term patency of PET grafts due to their susceptibility to bacterial infection and biofilm formation [4-6]. The development of infection starts primarily by bacterial adhesion onto the graft surface via weak, reversible, physical forces followed by an adhesion cascade to secure successful attachment. The adhered bacteria proliferate and develop an

irreversible attachment, forming dense microbial communities called biofilm [7]. Studies on pathogenic organisms responsible for PET graft infections have shown that *Staphylococcus aureus* is the infecting organism in ~70% of the cases, while *Staphylococcus epidermidis* is involved in ~30% resulting in prolonged hospitalization, graft failure, and patient death [8-9].

To overcome the aforementioned problems, surface modification of PET by polymer coating for drug delivery becomes thus one essential technique for further applications [10,11].The polymer film offers the opportunity to load and release various drugs to treat the main complications like inflammatory responses [12], thrombosis [13], and bacterial infection [14], while conserving the biocompatibility with biological tissues. In theory, casting of a polymeric film onto crimped PET grafts could be an ideal strategy to minimize the bacterial infection after implantation [7,11,14]. However, this method has severe limitations including relatively limited graft flexibility and ability to tensile, which make it difficult to be sutured with the connecting tissues. Additionally, the film would be incised when sewing with surrounding tissue which weakens the desired effect of the polymer coat.

Hence, we report a priority to coating of crimped PET grafts by a multifunctional network-structured film using a newly synthesized, biodegradable polyhexylene adipate-b-methoxy polyethylene oxide (PHA-b-MPEO) diblock copolymer. The employed copolymer is composed of a hydrophobic (polyhexylene adipate, PHA), and a hydrophilic block (methoxy polyethylene oxide, MPEO). For anti-bacterial effectiveness, the negatively charged, pH sensitive sulfadimethoxine (SD) moiety was tethered to the copolymer backbone [15] as schematically illustrated in Figure 2.

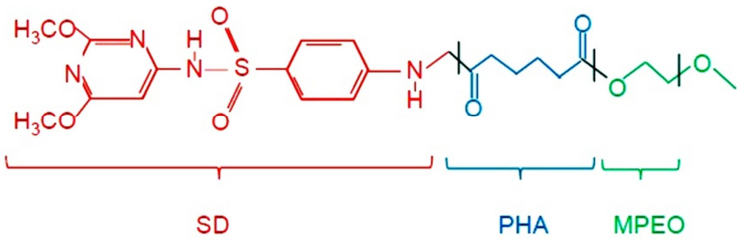

Figure 2. The molecular structure of the amphiphilic SD-PHA-b-MPEO di-block copolymer. The polymer is comprised of the hydrophobic block (polyhexylene adipate, PHA), and the hydrophilic block (methoxy polyethylene oxide, MPEO). The sulfadimethoxine (SD) moiety was immobilized to the chain end of the polymer backbone for anti-bacterial effectiveness.

The coating process was triggered by previous oxidization of PET surface using piranha solution (H_2O_2/H_2SO_4) to introduce a negatively charged hydroxyl group on the surface by selective cleavage of the ester bond within PET surface. In order to provide an irregular porous patterned film we varied humidity of the atmosphere and polymer concentration during the process of film formation, and took advantages of the repulsion forces between the modified surface and the employed polymer to equip a film that does not closely adhere to the PET surface. This versatile technique allows fabrication of network- structured film that does not tightly adhere to the PET surface after polymer casting. The developed film maintains the essential biocompatibility requirements and grafts flexibility along with the folding ability and provides the desired local anti-bacterial effect as schematically illustrated in Figure 3. Notably, the anti-bacterial activity was confirmed *in-vitro* against active human pathogens namely Gram-positive; *S. epidermidis* and *S. aureus* and Gram-negative; *E. coli* strains.

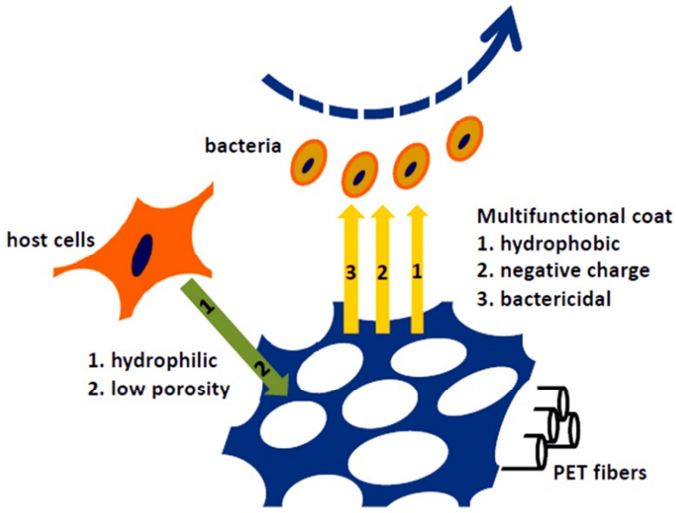

Figure 3. The mechanism of the multifunctional network- structured film on bacteria adhesion and host cell behavior. The formed coat inhibits the bacterial adhesion due to the negatively charged, bactericidal sulfadimethoxine group, and the hydrophobic PHA block, in addition to the bacterial cell-repelling characteristics of MPEO block. The hydrophilic properties of MPEO and the formed porous coat enable the host cells to bridge the filaments.

2. Material and Methods

2.1. Materials

Woven and knitted forms of crimped polyethylene terephthalate (PET, Dacron®) grafts (14 mm internal diameter, 30 cm length, 12 filaments per yarn bundle) were kindly provided by Vascutek GmbH, Germany. The biodegradable amphiphilic sulfadimethoxine-polyhexylene adipate-b-methoxy polyethylene oxide (SD-PHA-b-MPEO) diblock copolymer was kindly supplied by Prof. Dr. Andreas Greiner, Department of Chemistry, Marburg University, Germany. The bacterial strains; *Staphylococcus epidermidis* (isolated from a vein catheter of a patient), *Staphylococcus aureus* (ATCC 29213), and *Escherichia coli* (ATCC 25922) were supplied by the Institute for Medical Microbiology and Hospital hygiene, Marburg University, Germany. Hydrogen peroxide H_2O_2 (30%) was purchased from Carl Roth GmbH, Germany. The mouse L929 fibroblasts cell line was obtained

from DSMZ, Germany. Dulbecco`s modified Eagle´s medium (DMEM), Earle`s Balanced Salt Solution (EBSS), gamma irradiated Fetal Bovine Serum (FBS), trypsin, streptomycin, penicillin, and amphotericin B were purchased from PAA Laboratories GmbH, Germany. L-glutamine was provided by VWR, Germany. All other used chemicals were of analytical reagent grade.

2.2. Methods

2.2.1.Network-structured film coating

In the present study, two different forms of crimped PET cardiovascular grafts, woven and knitted, as shown in Figure 1, were used for network-structured film coating. All steps in the following experiments were performed for each form.

Firstly, the surface of PET graft was oxidized to acquire a negatively charged hydroxyl group using piranha solution composed of H_2O_2 (30%) and sulfuric acid (97%) at 1:1 v/v.

Briefly, woven and knitted slices (2x2 cm^2) of crimped PET were cleaned in 50% ethanol under sonication (Sonorex RK 100H, Bandelin, Germany) and then dipped into 20 ml piranha solution at 25°C for 15 minutes. The grafts were rinsed with distilled water and oven dried at 80°C for 1h. Afterwards, the oxidized grafts were dipped for 3h into polymer solution of SD-PHA-b-MPEO in dichloromethane (10 mg/ml). The desired network-structured film was then allowed to form by solvent evaporation at 25°C in a cap sealed glass chamber under saturated water vapor [16]. The obtained graft is abbreviated as PET-Net. For topographic comparison purposes, a polymer film was prepared with the same protocol using non-oxidized PET grafts. In all other described experiments, the cleaned, unmodified PET was used as control.

2.2.2.FTIR Analysis

Fourier transform infrared spectroscopy FTIR (Alpha, Bruker, Germany) was utilized to analyze the

oxidized surface of PET after piranha treatment in comparison to unmodified PET. The analysis was performed at 24 scans and at a resolution of 4 cm^{-1}. Scanning was conducted in the mid-IR range from 400-4000 cm^{-1}. Three measurements were carried out for each graft.

2.2.3. SEM visualization

The surface topography of the PET-Net was visualized using Scanning electron microscope SEM (Jeol JSM 7500 F, Japan) and compared to coated, unmodified PET. The grafts were mounted onto metal dishes using double-sided adhesive tape and conductive carbonic cement. A thin coat of platinum was prepared via a sputter coater (S150B, Edwards, England) under vacuum using an inert gas (argon) at 30 mA for 120 seconds before the grafts were observed.

2.2.4. Biocompatibility study

2.2.4.1. L929 cell adhesion and growth on PET-Net grafts

The biocompatibility property of PET-Net was investigated using mouse fibroblast cell line L929 as a model. Slices of unmodified PET and PET-Net (1x1 cm^2) were fixed onto sterile glass chips using inert, cell-nontoxic silicon glue and placed in a 12 well culture plate. The L929 cells were seeded at a density of $1x10^5$ cells per well in 2 ml of DMEM medium supplemented with 10% FBS, 1mM L-glutamine, penicillin (10.000 U/ml), streptomycin (10 µl/ml) and amphotericin B (25 µg/ml). The cultured grafts were incubated at 37°C and 8.5% CO_2. The medium was changed daily for 9 consecutive days.

The number of adhered cells on PET-Net and unmodified PET was counted after 24h cell culturing. The medium was removed and the grafts were rinsed twice with sterile PBS at pH 7.4. The grafts were detached from glass chips and dipped into EBSS buffer solution without Ca^{+2} or Mg^{+2} for 5 minutes at 25°C, followed by incubation in 1ml trypsin solution (5 mg/ml) at 37°C for 15 minutes

to isolate the adhered cells from the graft surface. The isolated cells were immediately counted using Neubauer chamber. The experiment was repeated in triplicate for each graft.

To assess the growth of L929 cells on the prepared PET-Net, a graft sample was taken each day, rinsed twice with sterile PBS at pH 7.4 and immersed in 1% paraformaldehyde for 1h to fix the adhered cells. The grafts were dried under dust-free airflow and platinum sputtered as described above for SEM observation.

2.2.5. Anti-adhesion efficiency of PET-Net grafts against bacterial strains

The *in-vitro* anti-adhesion efficiency of PET-Net grafts was assessed against Gram- positive (*S. epidermidis* and *S. aureus*), and against Gram-negative *E. coli* pathogens.

The bacteria were cultured on Col-S medium (Columbia Agar with 5% sheep blood, pH 7.3 ± 0.2, BD Biosciences, Germany) in an incubator (Heraeus BBD 6220,Germany) at 37°C, 5.5% CO_2 and 85% humidity for 24h. A fresh bacterial suspension from the last culture was prepared directly before use in sterile PBS at pH 7.4 containing 15 mM glucose. The optical density of the bacterial suspension was adjusted to a McFarland value of 1 (equivalent to $8x10^8$ CFU/ml) using a Densimat machine (bio Merieux, France).

Slices of PET-Net and unmodified PET (0.5x0.5 cm^2) were brought into contact with bacterial suspension and incubated for 24h as stated above. Afterwards, grafts were washed twice with sterile PBS at pH 7.4. To count the number of adhered bacteria, the grafts were incubated in 1ml trypsin solution (5 mg/ml) at 37°C under gentle stirring at 100 rpm/min for 20 minutes using HLC (HTMR 131, Germany) to detach the adhered bacteria from the surface. Ten microliters of the obtained bacterial suspension were spread onto Col-S medium in 90 mm petri dishes. The number of bacterial colonies was counted 24h after incubation. The experiment was repeated six times for each bacterial strain and the anti-adhesion efficiency was calculated using Equation (1):

$$\text{Anti-adhesion efficiency} = \left(\frac{A - B}{A}\right) x\ 100\% \quad (1)$$

Where, A is the number of grown colonies on the unmodified PET, and B is the number of grown colonies on the PET-Net.

2.2.6. Statistical analysis

The data were expressed as means ± standard deviations of the representative experiments. Statistical comparisons were made by analysis of T-distribution and the difference was considered to be significant at $p < 0.05$ for all evaluations.

3. Result

3.1. Surface characterization

3.1.1. FTIR analysis

Woven and Knitted forms of crimped PET grafts were surface oxidized by selective cleavage of the ester bond within the PET surface using piranha solution to produce negatively charged hydroxyl groups. The oxidized PET was confirmed by FTIR to detect the presence of the desirable groups on the surface. FTIR spectra of unmodified PET and oxidized PET are depicted in Figure 4. The spectra of unmodified PET showed a substantial strong intensity of carbonyl bonds (C=O) indicated by a stretching vibration at 1711 cm^{-1}, and a medium intensity of aromatic (C=C), (=C-H) and (C-H) bonds detected by stretching vibrations at 1407, 870, 721 cm^{-1}, respectively. At the same time, alkane (C-H) showed a stretching vibration at 1339 cm^{-1}, and the ester bond (C-O) was indicated by the presence of three strong stretching vibration bands at 1239, 1091 and 1015 cm^{-1}. The unmodified PET showed no peaks in the hydroxyl region (3000-3500 cm^{-1}), whereas a distinctive band appeared in this region in the spectra of oxidized PET, indicating the presence of the desired negative hydroxyl groups.

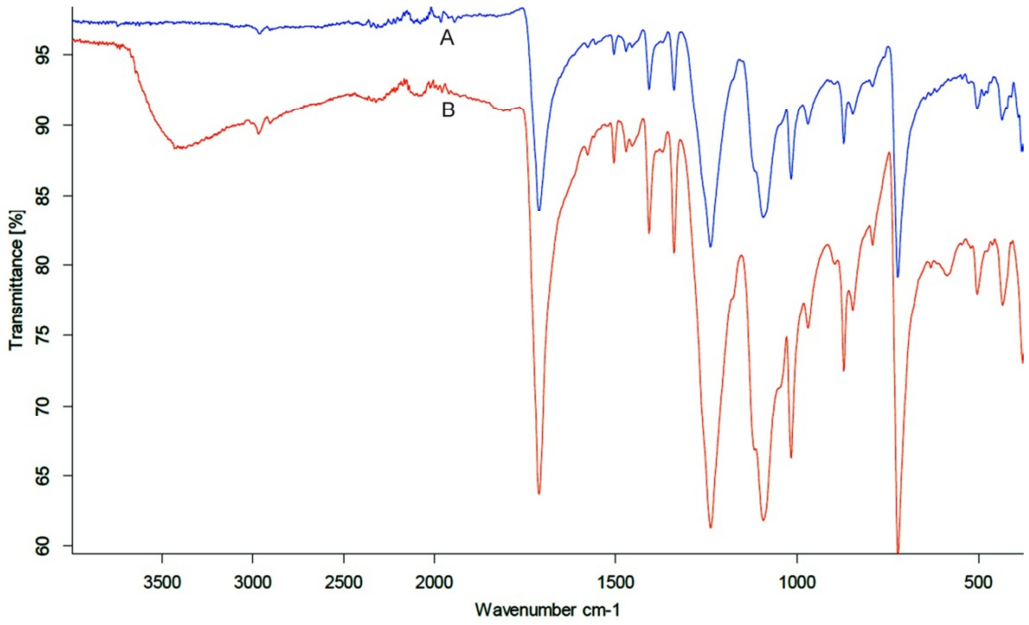

Figure 4. FTIR spectra of oxidized (B) and unmodified PET (A) grafts. The selective absorption of light in the region of the hydroxyl group (3000-3500 cm^{-1}) in oxidized PET is illustrated.

3.1.2. SEM visualizations

The surface modified and the unmodified PET grafts were dipped in the polymer solution to cast a film, followed by evaporation of the organic solvent under saturated humid conditions to obtain the appropriate coat characteristics. The topography of the obtained PET-Net was investigated using SEM and compared to the coated, unmodified PET (Fig. 5). SEM observations demonstrated formation of a porous architecture that displayed a variety of irregular pores resembling a network-structured film. Unlike the unmodified PET, the formed film on the oxidized PET was obviously not closely adhered to the surface and hence secured the flexibility of the graft fibers and its ability to tensile. In contrast, a porous film was closely associated with the unmodified PET which manifested a noteworthy reduction in fibers flexibility and tensile ability.

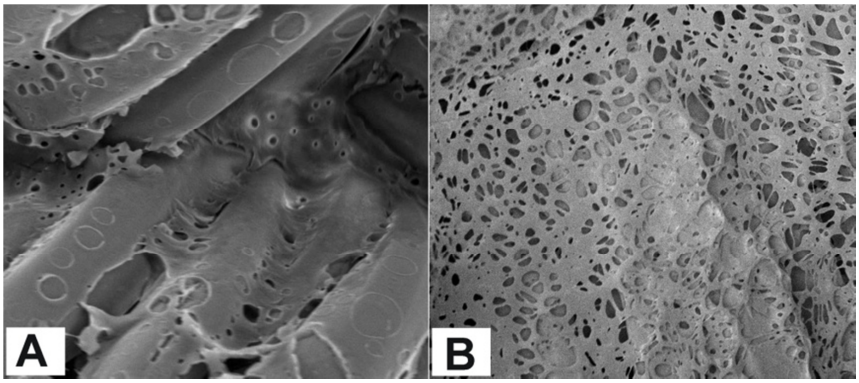

Figure 5. SEM micrographs visualize the coat architecture on woven PET. A closely adhered porous film was formed on the unmodified PET graft after dipping in the polymer solution (A), and a network- structured film was formed on woven PET after switching the surface charge into negative by piranha solution (B).

3.2. Biocompatibility study

The biocompatibility property of the network-structured coat to host cells was evaluated using L929 cells as a model. The cells were cultured on PET-Net and on unmodified PET to assess the cellular adhesion and growth over several days. The cellular behavior revealed a slight decrease in the number of adhered L929 cells onto PET-Net. Importantly, the difference did not meet the statistical significance (P= 0.1) as illustrated in Figure 6.

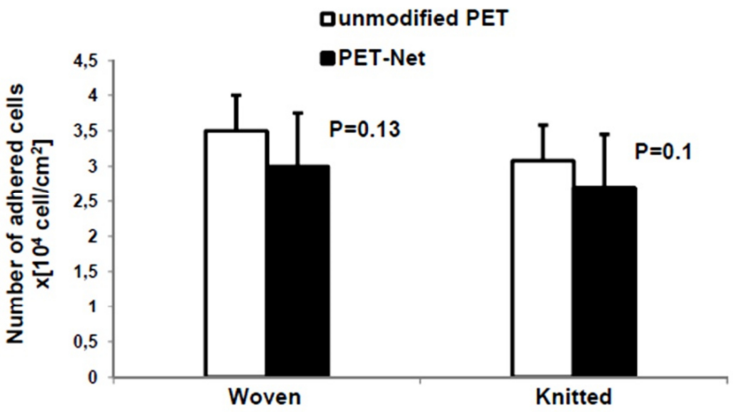

Figure 6. The number of L929 cells adhered on PET grafts after 24h cell culture. The adhered cells were counted (x10^4 cell/cm^2) after isolation from woven and knitted, PET-Net (black bars) and unmodified PET (white bars) using a Neubauer chamber. Results are given as mean ± standard deviation of three independent experiments.

The formed coat on woven and knitted PET-Net supported the cell adhesion and growth, and displayed compatible cellular behavior compared to unmodified PET at selected time intervals. The surfaces were similarly overgrown with a cellular monolayer after seven days (Fig. 7).

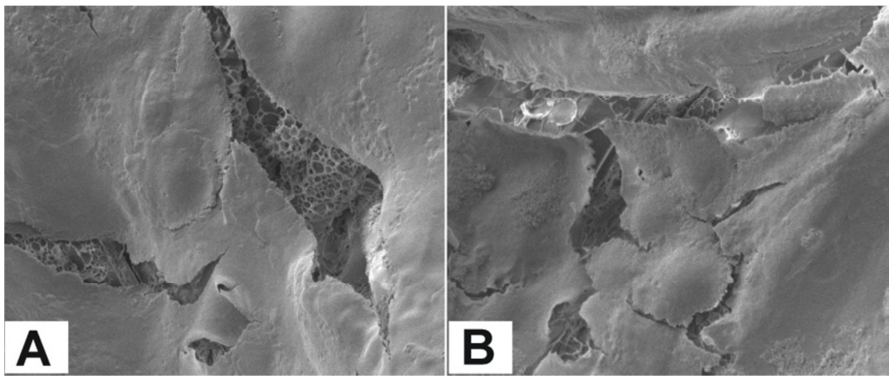

Figure 7. SEM micrographs of L929 cells grown on PET-Net grafts. The multifunctional network- structured coat supported cell growth on woven (A) and knitted (B) PET-Net.

3.3. Bacterial anti-adhesion efficiency of PET-Net

The *in-vitro* anti-adhesion efficiency of PET-Net against three bacterial strains was investigated in comparison to unmodified PET. The grafts were incubated in *S. epidermidis, S. aureus*, or *E. coli* suspensions at pathogen concentrations of 8 x10^8 CFU/ml for 24h. The attached bacteria were removed and cultured on agar blood medium. The CFUs numbers of the grown bacteria were counted thereafter for each strain as shown in Figure 8.

Our results demonstrated that the number of Gram-positive *S. epidermidis* and *S. aureus* bacteria adhered on PET-Net recorded a significant reduction ($p < 0.05$) compared to unmodified PET (Fig. 9. A and B). The adhesion of *S. epidermidis* previously isolated from a vein catheter decreased by 2.6 and 2.3 fold and of *S. aureus* decreased by 2.3 and 2.4 fold for woven and knitted PET-Net, respectively. To similar extent, Gram-negative *E. coli* bacteria demonstrated significant ($P = 0.003$) reduction by 2.9 fold for woven PET-Net and 2.7 fold for knitted PET-Net (Fig. 9 C). Depending on

the number of adhered bacteria, the anti-adhesion efficiency of PET-Net was calculated using the equation (1). The anti-adhesion efficiency against *S. aureus* was 56.3 % and 58.9% for woven and knitted PET-Net, respectively. Interestingly, woven and knitted PET-Net showed a higher anti-adhesion effectiveness (62.1 % and 56.9%, respectively) against *S. epidermidis* previously isolated from a vein catheter from a patient and thus especially relevant for the analysis. The anti-adhesion efficiency against Gram-negative *E. coli* was even more pronounced than that of the previously studied Gram-positive bacteria and showed 64.3 % and 63.1% for woven and knitted PET-Net, respectively.

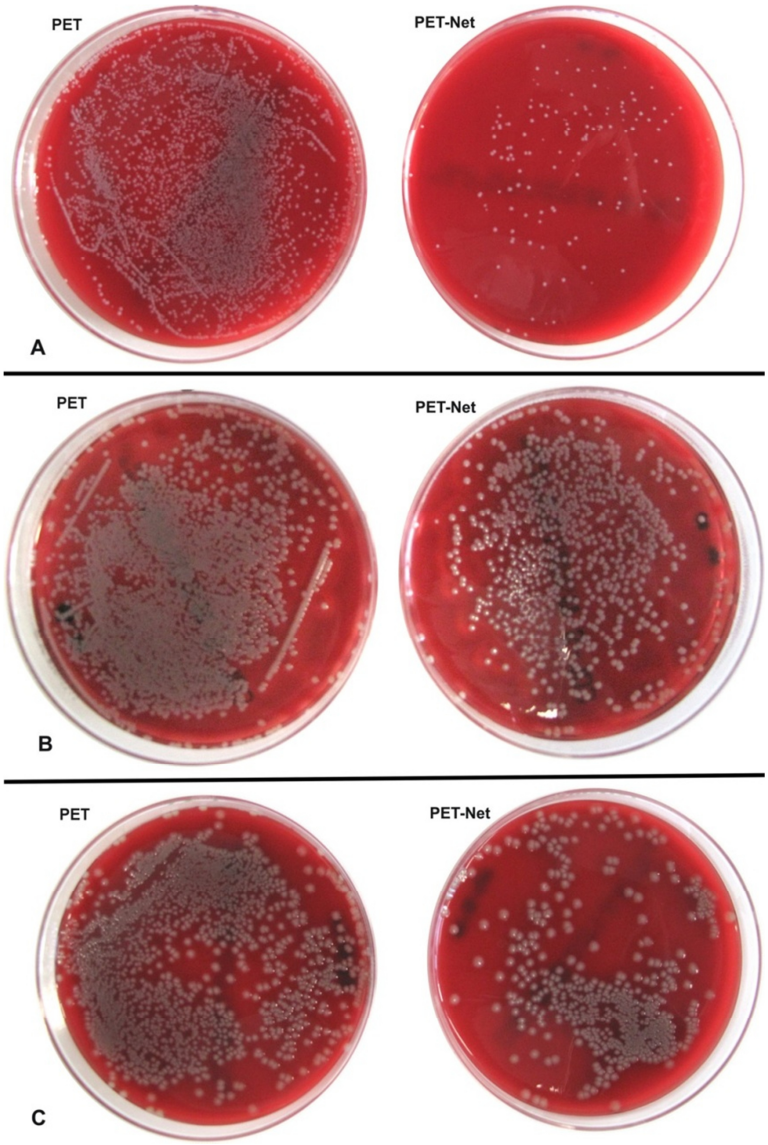

Figure 8. Col-S bacterial culture of isolated *S. epidermidis* (A), *S. aureus* (B), and *E. coli* (C) bacteria harvested from PET-Net (right) and unmodified PET (left) grafts. The grafts were infected at a pathogen concentration of 8 x 10^8 CFU/ml for 24h.

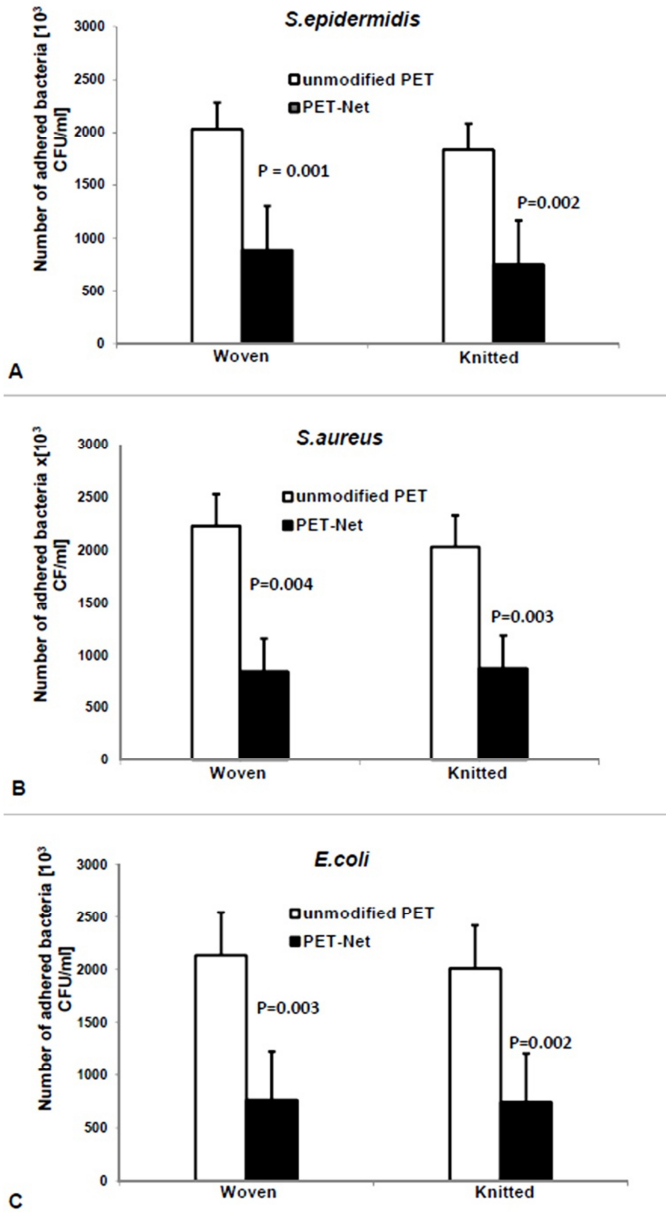

Figure 9. The number of bacteria adhered on woven and knitted unmodified PET and PET-Net grafts after 24h incubation. The number (x10^3 CFU/ml) of adhered *S. epidermidis* (A), *S. aureus* (B) and *E. coli* (C) bacteria was counted after isolation from the corresponding woven and knitted grafts and culture on Col-S medium. Results are given as mean ± standard deviation of three independent experiments.

4. Discussion

Cardiovascular prostheses successfully restore the function of damaged vessels and cardiac valves [1-3]. Despite of the associated complications with PET grafts, the woven and knitted forms of crimped PET grafts are still the most effective employed biomaterials [1-3]. However, infections and the host response destruct the graft and damage the surrounding tissue which often

necessitates graft removal upon surgical operation [4,17]. Importantly, previous coating of the implanted grafts with biocompatible and anti-bacterial polymeric film may minimize the serious deteriorations post implantation. In this study, we took priority over coating the crimped PET grafts with a newly synthesized SD-PHA-b-MPEO diblock co-polymer (Fig. 2), utilizing its multifunctional advantages mainly the negative charge, hydrophobicity, and the bactericidal effect of the sulfadimethoxine (SD) moiety and pH responsiveness. The structure of the employed polymer was proven and characterized using nuclear magnetic resonance (NMR), infrared (IR) and UV spectroscopy before use [15].

The formed porous film displayed a local bactericidal effect and satisfied biocompatibility with the host cell while maintaining the tensile ability of the grafts. However, it was critical to conserve this flexibility and tensile ability of crimped PET after coating. Indeed, many factors influence the coating process of PET graft mostly; the chemical and physical properties of the used polymer, the topographic nature of filaments that form the graft surface and the coating conditions [18]. Thus, we intended to form the polymeric film by evaporating the water-immiscible polymer solvent under saturated humid atmosphere. Under these conditions, network architecture was preferentially produced [16]. A rate-determining step during our coating technique was that the PET surface initially had to be oxidized with piranha solution to acquire a negative charge comparable to that on the polymer surface (Fig. 4). As a result of the divergent hydrophobic properties of the polymer and the oxidized PET, the electrostatic repulsion of the negatively charged surfaces precluded the close adhesion of the polymer casted on the PET filaments (Fig. 5). This ensured continuous flexibility and mobility of the PET texture. Furthermore, the porous architecture attained suitable characteristics to PET surface in terms of cell adhesion and growth, which hold promise for sufficient coverage of the graft with host cell. This consideration is based on the fact that the adhesion and growth of the host cell on PET depend on surface

hydrophobicity, porosity, electronegativity, mechanical properties, and in particular the distance between individual filaments in the yarn [19,20]. Accordingly, the hydrophobic block of the polymer and the negative charge on its surface hampered the cell adhesion to a small non-significant extent as shown by the decrease in the number of adhered L929 cells on PET-Net (Fig.6). In contrast, the formed network-structured coat provided a benefit to reduce the interval distance between the discrete filaments in the yarn. Additionally, the hydrophilic block of the polymer supported cell adhesion and growth and enabled the cells to bridge the filaments [19] (Fig. 3). As a result, L929 cells readily overgrew the PET-Net after 7 days and a cellular monolayer was observed which was comparable to that observed on unmodified PET (Fig. 7).

In general, bacterial adhesion and biofilm formation on the graft surface disturb host cell lining and stimulate the graft rejection [6]. Consequently, the anti-bacterial effect of the formed coat on PET-Net was investigated *in-vitro* against three different bacterial strains, namely *S.epidermidis, S.aureus,* and *E.coli* representing the most common Gram-positive and Gram-negative pathogens (Fig. 8).

The calculated anti-adhesion efficiency of PET-Net against aforementioned bacteria indicated highly significant reduction on adhesion of all aforementioned strains compared to unmodified PET (P=0.003) (Fig. 9). Notably, we reinforced our results by using a violent pathogenic Gram-positive *S.epidermidis* strain previously isolated from a patient`s vein catheter. Indeed, bacteria tend to adhere on and colonize preferably neutral and hydrophilic rather than hydrophobic surfaces [4]. This is avoided in the presence of polyhexylene and sulfadimethoxine groups in the formed multifunctional coat which switch the surface into hydrophobic and render the graft surface negatively charged. Additionally, the bacterial cell-repelling characteristics of polyethylene oxide guided synergistic antibacterial effect of the sulfadimethoxine group that make the modified PET graft even more unsuitable for bacterial adhesion and colonization. Furthermore, bacterial

adhesion could be influenced not only by electronegativity and hydrophobicity but also by surface porosity [21,22]. Therefore, the low porosity of the PET-Net makes it less favorable to bacterial adhesion. Interestingly, the formed multifunctional coat might offer additional advantages against bacterial biofilm formation due to pH responsiveness property of sulfadimethoxine group in range from 5.6 – 6 [15]. In particular, biofilm formation is initiated when bacteria attach to a surface and encase themselves in an acidic polysaccharide matrix [23]. In the presence of the pH responsive sulfadimethoxine group, the surface erosion of the film is accelerated at a slightly acidic pH and is accompanied by local release of sulfadimethoxine group in the surrounding area, providing an additional local anti-bacterial effect in the surrounding media.

5. Conclusion

We utilized a multifunctional network-structured film to preserve the flexibility and tensile ability of crimped PET grafts using amphiphilic SD-PHA-b-MPEO diblock copolymer. The produced coat offered a biocompatible contacting surface and held a bacterial anti-adhesion effect against both Gram positive and Gram negative bacteria. These data point out the utility of our new strategy to decrease the infection rate associated with cardiovascular grafts and increase graft patency.

6. Acknowledgements

We would like to thank Prof. Dr Andreas Greiner and Dr. Yasser Assem, Department of Chemistry, Marburg University, Germany for kind support.

7. References

[1] Desai M, Seifalian A, Hamilton G. Role of prosthetic conduits in coronary artery bypass grafting. Eur J Cardiothorac Sur. 2011;40: 394-98

[2] Butany J, Collins J. Analysis of prosthetic cardiac devices: a guide for the practising pathologist. J ClinPathol. 2005;58:113-24

[3] William F. The williams dictionary of biomaterials, Liverpool university press, Liverpool. 1999

[4] Sabe M, Shrestha N, Menon V. Contemporary drug treatment of infective endocarditis. Am J Cardiovasc Drugs. 2013;13:251-8

[5] Tayebjee M, Joy E, Sandoe J. Can implantable cardiac device infections be defined as early or late based on the cause of infection?.J Med Microbiol. 2013;62:1215-9

[6] Karchmer A, Longworth D. Infections of intracardiac devices. Cardiol Clin. 2003;21: 253-71

[7] Rodrigues L. Inhibition of bacterial adhesion on medical devices. In “Bacterial Adhesion”. Goldman. 2010;351-67

[8] Holmes D, Mack M, Kaul S, et.al. Expert consensus document on transcatheter aortic valve replacement. J Am Coll Cardiol.2012;59:1200-54

[9] McCann M, Gilmore B, Gorman S. Staphylococcus epidermidis device related infections: pathogenesis and clinical management. J Pharm Pharmacol 2008;60:1551-71

[10] David R. Holmes J, A new drug-eluting stent that does not live up to its promise, Nature Reviews Cardiology 6. 2009;500-501

[11] Niekraszewicz A, Kucharska M, Kardas I, Wiśniewska-Wrona M, Kustosz R, Jarosz A. Chitosan coatings to seal cardiovascular prostheses. Fibres & Textiles 2011;19:106-11

[12]Contreras-Garcia A, Alvarez-Lorenzo C, Taboada C, Concheiro A, Bucio E. Stimuli–responsive networks grafted onto polypropylene for the sustained delivery of NSAIDs**.** Acta Biomaterialia 2011;7: 996-1008

[13] Hirlekar R, Patel M, Jain S, Kadam V. Drug eluting coronary artery stents. Curr Drug Deliv.2010;7:421-7.

[14] Cai W, Wu J, Xi C, Meyerhoff M. Diazeniumdiolate-doped poly(lactic-co-glycolic acid)-based nitric oxide releasing films as antibiofilm coatings. Biomaterials. 2012;33:7933-44

[15] Assem Y, Greiner A. Biodegradable amphiphilic block copolymers: synthesis, characterization and properties evaluation. Philipps university. Marburg. 2011

[16] Xiong X, Lin M, Zou W, Liu X. Kinetic control of preparing honeycomb patterned porous film by the method of breath figure. Reactfuncpolym. 2011;71:964-71

[17] Vroman L. The life of an artificial device in contact with blood: initial events and their effect on its final state. Bull NY Acad Med.1988;64:352-57
[18] XS W. Synthesis and properties of biodegradable lactic/glycolic acid polymers. In: Wise et al editors. Encyclopedic handbook of biomaterials and bioengineering. New York: Marcel Dekker.1995.p.1015-54
[19] Eskin S, Trevino L, Chimoskey J. Endothelial cell culture on Dacron fabrics of different configurations. J Biomed Mater Res. 1978;12:517-24
[20] Oloffs A, Grosse-Siestrup C, Bisson S, Rinck M, Rudolph R, Gross U. Biocompatibility of silver-coated polyurethane catheters and silver-coated Dacron material. Biomaterials. 1994;15:753-55
[21] Friedlander R, Vlamakis H, Kim P, Khan M, Kolter R, Aizenberg J. Bacterial flagella explore microscale hummocks and hollows to increase adhesion.PNAS.2013;110:5624-9
[22] Katsikogianni M, Syndrevelis C, Amanatides E, Mataras D, Missirlis Y. Plasma treated and a-C:H coated PET performance in inhibiting bacterial adhesion. Plasma Process. Polym. 2007;4:1046-51
[23] Donlan M, Costerton W. Biofilms: survival mechanisms of clinically relevant microorganisms. ClinMicrobiol Rev. 2002;15:167

Chapter 3

Covalent Immobilization of Lysozyme onto Woven and Knitted Crimped Polyethylene Terephthalate Grafts to Minimize the Adhesion of Broad Spectrum Pathogens

Al Meslmani B, Mahmoud G , Leichtweiß T, Strehlow B, Sommer F, Lohoff M, Bakowsky U.

Prepared to submit to *Biomacromolecules* Journal

Abstract

Crimped polyethylene terephthalate PET is considered as the gold standard cardiovascular graft to restore the function of damaged vessels and heart valve. Graft-associated infections mostly the formation of bacterial biofilm entirely determines the short-term graft patency. We attempted to enzymatically inhibit the initial bacterial adhesion to PET grafts using lysozyme to eradicate predominantly Gram-positive bacteria. Woven and knitted forms of crimped PET grafts were surface-modified by Denier reduction to produce a functional carboxyl group. Lysozyme was covalently immobilized on the created carboxyl group by the end-point method. The surface-modified grafts were characterized by Fourier-transform infrared spectroscopy and X-ray photoelectron spectroscopy. Most importantly, the bacterial anti-adhesion efficiency was empirically evidenced using *Staphylococcus aureus*, *Staphylococcus epidermidis* and *Escherichia coli*. Our figures of merit revealed lysozyme immobilization yield of 15.7 µg/cm^2 as determined by the Bradford assay. The activity of immobilized lysozyme on woven and knitted PET manifested 58.4% and 55.87% using *Micrococcus lysodeikticus* cells, respectively. Noteworthy, the adhesion of vein catheter-isolated *S.epidermidis* decreased by 6 and 8 fold and of *S.aureus* by 11 and 12 fold, while the Gram-negative *E.coli* showed only a decrease by 3 and 4 fold. The anti-adhesion efficiency was specific for bacterial cells and no significant effect was observed on adhesion and growth of L929 cells used as a model. In conclusion, immobilization of lysozyme onto PET grafts can modulate the initial adhesion of pathogenic bacteria and inhibit the graft-associated infection.

Key words: Crimped cardiovascular PET; Lysozyme; Bacterial adhesion; Biofilm.

1. Introduction

The utilization of polyethylene terephthalate, (PET) (Dacron®) in cardiovascular prosthesis has given rise to critical infections, mainly prosthetic valve endocarditis (PVE) and prosthetic vascular graft infection (PVGI) [1,2,3]. The development of infection starts primarily by bacterial adhesion onto graft surface via weak, reversible, physical forces followed by an adhesion cascade to secure successful attachment. The adhered bacteria proliferate and develop an irreversible attachment forming dense microbial communities called biofilm [4]. The formed biofilm exhibits a great ability to evade host defenses and to resist antimicrobial therapy and the human immune system [4,5]. Studies on pathogenic organisms responsible for PET graft infections have shown that *Staphylococcus aureus* is the infecting organism in ~70 % of cases, and *Staphylococcus epidermidis* encounters ~30% of the cases, resulting in prolonged hospitalization, graft failure, and patient death [6,7].

Different strategies have been developed to prevent bacterial colonization on cardiovascular prostheses after implantation. The most commonly used approaches are focused primarily on bonding of anti-infective agents onto-graft surface, mainly silver [8], quaternary ammonium [9] or antibiotics [10], in addition to systemic antibiotics as prophylaxis [11]. Alternatively, recent approaches to prevent bacterial adhesion and to eradicate the bacteria upon contact with the biomaterial surface were applied. For instance, strategies were used to block bacterial adhesion including; changing surface morphology [12], modifying surface features using either bio surfactants [13], or plasma [14]. In addition, soluble agents toxic to bacteria were used [15]. Nevertheless, previous strategies were limited by difficulties related to short active duration, high cost, and high host-cytotoxic potential even at low concentrations [16]. Furthermore, contradictory results were also reported by several studies concerning biofilm eradication [17,18].

Unlike previous studies, we aimed to inhibit the bacterial adhesion enzymatically using an enzyme

with lytic activity against bacteria. Accordingly, an antibacterial graft resisting broad-spectrum pathogens was developed. Lysozyme, or 1,4-β-N-acetylmuramidase, is an enzyme that displays lytic activity especially for Gram-positive bacteria such as *S.aureus* and *S.epidermidis* [19,20]. Lysozyme damages the bacterial cell wall by catalyzing the β(1-4) glucosidic bonds of murein resulting in an effective protection against bacterial adhesion and biofilm formation. This strategy provides many advantages compared to antibiotic or other agents including long-term duration, nontoxicity, local application without adverse effect on normal flora and inability of bacteria to develop a resistance against the enzyme.

To the best of our knowledge, the covalent immobilization of lysozyme enzyme on woven and knitted forms of crimped PET cardiovascular grafts (Fig.1) is rarely addressed. In the current study, a hen egg white lysozyme was immobilized by the covalent end-point attachment technique to maintain its chemical stability and bioactivity after the immobilization process.

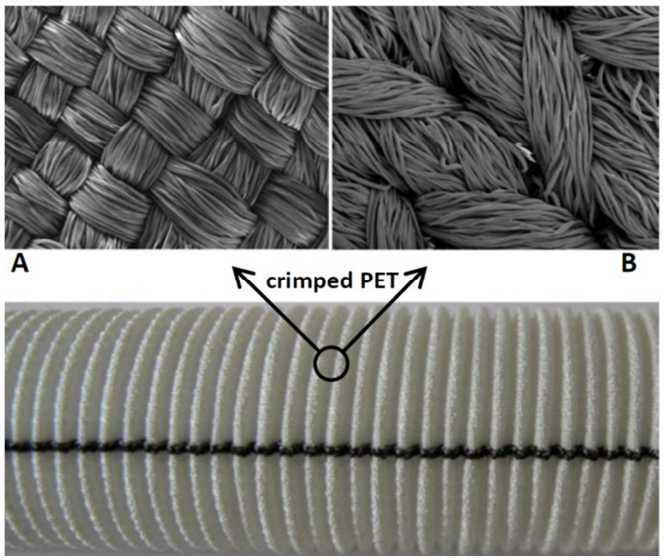

Figure1. SEM micrographs of woven (A) and knitted (B) crimped PET grafts. The multifilament PET threads in woven grafts are fabricated in an over-and-under pattern, while in knitted grafts are looped. The crimped technique (shown in the picture) is utilized to increase the flexibility, distensibility, and kink-resistance of grafts.

The woven and knitted forms were surface-modified as schematically shown in Figure 2. Denier reduction was carried out to selectively cleave the ester linkage within the PET surface, resulting in a free carboxyl group that was used as an anchor site for covalent immobilization of lysozyme. The surface-modified PET was characterized by FTIR and XPS. The immobilization efficiency of the enzyme was determined by the Bradford assay and its activity compared to free enzyme using *Micrococcus lysodeikticus* cells was detected. The bacterial anti-adhesion efficiency of the enzyme-immobilized grafts was studied against two Gram-positive (*S.aureus, S.epidermidis*) and one Gram-negative pathogen (*E.coli*). The host cell behavior on the modified grafts was evaluated using mouse L929 fibroblasts as a model.

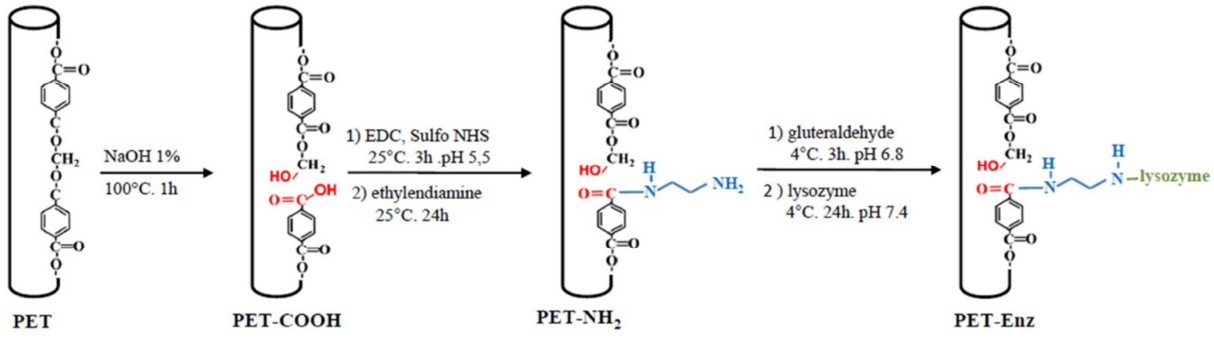

Figure 2. Schematic illustration of covalent immobilization of lysozyme on the PET surface. The intrinsic ester linkage within the PET structure was cleaved by alkaline treatment to produce functional carboxyl group on the surface (PET-COOH). The PET-NH_2 was obtained after grafting ethylendiamine on PET-COOH, while PET-Enz was obtained after immobilization of lysozyme by the end-point method.

2. Materials and methods

2.1. Materials

Woven and knitted forms of crimped PET grafts (14mm internal diameter, 30 cm length and 12 filaments per yarn bundle) were kindly provided by Vascutek GmbH, Germany. The bacterial strains *Staphylococcus aureus* (ATCC 29213), *Staphylococcus epidermidis* (isolated from a vein catheter of a patient), and *Escherichia coli* (ATCC 25922) were supplied from the Institute of

Medical Microbiology and Hospital hygiene, Marburg University, Germany. Lyophilized *Micrococcus lysodeikticus* (ATCC 4698) cells were purchased from Sigma Aldrich, Germany. Lyophilized powder lysozyme (EC 3.2.1.17) obtained from hen egg white (activity ≥40,000 units/mg protein), N-hydroxysulfosuccinimide (Sulfo-NHS), 1-Ethyl-3-(3-dimethyl amidopropyl) carbodiimide hydrochloride (EDC), glutaraldehyde, and ethylendiamine were purchased from Sigma Aldrich, Germany. Sodium hydroxide was supplied by Carl Roth, Germany. Paraformaldehyde, Tris buffer, methylene blue, and Giemsa stain were purchased from Merck, Germany. 2-(N-morpholino) ethanesulfonic acid (MES) was acquired from Serva, Germany. The mouse L929 fibroblast cell line was from DSMZ, Braunschweig, Germany. Dulbecco's modified Eagle's medium (DMEM), Earle's Balanced Salt Solution (EBSS), Fetal Bovine Serum (FBS), trypsin, streptomycin, penicillin, and amphotericin B were purchased from PAA Laboratories GmbH, Germany. L-glutamine was purchased from VWR, Germany. All other used chemicals were of analytical reagent grade.

2.2. Methods

2.2.1. Surface modification of crimped PET grafts

In the present study, two different forms of crimped PET cardiovascular grafts woven and knitted were used for surface modification (Fig. 1). All steps in the subsequent experiments were performed for each form. To introduce a functional carboxyl group on the surface of the crimped PET grafts, modified Denier reduction was utilized as previously reported by Kissa [21], and schematically illustrated in Figure 2. Briefly, slices (2x2 cm^2) from woven and knitted forms of crimped PET grafts were immersed in 20 ml of 50 % ethanol for 15 minutes in an ultrasonic water bath (Sonorex RK 100H, Bandelin, Germany) to clean the surface. Subsequently, the grafts were rinsed several times with distilled water under stirring and then oven dried at 55°C for 2h. The

cleaned grafts were dipped in 20 ml of 1% NaOH solution and incubated in a boiling water bath for 1h. The modified grafts were rinsed with distilled water and oven dried for 2h at 55°C. The obtained grafts are abbreviated as PET-COOH.

2.2.2. Grafting of ethylendiamine onto PET-COOH

Ethylendiamine was ligated to the previously produced carboxyl group using the adapted zero-length cross linker reaction known as carbodiimide plus sulfo-NHS as previously reported [22]. Crimped PET-COOH were immersed in 15 ml of MES buffer (0.1 M, pH 5.5) and hydrated for 2h. The carboxyl group on the surface was activated by 0.1 M of EDC and 5 mM of Sulfo-NHS and incubated under gentle stirring at 50 rpm/min (IKA C-MHGHS7, Germany) at room temperature for 3h. A solution of 50 mM of ethylenediamine was slowly added to the activated PET-COOH. The conjugation between one terminal amino group of ethylendiamine and one carboxyl group on the surface of PET-COOH was carried out overnight at room temperature while stirring. The obtained grafts were rinsed with distilled water under sonication for 5 minutes and dried under dust-free airflow. The gained grafts are abbreviated as PET-NH_2.

2.2.3. Immobilization of lysozyme enzyme onto PET-NH_2

Lysozyme enzyme was covalently immobilized onto PET-NH_2 using the homobifunctional cross-linker glutaraldehyde as described elsewhere [23]. Briefly, PET-NH_2 were immersed in 10 ml of sodium phosphate buffer (0.1 M, pH 6.8) containing 150 µl of 50 % glutaraldehyde and incubated at 4°C under gentle stirring at 50 rpm/min for 3h. Afterwards, the grafts were rinsed with distilled water under sonication for 5 minutes and dipped into 10ml of lysozyme solution (10 mg/ml) in phosphate buffered saline (PBS, 0.5 M, pH 7.4). The reaction was completed overnight at 4°C. The excess aldehydes and formed Schiff bases were reduced by adding 500 µl Tris buffer (0.2 M, pH

8.5) and incubation for 1h at 4°C. Finally, the grafts were washed with phosphate buffer and rinsed with distilled water under sonication for 5 minutes, and dried under dust-free airflow. The obtained grafts were stored at 4°C and are abbreviated as PET-Enz.

2.2.4. Surface characterization after modification

2.2.4.1. FTIR analysis

FTIR Spectrometer (Alpha, Bruker, Germany) was utilized to detect the functional carboxyl group on the surface of modified PET-COOH compared to unmodified PET. The analysis was performed at 24 scans, and at a resolution of 4 cm^{-1}. Scanning was conducted in the mid-IR range from 400-4000 cm^{-1}. Three different measurements were carried out for each graft.

2.2.4.2. XPS analysis

The chemical composition and survey spectra of modified and unmodified PET surfaces were investigated using XPS (PHI Versaprobe 5000, Physical Electronics, USA). The XPS spectra of PET-Enz grafts were collected along with the native lysozyme and the unmodified PET as controls. XPS spectra were acquired at a chamber pressure in the range of 10^{-8} mbar using monochromatized Al 1486.6 eV X-ray beams with an analytical spot size of 1400 µm x 200 µm. Two pass energies were chosen; 187.75 eV for survey scans and 23.5 eV for higher resolution scans. The binding energy scale was calibrated by shifting the C 1s aliphatic carbon peak to 284.8 eV. The XPS spectra were collected at the take-off angle 45° corresponding to a detection depth of about 4 nm for the relevant elements.

2.2.4.3. Determination of the concentration of immobilized enzyme

The concentration of covalently immobilized lysozyme on PET-Enz grafts was determined using an adapted dye-interaction method based on the Bradford assay [24]. Briefly, dye reagent was prepared from Coomassie Brilliant Blue G-250 (10 mg) in 5 ml of 95% ethanol and 10ml of 85% (w/v) phosphoric acid. The resulting solution was diluted to a final volume of 100 ml. various known concentrations of native lysozyme in 100 µl aqueous solution were added to 5 ml of the previously prepared dye reagent, and agitated using a vortex (Reax 2000, Heidolph, Germany). The mixture was kept at room temperature for 10 minutes, and then centrifuged at 5000 rpm/min for 15 minutes to separate the formed enzyme-dye complex. The absorbance of the supernatant that contains the free dye was measured within 30 minutes at 465 nm using a spectrophotometer (Thermo Fischer 1510. Finland). The linear inverse relationship between the absorbance at 465 nm caused by the residual dye and the concentration of enzyme in the aqueous solution was ascertained and used as a calibration curve to determine the amount of immobilized lysozyme enzyme.

Accordingly, slices (1x1 cm^2) of crimped PET- Enz grafts and PET-NH_2, as control were immersed in 5 ml dye reagent for 3h and gently mixed. The absorbance of dye solution above the graft was measured at 465 nm. The amount of immobilized enzyme was calculated using the previously constructed calibration curve. Since only a small amount of dye could be physically adsorbed onto dipped grafts, the removed grafts were rinsed again with 5ml of solution (5% ethanol, 10% phosphoric acid, 85% distilled water V/V/V) under sonication for 5 minutes and the absorbance of the dye in the washing solution was considered. The experiment was repeated in triplicate.

2.2.5. Evaluation of enzyme activity

The activity of lysozyme was determined based on a turbidity assay using *Micrococcus lysodeikticus* cells as a substrate [25].

2.2.5.1. Activity of free enzyme

A *Micrococcus lysodeikticus* cell suspension (0.02 % w/v; A_{450nm}~ 0.7) was prepared in phosphate buffer (66 mM, pH 6.24). The lytic reaction was carried out in a quartz cuvette (3 ml) with 1cm light path at 25°C using a spectrophotometer. First, the substrate suspension was filled into the cuvette that was placed into a thermostatic measuring cell and incubated for 5 minutes to achieve temperature equilibration. Afterwards, 100 µl of freshly, pre-cooled lysozyme solution (400 U/ml in phosphate buffer) was added to the substrate cell suspension. The change in the absorption (ΔA_{450nm}/minute) was recorded for 5 minutes. A blank assay without lysozyme was also performed to account for any autolytic degradation of the substrate. The experiment was carried out in triplicate, and one activity unit was defined as the absorption reduction of 0.001 per minute as illustrative in the equations:

$$\textit{Enzyme activity (unit/mg) solid} = \frac{\Delta A_{450nm/min}\ \text{test} - \Delta A_{450nm/min}\ \text{blank}}{(0.001)(0.1)(\text{mg used sample})} \quad (1)$$

$$\textit{(unit/mg) Protein} = \frac{(\text{unit/mg})\ \text{solid}}{\text{protein (\%)}} \quad (2)$$

2.2.5.2. Activity of immobilized enzyme

The activity of immobilized lysozyme was estimated by addition of pre-cold PET-Enz graft into 2.5 ml *Micrococcus lysodeikticus* cell suspension (0.02 % w/v) in phosphate buffer (66 mM, pH 6.24) at 25°C. The ΔA_{450nm} per minute of the substrate suspension was determined for 5 minutes. The

initial absorption of the lysozyme free-substrate suspension was also determined before the addition of PET-Enz. A blank assay was also conducted using pre-cold PET-NH_2 to detect any changes in absorption due to non-enzymatic effects. The experiment was carried out in triplicate for each graft form and the enzyme activity was calculated as described above taking into account the concentration of enzyme per unit surface area.

2.2.5.3. Anti-adhesion efficiency of PET-Enz grafts

The anti-adhesion efficiency of immobilized lysozyme on crimped PET against bacteria was assessed *in-vitro* against *S.aureus*, *S.epidermidis*, and *E.coli* strains as Gram-positive and Gram-negative microorganisms**.**

The bacteria were cultured on Col-S medium (Columbia Agar supplemented with 5% sheep blood, pH 7.3±0.2, BD Biosciences, Germany) in a closed incubator (Heraeus BBD 6220, Germany) at 37°C, 5.5% CO_2 and 85% humidity for 24h. A fresh bacterial suspension was prepared directly before use in sterile PBS at pH 7.4 containing 15 mM of glucose. The optical density of the bacterial suspension was adjusted to a McFarland value of 1 (equivalent to $8x10^8$ CFU/ml) using a Densimat machine (bio Merieux, France). Slices of PET-Enz and PET-NH_2 (0.5x0.5 cm^2) were brought in contact with the bacterial suspension and incubated at 37°C, 5.5 % CO_2 and 85 % humidity for 24h. Afterwards, grafts were washed twice with sterile PBS at pH 7.4. To count the adhered bacteria, the grafts were incubated in 1 ml trypsin solution (5 mg/ml) at 37°C under gentle stirring at 100 rpm/min for 20 minutes using HLC (HTMR 131, Germany) to remove the adhered bacteria from the grafts surface, followed by spreading 10 µl of the resulting suspension on 90 mm petri dishes containing Col-S medium. The number of bacterial colonies was counted after 24h incubation at 37°C, 5.5 % CO_2 and 85 % humidity. The test was repeated six times for each bacterial strain and the anti-adhesion efficiency was calculated using equation (3):

Anti-adhesion efficiency = $\left(\frac{A-B}{A}\right)\times 100\%$ (3)

A is the number of grown colonies on the control sample of the PET-NH_2 and B is the number of grown colonies on the PET-Enz.

2.2.5.4. Staining of bacteria

Bacteria adhered to unmodified PET and PET-Enz grafts were also investigated via methylene blue staining. After removal from the bacterial suspension, grafts were washed with sterile PBS at pH 7.4 and the bacteria were fixed in formalin solution (5%) for 5 minutes and rinsed with sterile water before a methylene blue drop was added. Thirty seconds later, grafts were directly washed with sterile water and dried at room temperature under a dust-free airflow. The stained bacteria were visualized at the same magnification for comparison purposes using an optical microscope (NLO-UV, Zeiss, Germany) equipped with a camera (Moticam 2000, USA).

2.2.6. Biocompatibility study

2.2.6.1. L929 cell adhesion and growth on PET-Enz grafts

The biocompatibility property of PET-Enz grafts was investigated using the L929 cells as model. Slices of unmodified PET and PET-Enz grafts (1x1 cm^2) were fixed onto sterile glass chips using inert cell-nontoxic silicon glue and set in a 12 well culture plate. L929 cells were seeded at a density of 10^5 cells per well in 2 ml of DMEM medium supplemented with 10 % gamma irradiated fetal bovine serum, 1 mM L-glutamine, penicillin (10.000 U/ml), streptomycin (10 µl/ml) and amphotericin B (25 µg/ml). The cultured grafts were incubated at 37°C and 8.5 % CO_2. The medium was changed every day for 9 consecutive days. A graft sample was detached daily, rinsed twice with sterile PBS at pH 7.4 and immersed in 1% paraformaldehyde for 1h. Subsequently, the adhered cells after 24h cell culturing were stained with Giemsa stain (5%) for 10h followed by

color differentiation using diluted acetic acid (0.5%). The treated grafts were dried at room temperature under a dust-free airflow and viewed using an optical microscope (Stemi 2000-C, Carl Zeiss, Germany) equipped with Camera (Canon G10, Japan). For scanning electron microscopy (SEM) studies, the cultured grafts were rinsed twice with sterile PBS, and fixed with 1% paraformaldehyde for 1h. After washing with distilled water, dehydration was performed by slow water replacement using a series of ethanol solutions (50%, 70%, 80%, and 95%) for 90 minutes receiving final dehydration in absolute ethanol for 120 minutes. The samples were then dried using a critical point dryer (Bal-Tec, CDP 030, Germany) followed by gold sputtering via Sputter coater (S150, Edwards, England) under vacuum using an inert dusting gas (argon) at 25 mA for 120 seconds, before they were visualized by SEM.

2.2.6.2. Counting of L929 cells adhered to PET-Enz grafts

The number of adhered cells on unmodified PET and PET-Enz grafts was counted 24h after cell culture. The medium was removed and the grafts were rinsed twice with sterile PBS at pH 7.4. The grafts were detached from the glass chips and dipped into EBSS buffer solution without Ca^{+2} or Mg^{+2} for 5minutes at 25°C, followed by incubation in 1 ml trypsin solution (5 mg/ml) at 37°C for 15 minutes to remove the adhered cells from the graft surface. The isolated cells were immediately counted using a Neubauer chamber. The experiment was repeated in triplicate for each graft.

2.2.7. Morphological analysis using SEM

Scanning electron microscope (Hitachi S-510, Japan) was used to examine the adhesion and growth behavior of L929 cells on the surface of unmodified PET and PET-Enz grafts. The grafts were dried as described above and were mounted onto metal dishes using double-sided adhesive

tape and conductive carbonic cement. The grafts were gold sputtered as described above. All images were taken at 25 kv under the same magnification for comparison studies.

2.2.8. Statistical analysis

The data are expressed as means ± standard deviations of the representative experiments. Statistical comparisons were made by analysis of T-distribution and the difference was considered to be significant at a $p < 0.05$ for all evaluations.

3. Results

3.1. FTIR spectroscopy of surface functionalized PET-COOH graft

Woven and knitted forms of crimped PET grafts were modified using the Denier reduction to introduce functional carboxyl groups on the surface. The created carboxyl group was activated by carbodiimide/sulfo-NHS and further used for conjugation of ethylendiamine as a spacer between the carboxyl group and lysozyme (Fig.2).

FTIR was used to characterize PET-COOH after modification to detect the presence of the desirable functional group on the surface. FTIR spectra of unmodified PET and PET-COOH are depicted in Figure 3. The spectra of unmodified PET surface showed a substantial strong intensity of carbonyl bonds (C=O) indicated by the stretching vibration at 1711 cm^{-1}, and a medium intensity of aromatic (C=C), (=C-H) and (C-H) bonds detected by stretching vibrations at 1407, 870, 721 cm^{-1}, respectively. At the same time, alkane (C-H) showed a stretching vibration at 1339 cm^{-1}, and the ester bond (C-O) demonstrated three strong stretching vibration bands at 1239, 1091 and 1015 cm^{-1}. The unmodified PET surface showed no peaks in the hydroxyl region of the carboxyl group (3000-3500 cm^{-1}), whereas a broad shoulder appeared in this region in the spectra of PET-COOH, indicating the presence of the desirable carboxyl group.

In addition, the preliminary FTIR spectrum of PET-NH_2 was almost the same as that of the unmodified PET graft (data not shown). This is because the absorption frequencies of amide bonds based on (C=O) and (C-N) at (1650-1690 cm^{-1} and 1030-1220 cm^{-1}, respectively) overlap with that of the ester groups in unmodified PET. However, the grafted ethylendiamine and lysozyme were confirmed using XPS.

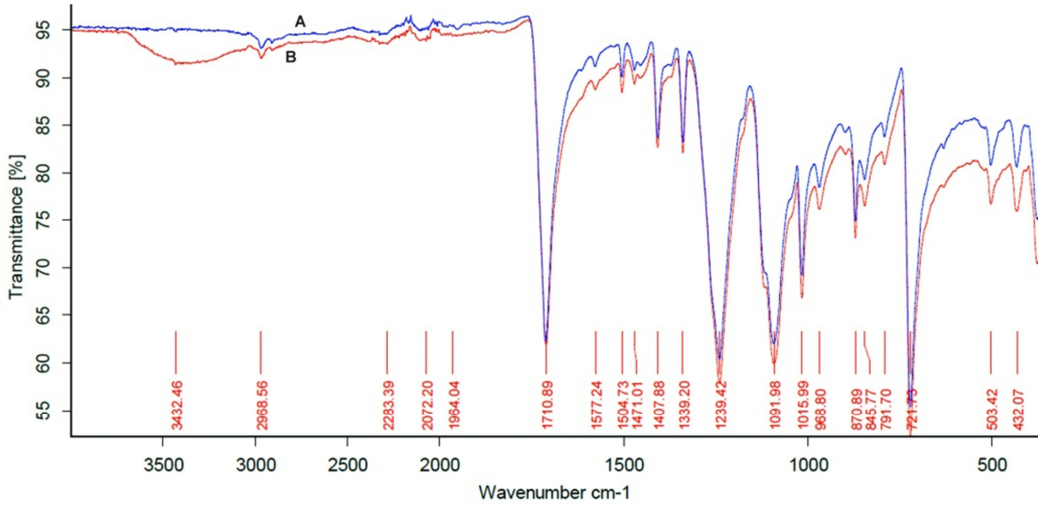

Figure 3. FTIR spectra of unmodified PET (A) and PET-COOH (B). The selective absorption of light in the region of the hydroxyl group derived from the carboxyl group (3000-3500 cm^{-1}) in PET-COOH is illustrated.

3.2. XPS surface analysis of PET-NH_2 and PET-Enz grafts

The chemical composition of native lysozyme, unmodified PET, PET-NH_2 and PET-Enz grafts were calculated from XPS spectra and illustrated in Table 1. The results revealed a small amount of intrinsic silicon corresponding to the unmodified PET. A nitrogen component was observed on the surface only after grafting of ethylendiamine and markedly increased after enzyme immobilization based on the amino groups of the grafted molecules. Notably, chlorine and sulfur traces, which were present in native lysozyme, were only obviously observed on the surface of PET-Enz as a result of successful enzyme immobilization.

Furthermore, the XPS detail spectra for all samples outlined two main peaks corresponding to carbon and oxygen (data not shown), while additional peaks from nitrogen and sulfur were only found in native lysozyme and PET-Enz spectra (Fig.4). The N-1s signal at 399.6 eV and the most intense signal in S-2p at 163 eV were present in both samples and were contributed to nitrogen and sulfur species from the lysozyme. An additional minor S-2p peak can be found in the PET-Enz spectrum at 168 eV and may indicate the presence of $(SO_3)^{-2}$ species.

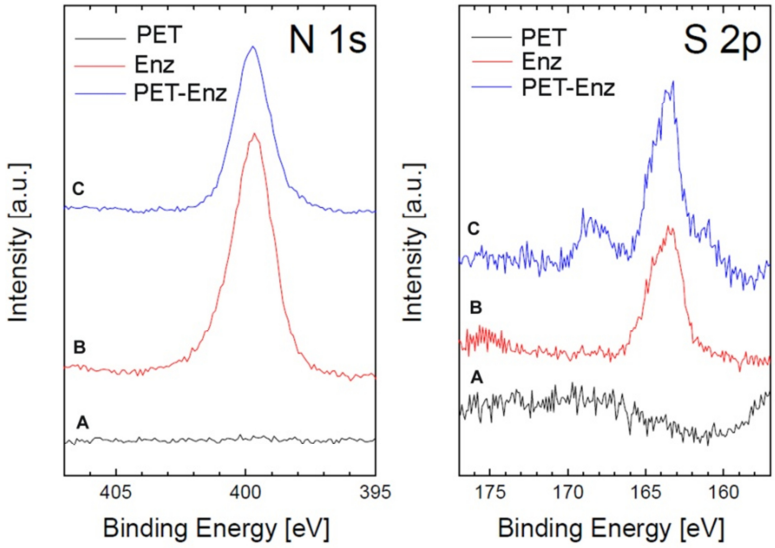

Figure 4. XPS survey scans spectra for nitrogen (N-1s) and sulfur (S-2p) of unmodified PET (A), native lysozyme (B) and PET-Enz graft (C). Nitrogen and sulfur peaks solitary appeared in the spectra of native lysozyme and PET-Enz.

Table1. XPS Study of PET grafts after surface modification and enzyme immobilization

PET Grafts	**Atomic Compositions (%) for Modified/Unmodified Grafts**					
	Carbon (C_1s)	**Oxygen (O_1s)**	**Silicon (Si_2p)**	**Nitrogen (N_1s)**	**Chlorine (Cl_2p)**	**Sulfur (S_2p)**
Native lysozyme	65.2	14.6	-	19.1	0.4	0.7
Unmodified PET	71.5	27.9	0.6	-	-	-
PET-COOH *	69.5	29.8	0.7	-	-	-
PET-NH_2 †	72.8	26.3	0.6	0.3	-	-
PET-Enz‡	58.8	30.8	0.1	9.6	0.2	0.5

*PET-COOH was obtained after Denier reduction of PET.

†PET-NH_2 was obtained by grafting ethylendiamine onto PET-COOH.

‡PET-Enz was obtained by immobilization of lysozyme onto PET-NH2.

3.3. Efficiency of enzyme immobilization onto PET-Enz grafts

The concentration of covalently immobilized lysozyme onto PET surface was determined using the Bradford assay. The blank assay was carried out on PET-NH_2, and the concentration of immobilized lysozyme was calculated from the prepared standard curve. The mean concentration of immobilized enzyme per unit surface area was appraised to be 15.7 µg/cm^2 based on three independent experiments.

3.4. Enzyme activity of free lysozyme *versus* immobilized lysozyme

To assess the influence of the immobilization process on lysozyme performance, the enzyme activity was detected against *Micrococcus lysodeikticus* cells compared to free lysozyme. Immobilized lysozyme onto woven and knitted PET manifested 58.4 % and 55.87 % of free enzyme activity, respectively. Thus, despite a significant reduction as compared to free enzyme (P=0.007), the remaining activity of immobilized enzyme was still noteworthy and suggested that the desired effect on bacterial adhesion was possible. In addition, the enzyme activity was comparable on woven and knitted PET grafts and did not indicate any significant difference (P> 0.05) (Fig.5).

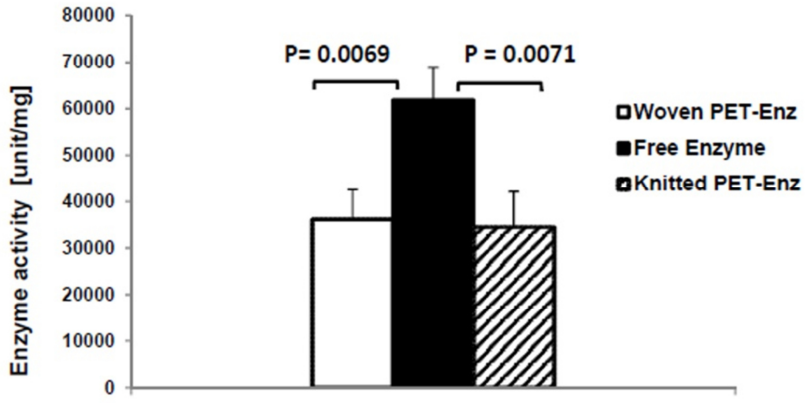

Figure 5. Activity of lysozyme on woven (white bar), knitted (striated bar) PET-Enz grafts, and free enzyme (black bar). The lysozyme activity (unit/mg) was turbidimetric measured using *Micrococcus lysodeikticus* cells as substrate. Results are given as mean ± standard deviation of three independent experiments.

3.5. Anti-adhesion efficiency of PET-Enz against bacterial strains

The *in-vitro* anti-adhesion efficiency of PET-Enz grafts against three bacterial strains was investigated. The grafts were incubated with *S.aureus*, *S.epidermidis* and *E.coli* suspensions at pathogen concentrations of $8x10^8$ CFU/ml for 24h. The attached bacteria were removed and counted by determining the number of CFUs after culture on agar blood medium, as shown in Figure 6.

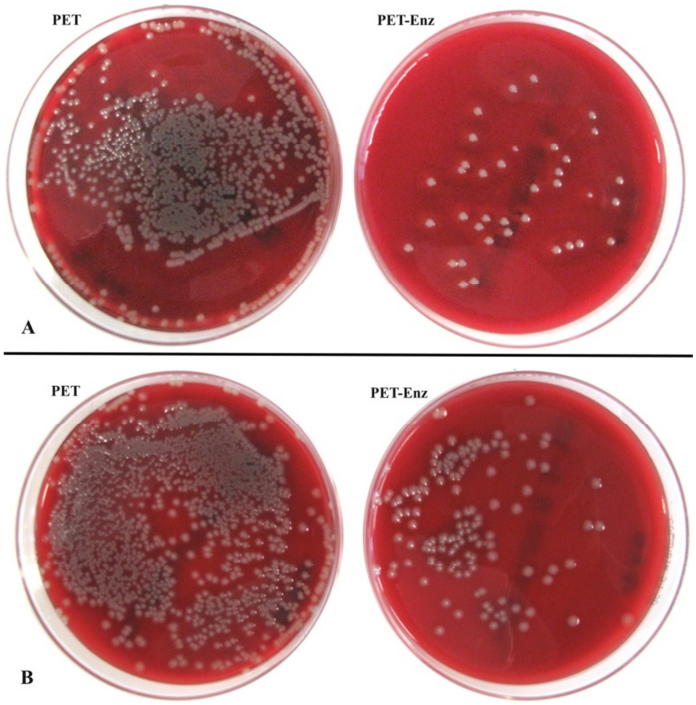

Figure 6. Col-S bacterial culture of isolated *S.aureus* (A) and *E.coli* (B) bacteria harvested from unmodified PET (left) and PET-Enz (right) grafts. The grafts were infected at pathogen concentrations of 8 x 10^8 CFU/ml for 24h.

Our results revealed that the number of Gram-positive *S.aureus* and *S.epidermidis* bacteria adhered on PET-Enz was reduced with a high statistical significance ($p < 0.0001$) as compared to unmodified PET (Fig.7 A and B). The adhesion of *S.epidermidis* isolated from a vein catheter decreased by 6 and 8 fold and of *S.aureus* by 11 and 12 fold. Gram-negative *E.coli* bacteria manifested lower, but still highly significant ($P < 0.0001$) reductions by 3 and 4 fold (Fig. 7C). The

number of adhered *E.coli* onto grafts was greater than that of *Staphylococcus* strains (P= 0.03). Furthermore, the number of bacteria adhered on all studied grafts demonstrated the pattern to be higher on woven than on knitted PET grafts, however this difference did not reach statistical significance(P > 0.05).

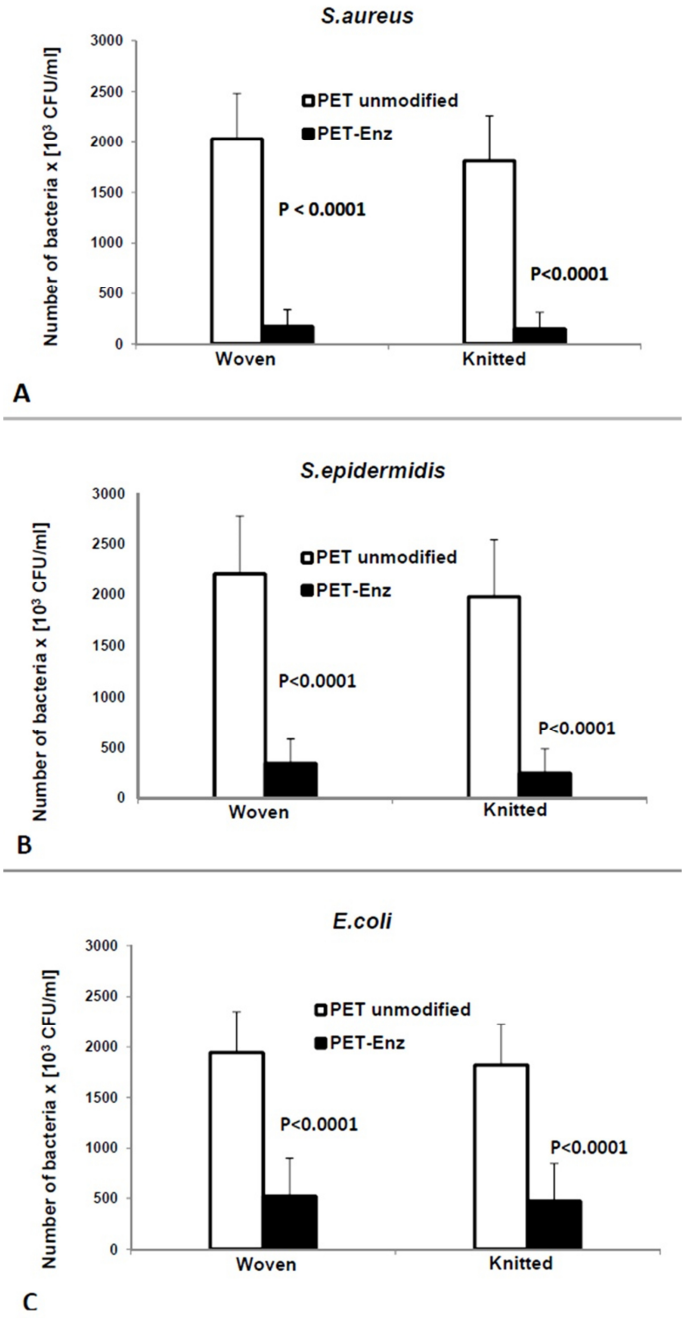

Figure 7. The number of adhered bacteria on PET and PET-Enz grafts. The number (x10^3 CFU/ml) of adhered bacteria was counted after isolation from the corresponding woven and knitted grafts. The isolated *S.aureus* (A), *S.epidermidis* (B) and *E.coli* (C) bacteria were cultured on Col-S medium. Results are given as mean ± standard deviation of three independent experiments.

Depending on the number of adhered bacteria, the anti-adhesion efficiency of PET-Enz grafts was calculated based on Equation 3. The anti-adhesion efficiencies of woven and knitted PET-Enz against *S.aureus* were 81.5 % and 80.8 % respectively, while against *S.epidermidis* were 84.5 % and 87.8 %, respectively. The anti-adhesion efficiency against *E.coli* was 73.3 % and 74.1 % for woven and knitted PET-Enz, respectively. These results correlated well with the data acquired by optical microscope after methylene blue staining (Fig. 8).

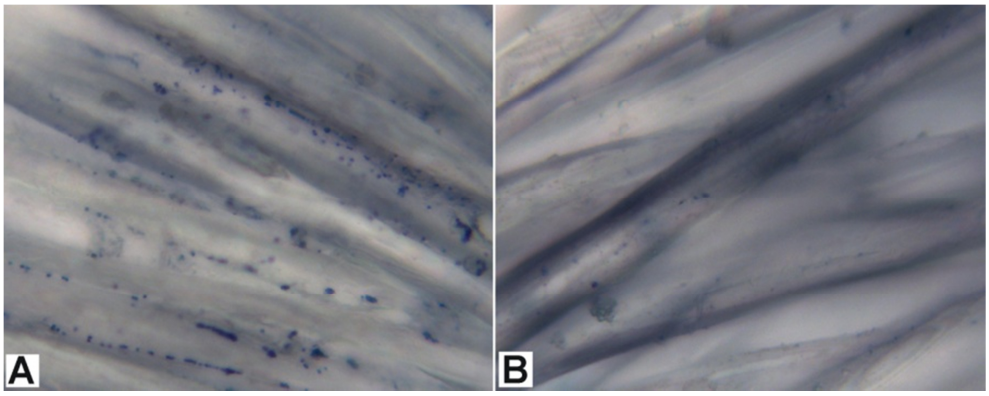

Figure 8. Micrographs of methylene blue stained, adhered *S.aureus* bacteria on woven PET (A), and on woven PET-Enz (B) grafts 24h after bacteria incubation. The PET-Enz demonstrated observable lower hospitability to bacteria than the unmodified PET.

3.6. L929 cell adhesion and growth on modified PET-Enz grafts

The biocompatibility property of PET-Enz grafts with host tissue was evaluated *in-vitro* using L929 cells. Our results revealed no effect of immobilized enzyme on cell adhesion and growth. Both unmodified PET and PET-Enz grafts were first covered with a confluent cellular monolayer after seven days as observed by SEM (Fig.9). Furthermore, the cells count adhered to PET-Enz grafts recorded no significant difference compared with unmodified PET ($p > 0.05$) (Fig.10). These results correspond well with data acquired by optical microscope after Giemsa stain (Fig.11), and confirmed that the modifications in PET-Enz grafts did not provoke any variation in cellular behavior on the grafts surfaces.

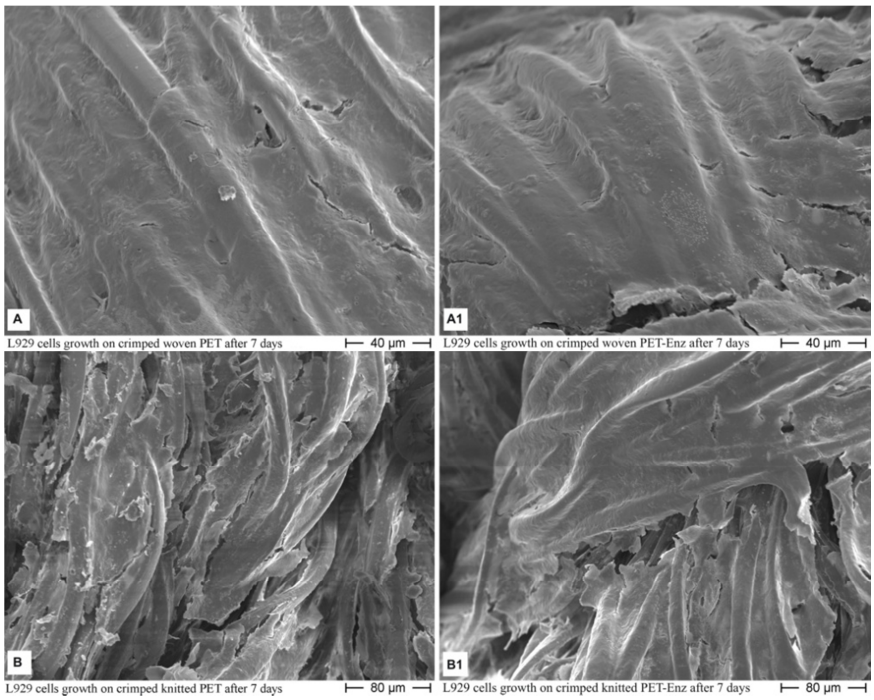

Figure 9. SEM micrographs of L929 cells grown on woven (A1) and on knitted (B1) PET-Enz grafts after 7 days. Cell growth on the corresponding unmodified woven (A) and knitted (B) PET demonstrated similar behavior.

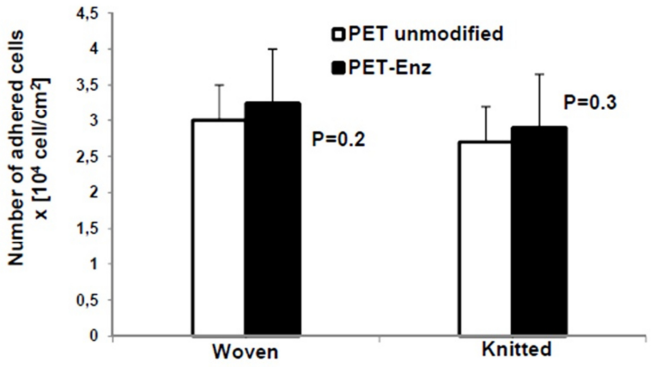

Figure 10. Number of adhered L929 cell on woven and knitted; PET-Enz (black bars) and unmodified PET (white bars). L929 cells were isolated and counted (x10^4 cell/cm^2) using a Neubauer chamber. Results are given as mean ± standard deviation of three independent experiments.

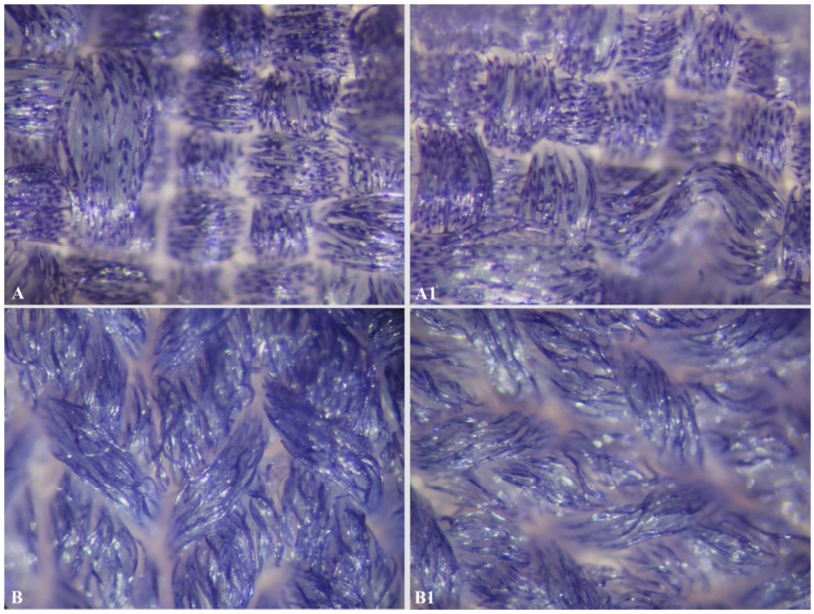

Figure 11. Micrographs of Giemsa stained, adhered L929 cells to woven (A1) and knitted (B1) PET-Enz grafts after 24h cell culturing. The cell adhesion on the corresponding unmodified; woven (A) and knitted (B) PET depicted similar profile.

4. Discussion

The impact and utility of PET grafts in vascular prostheses and heart valve sewing cuffs are limited due to the associated infections and biofilm formation [1,2,26]. The development of cardiovascular grafts resistant to biofilm formation is critical and is the major challenge to graft's long-term patency. Herein, we modified PET grafts with the lysozyme to take advantage of its capacity to lyse β (1-4) glucosidic bonds in the bacterial cell wall, resulting in an effective protection against bacterial adhesion and biofilm formation [4,19,20].

The ligation of lysozyme on surfaces of woven and knitted forms of crimped PET cardiovascular grafts was initiated by Denier reduction to produce a functional carboxyl group on the PET surface (Fig. 2) [21]. Using FTIR, the presence of the desired functional group on PET-COOH was proved by a broad shoulder of hydroxyl from the carboxyl group (Fig. 3) [27]. Additionally, enrichment of the PET surface with carboxyl groups decreased the surface hydrophobicity and static water contact

angle, hence increasing in the wettability of PET-COOH was observed. A similar observation was previously reported and studied [21]. The generated functional group on PET-COOH was conjugated to one terminal amino group of ethylendiamine via an amide bond to form PET-NH_2. The second amino group in ethylendiamine was further used as an anchor for enzyme immobilization to produce PET-Enz grafts. To avoid the reaction between the amino and carboxyl groups on the enzyme molecule, we used glutaraldehyde to activate the amino group of ethylendiamine on the surface of PET-NH_2 by the end-over end method. This ensured that the interaction occurred only on the surface of the desired graft.

Quantitative analysis of atomic concentrations obtained from XPS spectra of all grafts showed a marked reduction in carbon after Denier reduction (Table 1). This is attributed to the removal and loss of some molecules from the surface due to alkaline treatment [21]. Furthermore, PET-NH_2 contained nitrogen and had a low oxygen concentration, thus verifying the formation of amide bonds between the carboxyl group on the graft surface and the amino group in ethylendiamine molecule. The increase in nitrogen concentration on PET-Enz and the simultaneous appearance of chlorine and sulfur confirmed the successful lysozyme immobilization. This was confirmed by XPS spectra of native lysozyme and unmodified PET versus PET-Enz (Fig. 4). Corresponding to the XPS spectra of PET-Enz, the surface concentration of lysozyme as detected by the Bradford assay confirmed the successful immobilization of lysozyme on the surface.

It was critical to prove the integrity of tertiary structure and active sites after immobilization of the enzyme. Therefore, we investigated the activity of immobilized enzyme on standard *M. lysodeikticus* cells [25]. Despite a minor reduction of the immobilized enzyme activity on woven and knitted PET grafts, we confirmed the maintained activity compared to free enzyme (Fig. 5).

Accordingly, we found obvious anti-adhesion efficiency of the immobilized enzyme against three bacterial strains, namely *S.aureus, S.epidermidis*, and *E.coli* representing common Gram-positive

and Gram-negative pathogens. The results obtained using Equation 3 indicated a significant effect of PET-Enz grafts on adhesion of all bacterial strains compared to unmodified grafts. The decrease in the number of adhered bacteria on PET-Enz grafts (Fig.7) showed high statistical significance.

Despite the detected activity of lysozyme, the results demonstrated a better activity of PET-Enz grafts against Gram-positive than Gram-negative bacteria. This attributed to that lysozyme, a glycoside hydrolase, cleaves the β (1-4) glucosidic bond between N-acetylmuramic acid and N-acetyl-D-glucosamine residues in peptidoglycan of bacterial cell wall [19,20]. The targeted glucosidic β(1-4) bonds in a Gram-positive cell wall are uncovered and found in large quantities compared to the Gram-negative cell wall which contains an outer membrane [4,20]. Consequently, the enzyme on PET-Enz grafts can easily access these structures on Gram-positive bacteria, leading to pressure imbalance within the bacterial cell wall causing cell lysis and death (Fig.8) [4,19,20]. We notably reinforced our results by using a truly pathogenic Gram-positive *S. Epidermidis* bacterial strain isolated from a patient's vein catheter. The PET-Enz significantly minimized the initial adhesion of the active pathogenic bacteria, a finding that promises eradication of subsequent biofilm formation.

In contrast, the outer membrane of Gram-negative bacteria, the β (1- 4) glucosidic bonds are hidden under a layer of lipoproteins and only few exist in the pili on the cell surface. Accordingly, the enzyme activity is limited mainly to the pili and the burdened bacterial adhesion is without any effect on the wall structure [4,19,20]. In addition, peptidoglycan forms around 90 % of the dry weight of Gram-positive bacteria and only 10 % of Gram-negative strains [28]. Our PET-Enz grafts still retained activity against Gram-negative bacteria, may be explained by earlier findings stating that the irreversibly inactivated lysozyme showed antibacterial effects, suggesting that the antibacterial efficiency is not only attributable to its activity, but also to the alkaline nature of the enzyme [29].

In our study, woven grafts were more hospitable to bacterial adhesion than knitted grafts. Bacterial adhesion could, in theory, be influenced by factors other than lysozyme including graft porosity, surface tension, and electronegativity [30]. According to our results, the lower porosity of the woven PET may make it more favorable to bacteria adhesion.

To ensure complete healing after graft implantation, coating of the graft by the natural host cells is critical. This process can be disturbed by successful bacterial adhesion and biofilm formation on the grafts surface. Consequently, absence of biocompatibility at the graft tissue interface is crucial for initiation of the infection process [7]. Thus, the ability of PET-Enz grafts to support host cell adhesion and growth is decisive, which, apart from lysozyme, can be influenced by surface hydrophobicity, porosity, roughness, mechanical properties, and in particular the distance between individual filaments in the yarn. All PET grafts in our study were readily overgrown by L929 cells used as a model to evaluate the cell hosting. No significant difference in the number of attached cells after enzyme immobilization was observed. A trend towards an increased number of adhered cells on PET-Enz graft compared to unmodified grafts showed no statistical significance (Fig.10 and 11). Altogether, these findings outline conformity of the modified grafts with the biocompatibility requirements for biomedical applications.

5. Conclusion

Immobilization of lysozyme enzyme on crimped PET cardiovascular grafts inhibited the initial adhesion of Gram-positive bacteria and to a lower extent in case of Gram-negative bacteria. The acceptable biocompatibility property of modified grafts highlights our strategy as a novel biocompatible, anti-bacterial platform for PET cardiovascular grafts to decrease the incidence of graft-associated infections.

6. Acknowledgements

We would thank Prof. Dr. Juergen Janek, Institute of Physical Chemistry, Justus-Liebig-University, Giessen, Germany, for the generous support.

7. References

[1] Saby L, Laas O, Habib G, et.al. Positron emission tomography/computed tomography for diagnosis of prosthetic valve endocarditis. *J Am Coll Cardiol.*2013;61:2374-82

[2] Tayebjee M, Joy E, Sandoe J. Can implantable cardiac device infections be defined as early or late based on the cause of infection?. J Med Microbiol. 2013;62:1215-9

[3] Bergamini T, Dennis B, Dean G, Hermann K, Towene J. Infection of vascular prostheses caused by bacterial biofilms. J Vasc Surg.1988;7: 21-30

[4] Rodrigues L. Inhibition of bacterial adhesion on medical devices. In: Rodrigues L editor "Bacterial Adhesion". Goldman. 2010;351-67

[5] Coenye T, Nelis H. In vitro and in vivo model systems to study microbial biofilm formation. J Micro Meth. 2010; 83:89-105

[6] Holmes D, Mack M, Kaul S, et.al. Expert consensus document on transcatheter aortic valve replacement. *J Am Coll Cardiol.*2012;59:1200-54

[7] McCann M, Gilmore B, Gorman S. Staphylococcus epidermidis device related infections: pathogenesis and clinical management. J Pharm Pharmacol 2008;60:1551-71

[8] Oloffs A, Grosse-Siestrup C, Bisson S, et.al. Biocompatibility of silver-coated polyurethane catheters and silver-coated Dacron material. Biomaterials. 1994;15:753-55

[9] Gong S, NaNiu L, Kemp L, et al. Quaternary ammonium silane-functionalized, methacrylate resin composition with antimicrobial activities and self-repair potential. Acta Biomaterialia. 2012;8: 3270-82

[10] Bisdas T, Beckmann E, Marsch G, et.al. Prevention of vascular graft infections with antibiotic graft impregnation prior to implantation: in vitro comparison between daptomycin, rifampin and nebacetin. Eur J Vasc Endo vasc Surg. 2012;43:448-56

[11] Stortecky S, Wenaweser P, Diehm N, et.al. Percutaneous management of vascular complications in patients undergoing transcatheter aortic valve implantation*. J Am Coll Cardiol.* 2012;5:515-24

[12] Wanga J, Huangb N, Yangb P, et.al. The effects of amorphous carbon films deposited on polyethylene terephthalate on bacterial adhesion. Biomaterials. 2004;25: 3163-70

[13] Das P, Mukherjee S, Sen R. Anti-adhesive action of a marine microbial surfactant. Colloids Surf B Biointerf. 2009;71:183-6

[14] Katsikogianni M, Syndrevelis C, Amanatides E, Mataras D, Missirlis Y. Plasma treated and a-C:H coated PET performance in inhibiting bacterial adhesion. Plasma Process Polym. 2007;4:1046-51

[15] Song J, Kong H, Jang J. Bacterial adhesion inhibition of the quaternary ammonium functionalized silica nanoparticles. Colloids Surf B Biointerf.2011;82:651-6

[16] Huhtala A, Alajuuma P, Burgalassi S, et al.A collaborative evaluation of the cytotoxicity of two surfactants by using the human corneal epithelial cell line and the WST-1 test. J. Ocul. Pharmacol. 2003;19:11-21

[17] Hernandez-Richter T, Schardey H, Wittmann F, et.al. Rifampin and triclosan but not Silver is effective in preventing bacterial infection of vascular dacron graft material. Eur J Vasc Endo vasc Surg. 2003;26:550-57

[18] Goefau-Brissonnie`re O, Fabre D, Leflon-Guibout V, et.al. Comparison of the resistance to infection of rifampin-bonded gelatin-sealed and silver/collagen-coated polyester protheses. J Vasc Surg. 2002;35:1260-63

[19] Pellegrini A, Thomas U, Fellenberg R, Wild P. Bactericidal activities of lysozyme and aprotinin against Gram-negative and Gram-positive bacteria related to their basic character. J Appl Micro.1992;72:180-7

[20] Chaignon P, Sadovskaya I, Ragunah C, et.al. Susceptibility of staphylococcal biofilms to enzymatic treatments depends on their chemical composition. Appl Microbiol Biotechnol. 2007;75:125-32

[21] Kissa E. Soil release finishes-Alkali treatment of polyester fibers. In: Lewin M. Sello S. editors. Handbook of fiber science and technology, New York: Marcel Dekker.1984, p.265-89

[22] Hermanson G. Bioconjugate Reagents, Zero Length Cross linkers. In: Hermanson G editor. Bioconjugate Techniques. 2th. Elsevier.1996; p.169-86

[23] Hermanson G. Bioconjugate Reagents, homobifunctional cross-linker glutaraldehyde. In: Hermanson G editor. Bioconjugate Techniques. 2th. Elsevier.1996; p. 470-72

[24] Kang I, Kwon B, Lee J, Lee H. Immobilization of proteins on poly(methyl methacrylate) films. Biomaterials. 1993;14:787-92

[25] Shugar D. The measurement of lysozyme activity and the ultraviolet inactivation of lysozyme. Biochimica et Biophysica Acta. 1952;8:302-9

[26] Dilsizian V, Achenbach S, Narula J. Adding or selecting imaging modalities for incremental diagnosis. A case study of ^{18}FDG PET/CT in prosthetic valve endocarditis. J Am Coll Cardiol Img. 2013;6:1020-21

[27] Griffiths P, Hasseth J. Fourier transform infrared spectroscopy.2nd Wiley-Blackwell. 2007

[28] Zdzbicka-Barabas A, Mak P, Skrzypiec K, et.al. Synergistic action of galleria mellonella anionic peptide 2 and lysozyme against gram-negative bacteria.Biochimica et Biophysica Acta.2012;1818:2623-35

[29] Qiu Y, Zhang N, An Y, Wen X. Biomaterial strategies to reduce implant-associated infections. Int J Artif Organs. 2007;30:828-41

[30] Abbott A, Rutter P. The influence of ionic strength, pH and a protein layer on the interactions between Streptococcus mutans and glass surfaces. J Gen Microbiol. 1983; 129:439-45

Chapter 4

Immobilization of Hydrophilic PLGA Nanoparticles Model onto Polyethylene Terephthalate and Polytetrafluoroethylene Cardiovascular Grafts

Al Meslmani B, Bakowsky U

Prepared to submit to *Tissue Engineering* Journal

Abstract

Polyethylene terephthalate PET and expanded polytetrafluoroethylene ePTFE grafts are essentially employed to replace the damaged blood vessels and heart valves. However, the emerged critical complications after implantation prominently distract the grafts patency leading to prolonged hospitalization. We attempted to treat the main complications by local delivery of drugs from immobilized poly lactic-glycolic acid (PLGA) nanoparticles using Fluorescein isothiocyanate labeled dextran (FD) as hydrophilic model. The woven crimped PET and ePTFE were surface functionalized to produce amino group that was used as anchor site for immobilization of PLGA nanoparticles. The modified surface was characterized using electro kinetic analyzer, Fourier transform infrared spectroscopy, and scanning electron microscope. Importantly, the stability of immobilized nanoparticles on the grafts surfaces was investigated under continuous flow conditions, and the biocompatibility of the coated grafts was evaluated *in-vitro* using mouse L929 fibroblasts cell line as model. The results revealed a higher negative surface potential values (up to -41mV) at high pHs characteristic for amino functionalized PET. While the medium stretching at 2955 cm^{-1} identified the amino group on the ePTFE surface. The FD-loaded PLGA nanoparticles prepared by double emulsion-solvent evaporation method displayed homogenous monolayer without aggregation on grafts surface and maintained a satisfactory stability over 24h under continuous flow. Additionally, the nano-immobilized grafts reported no significant effect on L929 cells adhesion and growth ($P>0.05$) compared to unmodified grafts. In conclusion, immobilization of nanoparticles on PET and ePTFE provide a stable and biocompatible model for local drug delivery proposed to treat the complications after implantation and enhance the grafts patency.

Key words: PET; ePTFE; tissue engineering; PLGA nanoparticles immobilization; hydrophilic model; biocompatibility.

1. Introduction

Cardiovascular prosthesis has displayed highly successful applications and gained further a large of interest. Polyethylene terephthalate PET (Dacron®) and expanded polytetrafluoroethylene ePTFE (Teflon®) are preferably utilized to replace the damaged vessels and covering the sewing rings of heart valves and vascular stent (Fig.1).

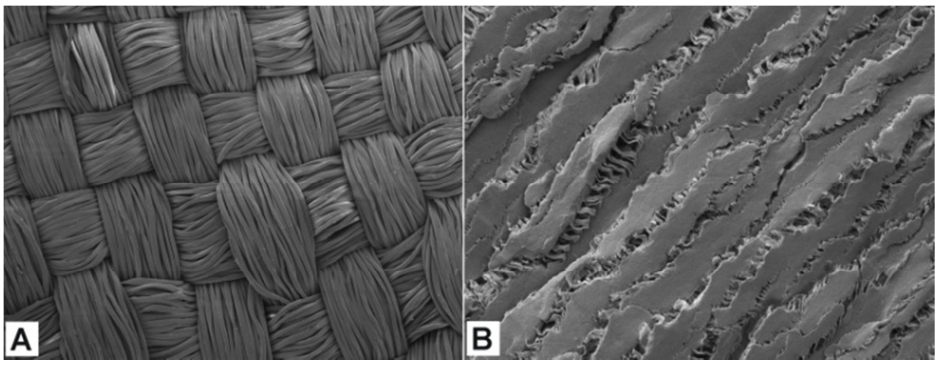

Figure 1. SEM micrographs of woven PET (A) and ePTFE (B) cardiovascular grafts. The filament in threads of woven PET are fabricated in an over-and-under pattern, while ePTFE is fabricated by heating, stretching, and extruding the polymer followed by cracking the developed grafts into non-woven porous tube.

The high flexible mechanical feature and micro-porous wall structure of PET give advantages for substitution of large diameter vessels [1,2,3], whereas the relatively inert characteristics of ePTFE offer the priority for small and medium diameter vessels intended to restore the normal blood flow and cardiac output [1-3]. However, the utilization of PET and ePTFE cardiovascular grafts was reported to associate with critical complications mainly; thrombosis, inflammation, and infection leading to prolonged hospitalization, graft failure, and patient death [4,5]. This stated low patency is still in prerequisite to improvement despite the significant progress in development of PET and ePTFE grafts using tissue engineering, antithrombotic therapy, and endothelial cell seeding. An attractive approach is the encapsulation of suitable drugs in polymer nanoparticles from which they well be locally delivered to treat the common complications [6]. Nanoparticles, as drug

delivery system, provide many considerable benefits essentially the biocompatibility, drugs protection, local application, and avoidance of drug-side effect, while the controlled and sustained release of drug to the site of effect is one of the most advanced [7-10]. In present study, the two mostly employed cardiovascular grafts; woven crimped PET and ePTFE were coated using PLGA nanoparticles loaded with Fluorescein isothiocyanate labeled dextran (FD) as hydrophilic model for wide range of medical applications. The surfaces of PET and ePTFE were modified to produce functional amino group that was used as anchor site for immobilization of PLGA nanoparticles as schematically illustrated in Figure 2. The modified surface was characterized using electro kinetic analyzer, Fourier transform infrared spectroscopy (FTIR), and scanning electron microscope (SEM). Importantly, the stability of immobilized nanoparticles on the grafts surfaces was investigated under continuous flow conditions, and the host cell behavior on the coated grafts was evaluated *in-vitro* using mouse L929 fibroblasts cell line as model.

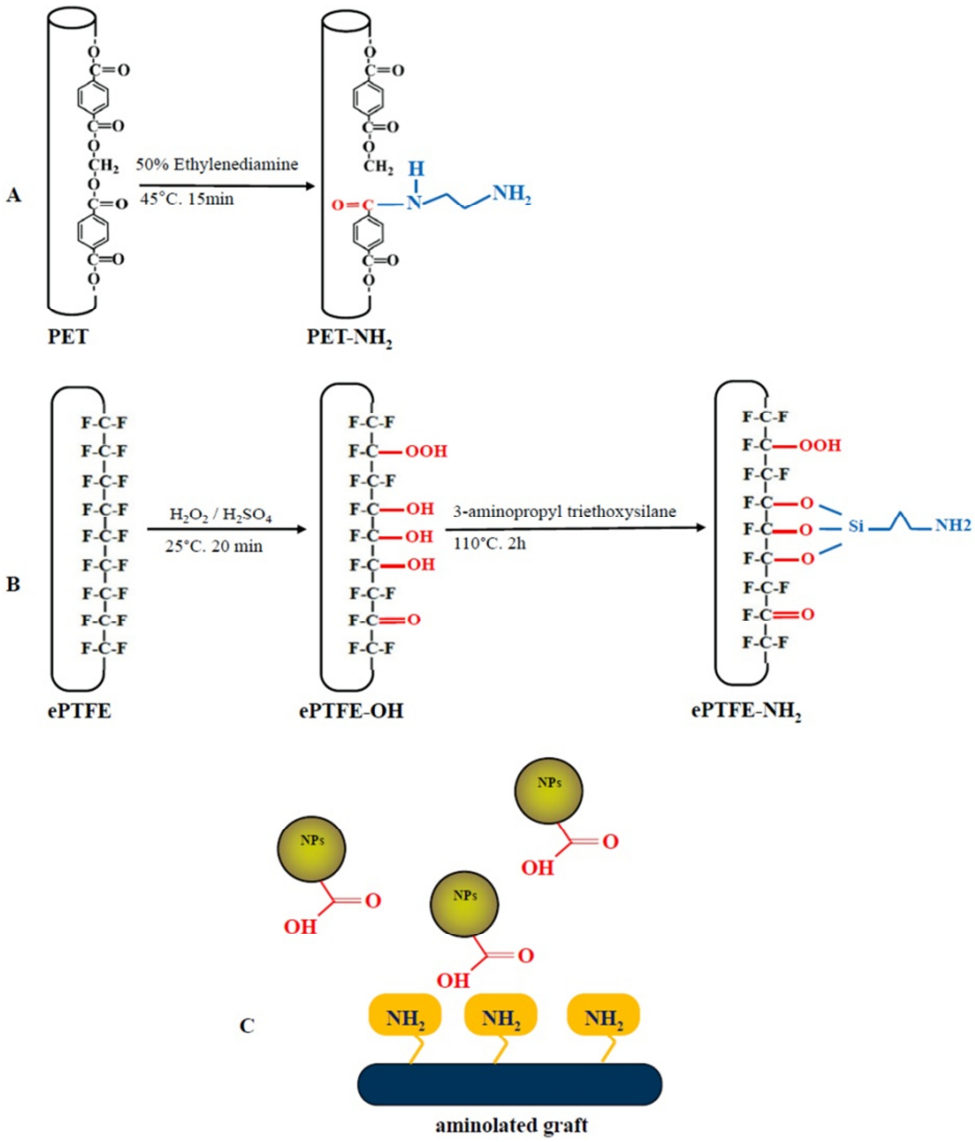

Figure 2. Schematic illustration of surface functionalization of; PET (A), ePTFE (B) and covalent immobilization of PLGA nanoparticles on the aminolated grafts (C). The intrinsic ester linkage within PET structure was cleavage by aminolysis reaction to produce functional amino group on the surface (PET-NH_2). While the oxidation reaction was utilized to introduce functional hydroxyl groups on ePTFE surface using piranha solution to yield ePTFE-OH. Subsequently, ePTFE-NH_2 was obtained by grafting 3-aminopropyl triethoxysilane on ePTFE-OH. The covalent immobilization of the nanoparticles was completed between the amino group on the aminolated graft and the carboxyl group on the PLGA nanoparticles using cross-linker glutaraldehyde.

2. Material and method

2.1. Material

Crimped woven polyethylene terephthalate PET (Dacron®,14 mm internal diameter, 30 cm length, 12 filaments per yarn bundle), and expanded polytetrafluoroethylene ePTFE (Teflon®, 10 mm internal diameter, 20 cm length, 0,35 mm wall thickness) were kindly provided by Vascutek GmbH, Germany. Poly lactic-glycolic acid (PLGA RG503H) was bought from Boehringer Ingelheim, Germany. Fluorescein isothiocyanate labeled dextran (FD 10S), Ethylenediamine, glutaraldehyde, 3-aminopropyl Triethoxysilane ≥ 98%, were purchased from Sigma Aldrich, Germany. 30 % H_2O_2 and Tween® 80 were acquired from Carl Roth GmbH, Germany. Paraformaldehyde and Giemsa stain were bought from Merck, Germany. Mouse L929 fibroblasts cells line were obtained from DSMZ, Germany. Dulbecco's Modified Eagle's Medium (DMEM), Earle's Balanced Salt Solution (EBSS), Gamma Irradiated Fetal Bovine Serum (FBS), trypsin, streptomycin, penicillin, and amphotericin B were purchased from PAA Laboratories GmbH, Germany. L-glutamine was bought from VWR, Germany. All other used chemicals were of analytical reagent grade.

2.2. Method

2.2.1. Surface functionalization of PET and ePTFE

In the present study, two different types of cardiovascular grafts, crimped woven polyethylene terephthalate (PET) and expanded polytetrafluoroethylene (ePTFE) were used for surface modification (Fig. 1). Each step in the subsequent experiments was done for each type.

Initially, slices from PET and ePTFE grafts (2x2 cm^2) were cleaned in 50 % ethanol under sonication (Sonorex RK 100H, Bandelin, Germany) for 15 minutes. Subsequently, the grafts were rinsed several times with distilled water under sonication and oven dried at 55°C for 2h before they were functionalized to produce reactive amino group on the surface (Fig. 2). The PET graft was surface

functionalized using modified aminolysis reaction according to the previously reported method [11]. The cleaned PET graft was dipped into 20 ml of 50 % ethylendiamine at 45°C for 15 minutes to selectively cleave the ester linkage within PET surface resulting in free amino group (Fig. 2A).The aminolated PET graft was thoroughly rinsed with distilled water under sonication and oven dried at 55°C for 2h. The obtained graft is abbreviated as PET-NH_2. Otherwise, the cleaned ePTFE graft was pre-oxidized using Piranha solution (30 % H_2O_2 and 96 % H_2SO_4 at 1:1 v/v) for 20 minutes at room temperature to produce functional hydroxyl groups [12], the oxidized graft was rinsed thoroughly with distilled water and oven dried at 100°C for 1h. Afterwards, the dried graft was dipped into 20 ml chloroform solution of 3-aminopropyl triethoxysilane (20 µl/10 ml) for 2h. The graft was rinsed in chloroform and oven dried at 110°C for 2h to produce functional amino group on the surface (Fig. 2B). The obtained graft is abbreviated as ePTFE-NH_2.

2.2.2. Surface characterization

2.2.2.1. Measurement of surface potential of PET-NH_2

Surface potential of PET-NH_2 was measured using an electro kinetic analyzer (Sur PASS/Fa. A. PAAR, Austria) to detect the desired functional group on the surface in comparison to unmodified PET. The zeta potential/pH value function was measured in 1mM NaCl solution at pressure 300 mbar and titration solutions: 0,1 M HCl and 0,1 M NaOH in a cylindrical measuring chamber particular for determination of the zeta potential of textile and fibers as shown in Figure 3A. Four potentials were measured at each pH value and two measurements per streaming direction of the electrolyte. The potential /pH function was expressed as the mean value of repetitive measurements.

2.2.2.2. FTIR Analysis

An FTIR (Alpha, Bruker, Germany) was utilized to detect the functional groups on the surface of oxidized and aminolated ePTFE compared to unmodified ePTFE. The analysis was performed at 24 scans and at resolution of 4 cm^{-1}. Scanning was conducted in the mid-IR range from 400-4000 cm^{-1}. Three measurements were carried out for each graft.

2.2.3. PLGA nanoparticles synthesis

PLGA nanoparticles (NPs) were prepared using adapted *double emulsion-solvent evaporation* method (W1/O/W2) as previously reported [13]. Briefly, 250 µl of aqueous FD (25 mg/ml) was emulsified in 5 ml organic phase of PLGA solution (50 mg) in chloroform/acetone (3:2 v/v) using a high-speed homogenizer (Ultra-Turrax T25, IKA, Germany) operating at 10,000 rpm for 30 sec to yield the primary W_1/O emulsion. The obtained primary W_1/O emulsion was then directly dropped into 20 ml of continuous aqueous phase (W2) containing 0.1 % (w/v) Tween®80 using an electronic pump (Perfusor, Braun, Germany) at a constant flow rate of 1 ml/min and was continuously gently magnetic stirred at 300 rpm under a fume hood for 4h to allow the solvent evaporation and nanoparticles hardening. The obtained nanoparticles were collected by centrifugation at 15,000 rpm for 10 minutes and washed twice with deionized water. After separation, the nanoparticles were re-suspended and were directly used for particles characterization and immobilization. For advanced study, the prepared nanoparticles were freeze-dried and stored at -20°C. Unloaded PLGA nanoparticles as control were also prepared without FD using the same procedure.

2.2.4.Nanoparticles characterization

2.2.4.1. Size and zeta potential measurements

The average size of PLGA nanoparticles, size distribution and the Zeta potential distribution were determined by MasterSizer (Zetasizer Nano-ZS, Malvern Instruments. UK) based on a laser light scattering technique. The samples was diluted in phosphate buffered saline (PBS, 0.5 M. pH 7.4) at 1/100 ratio and vortex before the analysis was completed at; 25°C, refractive index 1.59, medium refractive index 1.330, medium viscosity 0.88 mPas, dielectric constant 78.5, and at 17° scattering angle. The software DTS v 6.2 was used to calculate the particle mean diameter (Z-Ave), poly dispersity index (PDI) and average potential value (ζ potential). A Smoluchowsky constant F (Ka) of 1.5 was used to achieve zeta potential value from electrophoretic mobility. Each size and zeta measurement was performed with multiple runs, and all measurements were performed in triplicate directly after nanoparticle preparation.

2.2.4.2. Encapsulation efficiency

The concentration of loaded FD in the synthesized NPs was determined after extraction as described previously [13]. Twenty milligram from the freeze-dried NPs were dissolved in 1 ml chloroform/acetone, followed by addition of 4 ml PBS at pH 7.4 and agitated using orbital shaker maintained at 37 ◦C for 15 h at 30 rpm. The concentration of extracted FD in the PBS buffer was determined by fluorescent spectrophotometer (LS 50B Luminescence Spectrometer, Perkin-Elmer, Germany) at excitation wavelength λ_e 494nm and emission λ_m510 nm. A calibration curve was arranged using standard solutions prepared by dissolving 20 mg of unloaded NPs in 1 ml chloroform/acetone mixed with increasing amounts of FD in 4 ml PBS at pH 7.4. The encapsulation efficiency was calculated from the mean value of three repeated experiments using Equation (1):

$$Encapsulation\ efficiency\ = \left(\frac{\text{total FD} - \text{measured FD}}{\text{total FD}}\right) \times 100\% \qquad (1)$$

2.2.5. Immobilization of the NPs on PET-NH_2 and ePTFE-NH_2

PLGA nanoparticles were covalently immobilized onto PET-NH_2 and ePTFE-NH_2 using homobifunctional cross-linker glutaraldehyde as described elsewhere [14] and schematically illustrated in Figure 2C. Briefly, the aminolated PET-NH_2 and ePTFE-NH_2 were immersed in 10 ml of sodium phosphate buffer (0.1 M, pH 6.8) containing 150 µl of 50 % glutaraldehyde and incubated at 4°C under gentle stirring at 50 rpm/min for 3h to activate the amino groups on the surface. Afterwards, the grafts were rinsed with distilled water under sonication for 5 minutes and dipped into 10 ml of NPs suspension in phosphate buffered saline (PBS, 0.5 M, pH 7.4). The reaction between the activated amino group on the graft surface and the carboxyl group on the NPs was completed overnight at 4°C. Finally, the grafts were rinsed with distilled water and dried under dust-free airflow. The obtained grafts were stored at 4°C and are abbreviated as PET-NPs and ePTFE-NPs, respectively.

2.2.6. Stability of immobilized NPs under continuous flow condition

The stability of immobilized NPs on graft surface was performed under continuous flow condition. Slices (0.5x0.5 cm^2) of PET-NPs and ePTFE- NPs grafts were held tightly onto an inner side of silicone tube. The silicone tube was connected to a pump (Pump drive 5001, Heidolph, Germany) using silicone rubber pump tube (strength 1.6, Carl Roth, Germany). The prepared grafts attached-silicone tube and saline solution were incubated in water bath at 37°C for 15 minutes to achieve temperature equilibration. The flow rate was operated using saline at 100 rpm/min for 24h. A graft sample was removed every 6h, rinsed with distilled water and dried followed by sputter coating with a thin film of platinum via Sputter coater (S150B, Edwards, England) under vacuum using an inert argon dusting gas at 30 mA for 120 seconds before they were observed by scanning electron microscope.

2.2.7. Biocompatibility study

2.2.7.1. L929 cells adhesion and growth on PET-NPs and ePTFE-NPs

The biocompatibility of PET-NPs and ePTFE-NPs with host cells was evaluated *in vitro* using mouse L929 fibroblast cell line as model. Slices (0.5x0.5 cm^2) of PET-NPs, ePTFE-NPs and unmodified PET, ePTFE were fixed onto sterile glass chip using inert, cell-nontoxic silicon glue and placed in a 12 well culture plate. L929 cells were seeded at a density of $1x10^5$ cells per well in 2 ml of DMEM medium, supplemented with 10 % FBS, 1 mM L-glutamine, penicillin (10.000 U/ml), streptomycin (10 µl/ml) and amphotericin B (25 µg/ml). The cultured grafts were incubated at 37°C and at 8.5 % CO_2. The medium was changed daily for 9 consecutive days, and a graft sample was taken out daily, rinsed twice with PBS at pH 7.4 and immersed in 1% paraformaldehyde for 1h to fix the cells. The adhered cells after 24h culturing were stained by Giemsa stain (5 %) for 10h followed by color differentiation using 0.5 % acetic acid and dried at room temperature under dust free-airflow. The grafts were optically observed using microscope (Stemi 2000-C, Carl Zeiss, Germany) equipped with a camera (Canon G10, Japan). Furthermore, the fixed grown cells on grafts were observed using scanning electron microscopy after washing, drying, and preparation as previously described.

2.2.7.2. Counting of L929 cells adhered to PET-NPs and ePTFE-NPs

The number of adhered cells onto PET-NPs, ePTFE-NPs was counted 24h after cell seeding in comparison to unmodified PET and ePTFE grafts. The medium was removed and the grafts were rinsed twice with sterile PBS at pH 7.4. The rinsed grafts were detached from the glass chips and dipped into EBSS buffer solution without Ca^{+2} or Mg^{+2} for 5 minutes at 25°C, followed by incubation in 1 ml trypsin solution (5 mg/ml) at 37°C for 15 minutes to remove the adhered cells

from the graft surface. The isolated cells were immediately counted using a Neubauer chamber. The experiment was repeated in triplicate for each graft.

2.2.8. Scanning electron microscope

A scanning electron microscope SEM (Jeol JSM 7500 F. Japan) was used to assess the stability of immobilized NPs after exposed to flow condition, and to observe the grown cells on PET-NPs, ePTFE-NPs grafts in comparison to unmodified grafts. The tested grafts were mounted onto metal dishes using double-sided adhesive tape and conductive carbonic cement. The platinum sputter coating was performed as previously described. All images were taken at 5 kV under the same magnification for comparison studies.

2.2.9.Statistically analysis

The data were expressed as means ± standard deviations of representative experiments. Statistical comparisons were made by analysis of T-distribution. The difference was considered to be significant at $p < 0.05$ for all statistical evaluations.

3. Result

3.1. Surface characterization

FD-loaded PLGA nanoparticles as hydrophilic model were prepared for nano monolayer coating of crimped woven PET and expanded PTFE grafts. The grafts surfaces were modified to introduce functional amino groups used as anchor sites for covalent immobilization of the NPs (Fig.2). The PET was directly aminolyized by ethylendiamine, while ePTFE was pre-oxidized by Piranha solution to produce hydroxyl groups used for coupling of 3-aminopropyl triethoxysilane as a source of amino group on the surface.

The electro kinetic analyzer was used to detect the presence of the desirable reactive amino group on the functionalized PET-NH_2 based on surface zeta potential. The potential /pH function of unmodified PET and PET-NH_2 are depicted in Figure 3B. Negative surface potential was detected for all studied grafts. Notably, higher negative zeta potential values (up to -41mV) at high pHs was characteristic for PET-NH_2 compared to irregular function with a drastic reduced potential detected on unmodified PET identified the presence of basic amino group on the surface.

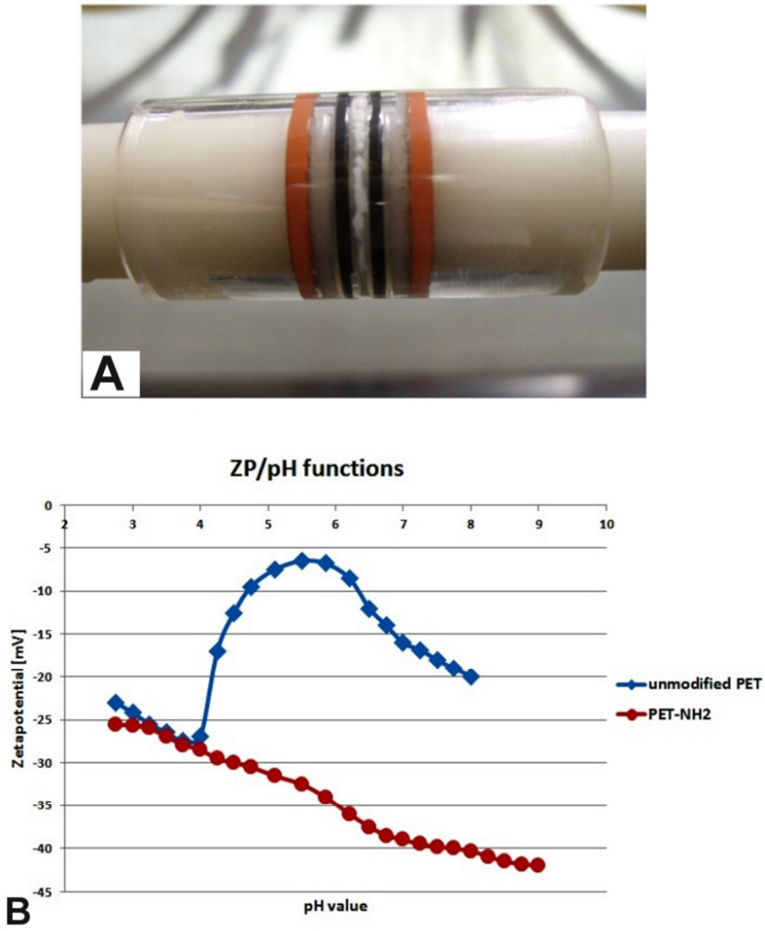

Figure 3. Measurement of the surface potential (A), and the zeta potential/pH value function of PET-NH_2 and unmodified PET (B). The PET sample was cut into slices and placed in a cylindrical measuring chamber. The measurement was carried out in 1mM NaCl solution at pressure 300 mbar and titration solutions: 0,1M HCl and 0,1M NaOH. The basic amino group on PET-NH_2 demonstrated higher negative zeta potential values at high pHs compared to irregular function with a drastic reduced potential detected on unmodified PET. Results are given as mean value of four measurements at each pH value.

Otherwise, the oxidized ePTFE-OH and aminolated ePTFE-NH_2 were characterized by FTIR to detect the presence of the functional groups on the surface. FTIR spectra of unmodified ePTFE, ePTFE-OH and ePTFE-NH_2 are depicted in Figure 4. The spectra of unmodified ePTFE surface showed a substantial strong intensity of (C-F) bonds indicated by the stretching vibration at 1000-1400 cm^{-1}. Additionally, a broad shoulder appeared at 3000-3500 cm^{-1} in the oxidized ePTFE-OH corresponding to hydroxyl group, and a medium intensity of (C=O) bonds detected by stretching vibrations at 1682 cm^{-1}. The absence of hydroxyl stretching vibration in the ePTFE-NH_2 accompanied with medium stretching at 2955 cm^{-1} recognized the desired amino group on the surface.

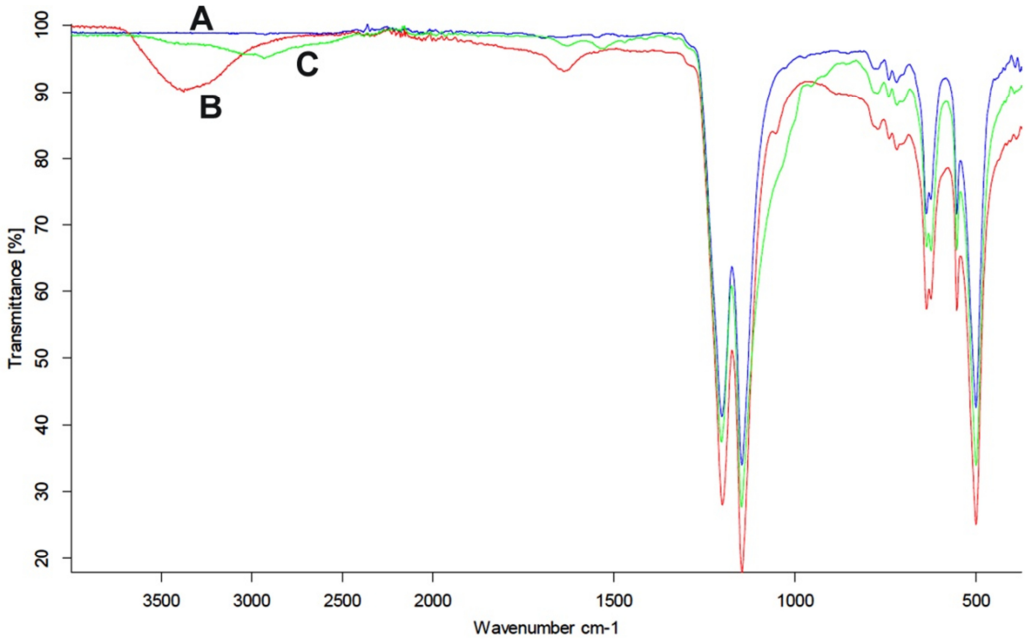

Figure 4. FTIR spectra of ePTFE-NH_2 (C), and ePTFE-OH (B) compared to unmodified ePTFE (A) grafts. The selective absorption of light in the region of the hydroxyl group at 3000-3500 cm^{-1} and of carbonyl group at 1682 cm^{-1} in ePTFE-OH is illustrated. While the medium stretching at 2955 cm^{-1} recognized the desired amino group on the surface of ePTFE-NH_2.

3.2. Nanoparticles characterization

PLGA nanoparticles were obtained be *double emulsion-solvent evaporation* method and directly characterized after syntheses. The size and zeta potential characterization of FD-loaded PLGA NPs and unloaded are illustrated in table 1. The produced loaded particles displayed an increased mean size and polydispersity index comparing to the unloaded particles without effect on the

average potential value. Furthermore, the encapsulation efficiency of FD in the NPs prepared at 1:10 FD/polymer rate manifested 41.3±3.8 %.

Table 1. Size and zeta potential characterization of unloaded and FD-loaded PLGA NPs

	Particle size nm	PDI*	ζ potential
Unloaded PLGA NPs	151.4±2.1	0.11±0.05	-23.3 ± 0.6
FD-loaded PLGA NPs	178.2±2.9	0.17±0.08	-22.6 ± 0.8

Data are shown as mean ± standard deviation from three experiments
*PDI: polydispersity index

3.3. NPs immobilization and stability evaluation under continuance flow condition

The topographic features of the NPs-immobilized grafts were visualized using SEM compared to unmodified grafts. The SEM observation detailed a homogenous monolayer of NPs on PET-NPs and ePTFE-NPs grafts as shown in Figure 5.

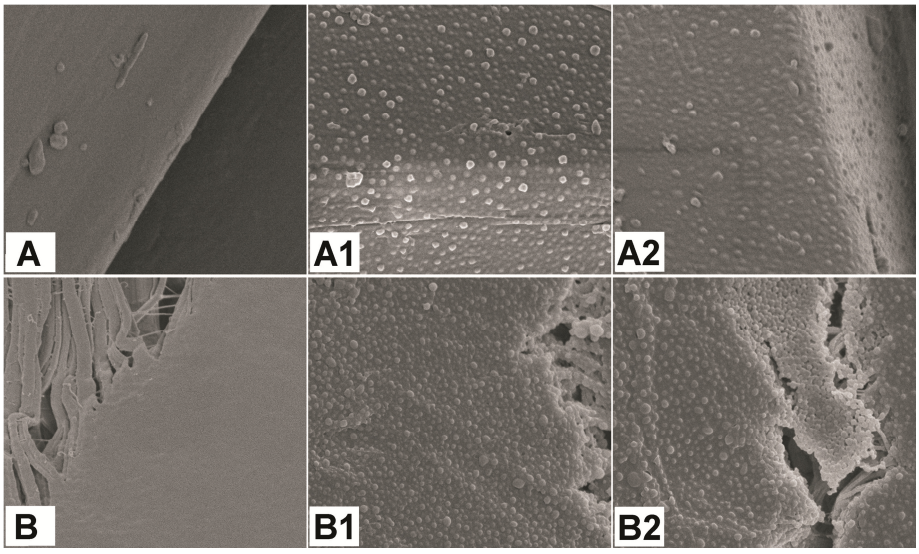

Figure 5. SEM micrographs of immobilized nanoparticles on PET-NPs and ePTFE-NPs (A1 and B1, respectively) compared to unmodified; PET (A) and ePTFE (B) grafts, and to the nano-immobilized grafts after continuous flow for 24h (A2 and B2, respectively). A homogenous monolayer of spherical, smooth surface nanoparticles on PET-NPs and ePTFE-NPs grafts was detected without aggregation on the surface. The identified nanoparticles displayed an observed stability under continuous flow over 24h.

The particles displayed a spherical shape with a smooth surface and no aggregation on the grafts surface was observed. Furthermore, the immobilized NPs on PET-NPs and ePTFE-NPs demonstrated satisfactory stability under appropriate human-mimic continuous flow conditions for 24h as both PET-NPs and ePTFE-NPs maintained an obviously monolayer coat of NPs.

3.4. L929 cells adhesion and growth on PET-NPs and ePTFE-NPs

The biocompatibility property of PET-NPs and ePTFE-NPs grafts with host tissue was evaluated *in-vitro* using L929 cells. Our results revealed no effect of immobilized nanoparticles on cell adhesion and growth comparing to unmodified PET and ePTFE grafts. The primary optical micrographs of adhered cells stained with Giemsa 24h after cell seeding demonstrated normal cell behavior on PET-NPs and ePTFE-NPs (Fig.6).

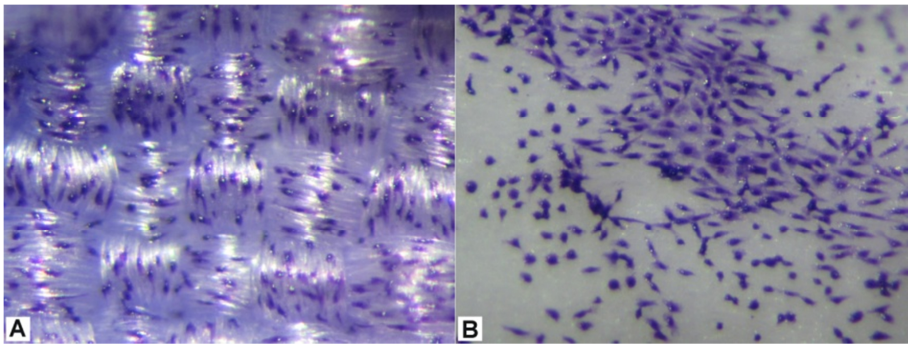

Figure 6. Micrographs of Giemsa stained, adhered L929 cells on PET-NPs (A) and ePTFE-NPs (B) grafts after 24h cell culture. The nano-immobilized grafts obviously supported cell adhesion.

These results correspond well with data acquired by counting the adhered cells to NPs-immobilized grafts which recorded no significant difference compared to unmodified grafts ($p > 0.05$) (Fig.7). Furthermore, both unmodified and NPs -immobilized grafts were first overgrown with a confluent cellular monolayer after seven days of cell culturing, that confirmed the biocompatibility of PET-NPs and ePTFE-NPs which did not provoke any variation in cellular adhesion and growth of the host.

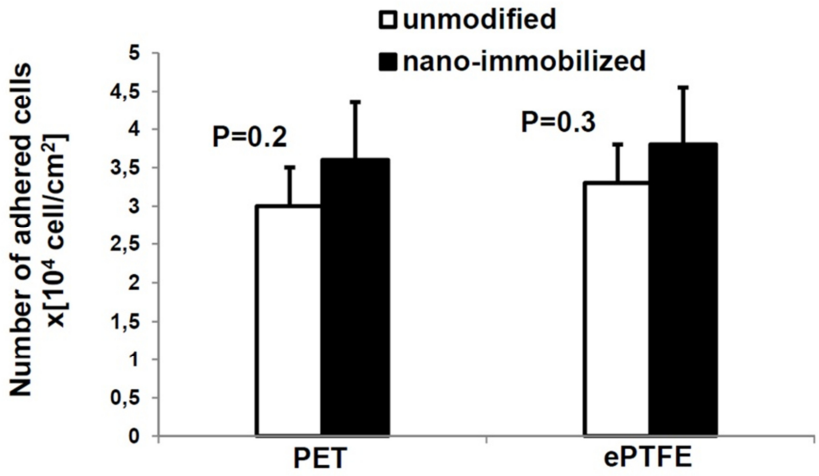

Figure 7. Number of adhered L929 cell on PET-NPs and ePTFE-NPs (black bars) in comparison to unmodified PET and ePTFE (white bars). L929 cells were isolated and counted ($x10^4$ cell/cm^2) using a Neubauer chamber. Results are given as mean ± standard deviation of three independent experiments.

4. Discussion:

The patency of synthetic cardiovascular grafts made of PET and ePTFE is limited due to many complications after implantation [4,5]. Considering the reported success to the vascular prostheses and artificial heart valve, the used PET and ePTFE grafts have a potential for thrombus and bacterial infections that obviously restricted the long-term patency [5,6]. Wherefore, we aimed to support the grafts patency by local delivery of hydrophilic drugs using PLGA nanoparticles as carrier and FD as water soluble drug model. The NPs were covalently immobilized

to PET and ePTFE grafts after surface functionalization (Fig. 2). The functional amino group was directly produced on PET by aminolysis reaction using ethylendiamine to selectively cleavage of the ester bond resulting in PET-NH_2 [11]. The produced amino group on PET-NH_2 was proven based on the variation of surface potential realized by evaluating the pH-dependence (potential/pH functions) of the specific dissociable groups on the surface (Fig. 3). The aminolated graft demonstrated a negative potential over a wide pH range due to ionization of the surface amino group with an isoelectric point at around pH 7-8 conforming the successful amino functionalization [15].

While ePTFE was amino-functionalized by grafting 3-aminopropyl triethoxysilane to the previously produced hydroxyl groups using Piranha solution to yield ePTFE-NH_2 [12]. The pre-oxidation process and the subsequent introducing of amino group on ePTFE was proven using FTIR corresponding to the broad shoulder in the range of hydroxyl group and the definite band of amino group [16] (Fig. 4). Afterwards, the produced amino groups on the surfaces were activated by glutaraldehyde and used further as anchor sites for covalent coupling to the carboxyl group in the PLGA nanoparticles. The nanoparticles were synthesized from biodegradable PLGA polymer for local, controlled release using FD as hydrophilic model, taking advantages of the high capacity of hydrophilic drugs by double emulsion-solvent evaporation method and the stability of obtained particles [13]. Additionally, for immobilization purpose, the intrinsic carboxyl groups in the PLGA made it our first choice for nanoparticles syntheses along with Tween®80 as surfactant at suitable concentration to stabilize the nano suspension. The surfactant adsorb at the particles surface between the superficially COOH groups leaving them free and available for coupling [17]. The marked increase in the size of the obtained FD-loaded NPs in comparison to unloaded NPs is attributed to expansion of polymeric matrix within FD encapsulation [13]. However, all particles seemed to possess the ideal surface charge suggesting that the surfactant and/or FD have no

masking effect on the superficial carboxylic groups [18]. However, the efficiency of NPs coating for cardiovascular grafts entails the stability during the massive blood flow to secure the local controlled release of encapsulated drug. Therefore, the stability of immobilized NPs was evaluated *in-vitro* under human-mimic conditions (Fig. 5). The surface visualization manifested permanence of monolayer coat on both PET-NPs and ePTFE-NPs after 24h substantial continuous flow providing an appropriate carrier for controlled drug delivery over the tested time. Nonetheless, the biocompatibility of the implanted grafts with natural host cells is critical and essential to ensure complete healing after graft implantation by comprehensive coverage with host cells. The ability of PET-NPs and ePTFE-NPs to support host cell adhesion and growth is decisive and displayed dependency on surface topography, hydrophobicity, and porosity [19,20]. Interestingly, the tested grafts were readily overgrown by L929 cells and shown no significant difference in the number of adhered cells on PET-NPs and ePTFE-NPs compared to unmodified grafts (Fig. 7). Furthermore, the hosting ability of the modified grafts was additionally confirmed by differential cell staining using Giemsa stain (Fig. 6). This highly emphasized the conformity of the nano-immobilized grafts with the biocompatibility requirements for biomedical applications.

5. Conclusion

Immobilization of nanoparticles on crimped woven PET and expanded PTFE cardiovascular grafts provide a stable and biocompatible drug carrier that highlights our strategy as an effective local, controlled drug delivery model to treat the most common complications after implantation and hence enhance the grafts patency.

6. Acknowledgements

We would thank Dr. Marion Frant, Institute for Bioprocessing and Analytical Measurement Techniques (iba), Heilbad Heiligenstadt, Germany for kind support.

7. References

[1] Williams S, Kosnik P, Kleinert L, Vossman E, Lye K, Shine M. Adipose stromal vascular fraction cells isolated using an automated point of care system improves the patency of expanded Polytetrafluoroethylene vascular grafts. Tissue Eng Part A. 2013;19:1295-02

[2] Wang X, Lin P, Yao Q, Chen C. Development of small-diameter vascular grafts. World J Surg 2007;31:682-9

[3] Voegele-Kadletz M, Wolner E. Bio artificial surfaces-blood surface interaction. Mater Sci and Eng. 2011;31:1195-200

[4] Tayebjee M, Joy E, Sandoe J. Can implantable cardiac device infections be defined as early or late based on the cause of infection?. J Med Microbiol. 2013;62:1215-9

[5] Dimitrievska S, Maire M, Diaz-Quijada G, Robitaille L, Ajji A, Yahia L, et al. Low thrombogenicity coating of nonwoven PET fiber structures for vascular grafts. Macromol Biosci. 2011;11:493

[6] Wickline S, Neubauer A, Winter P, Caruthers S, Lanza G. Applications of nanotechnology to atherosclerosis, thrombosis, and vascular biology, Arterioscler Thromb Vasc Biol 2006,26:435-41

[7] Sahoo SK, Labhasetwar V. Nanotech approaches to drug delivery and imaging. Drug Discov. 2003;8:1112-20

[8] Wickline SA, Neubauer A, Winter P, Caruthers S, Lanza G. Applications of nanotechnology to atherosclerosis, thrombosis, and vascular biology. Arterioscler.Thromb.Vasc. Biol 2006;26:435-41

[9] Whitesides GM. Nanoscience, nanotechnology, and chemistry. Small 2005;1:172-9

[10] Liu Y, Miyoshi H, Nakamura M. Nanomedicine for drug delivery and imaging. Int. J. Cancer 2007;120:2527-37

[11] Muthuvijayan V, Gu J, Lewis R. Analysis of functionalized polyethylene terephthalate with immobilized NTPDase and cysteine. ActaBiomaterialia. 2009;5:3382-93

[12] Löhbach C, Bakowsky U, Kneuer C, Jahn D, Graeter T, Schäfers HJ, Lehr CM. Wet chemical modification of PTFE implant surfaces with a specific cell adhesion molecule. Chem. Commun. 2002;2568-69

[13] Mao S, Xu J, Cai C, Germershaus O, Schaper A, Kissel T. Effect of WOW process parameters on morphology and burst release of FITC-dextran loaded PLGA microspheres. Int. J. Pharm. 2007;334:137-48

[14] Hermanson G. Bioconjugate reagents, homobifunctional cross-linker glutaraldehyde. In: Hermanson G editor. Bioconjugate Techniques. 2th. Elsevier. 1996; p.470-72

[15] Butterworth M, Corrad R, Johal J, Lascelles F, Maeda S, Armes P. Zeta potential measurements on conducting polymer-inorganic oxide nanocomposite particles. J. Coll&interfac. 1995;174:510-17
[16] Griffiths P, Hasseth J. Fourier transform infrared spectroscopy.2nd Wiley-Blackwell. 2007
[17] Giannavola C, Bucolo C, Maltese A, Paolino D, Vandelli MA, Puglisi G, et.al. Influence of preparation conditions on acyclovirloadedpoly-d,l-lactic acid nanospheres and effect of PEG coating on ocular drug bioavailability. Pharm. Res. 2003;20:584-90
[18] Muller RH. Charge determinations. In: Muller RH editor, Colloidal carriers for controlled drug delivery and targeting modification, characterization and in vivo. CRC, Baca Raton.1991
[19] Lei Y, Remy M, Labrugere C, Durrieu M. Peptide immobilization on polyethylene terephthalate surfaces to study specific endothelial cell adhesion, spreading and migration. J Mater Sci Mater Med. 2012;23:2761
[20] Yu F, Mücklich F, Li P, Shen H, Lehr C, Bakowsky U. In vitro cell response to a polymer surface micropatterned by laser interference lithography. Biomacromolecules. 2005;6:1160

Chapter 5

Development of Thrombus-resistant and Cell Compatible Crimped Polyethylene Terephthalate Cardiovascular Grafts Using Surface Co-immobilized Heparin and Collagen

Al Meslmani B, Strehlow B, Mohr E, Mahmoud G, Leichtweiß T, Bakowsky U.

Submitted to Journal of *Colloid and Surfaces B: Biointerfaces*

Abstract

Short-term patency of polyethylene terephthalate (PET) cardiovascular grafts is determined mainly by the inherent thrombogenicity and improper endothelialization following grafts implantation. The aim of the present study was to immobilize heparin to develop thrombus resistant grafts. Additionally, collagen was co-immobilized to enhance the host cell compatibility. The synthetic woven and knitted forms of crimped PET grafts were surface modified by Denier reduction to produce functional carboxyl groups. The produced groups were used as anchor sites for covalent immobilization of heparin or co-immobilization of heparin/collagen by the end-point method. The modified surface was characterized using Fourier transform infrared spectroscopy and X-ray photoelectron spectroscopy. The biological activity of immobilized molecules was investigated *in vitro* using direct blood coagulation test, and platelets deposition under flow condition. Furthermore, the biocompatibility of modified grafts with host cells was assessed using L929 cell as model. All modified grafts showed significant resistance against fibrin and clot formation. The number of deposited platelets on heparin-immobilized woven and knitted grafts obviously decreased by 3 fold and 2.8 fold per unit surface area respectively, while the heparin/collagen co-immobilized grafts showed only a decrease by 1.7 and 1.8 fold compared to unmodified PET. Heparin-immobilized grafts reported no significant effect on L929 cells adhesion and growth ($P>0.05$), conversely, collagen co-immobilization considerably increased cell adhesion almost ~ 1.3 fold and 2 fold per unit surface area for woven and knitted grafts respectively. Our results emphasize that immobilization of heparin minimized the inherent thrombogenicity of the PET grafts. The simultaneous co-immobilization of collagen supported host cell adhesion and growth required for the grafts biocompatibility.

1. Introduction

Polyethylene terephthalate (PET) Dacron® grafts are promising alternatives for autologous grafts. The wide cardiovascular applications of PET grafts including; vascular prostheses [1,2], heart valve sewing cuffs [3,4], and surgical meshes [5] are associated with haemocompatibility problems [6,7]. One of the prominent shortcomings of PET is the substantial thrombogenic property that impaired ultimately the patency of the graft and hence, the patient`s life quality. After implantation, the blood coagulation cascade is mostly triggered at the graft-blood interface by the adsorption of plasma proteins on the graft surface followed by activation of platelets and complements in blood serum, and finally leads to formation of non-soluble fibrin and thrombosis [6,7]. However, the previous studies suggest that the sequences of protein deposition, fibrin formation, and platelets aggregation on graft surface showed dependency mainly on the surface properties [7].

One potential strategy to reduce the thrombogenicity of prosthetic material is by immobilization of bioactive molecules to the graft surface. Recently, several studies have reported to the coating of heparin on surface as an effective method to create a thrombus-resistant graft [8-10]. Heparin, an anticoagulant non-branched mucopolysaccharide, prevents blood coagulation cascade by two ways; either directly by capture and inactivation of thrombin, or indirectly by stimulation of anti-thrombin enzyme (AT III). Thrombin is an enzyme controls the conversion of soluble fibrinogen to precipitated fibrin fibers [11]. Additionally, a successful way to limit graft failure is to provide rapid, uniform, and complete coverage with an endothelial layer. Accordingly, cell growth on graft surface was enhanced using biomolecules such as insulin, transferrin, and peptides [12-14], whereas, tropoelastin, gelatin and collagen were used to stimulate cell adhesion and growth [15-17]. To the best of our knowledge, the covalent immobilization of heparin on woven and knitted forms of crimped PET cardiovascular grafts (Fig.1) is rarely addressed. We aimed to improve the

blood compatibility properties to reduce thrombosis and platelets deposition on two different forms of crimped PET grafts by surface modification.

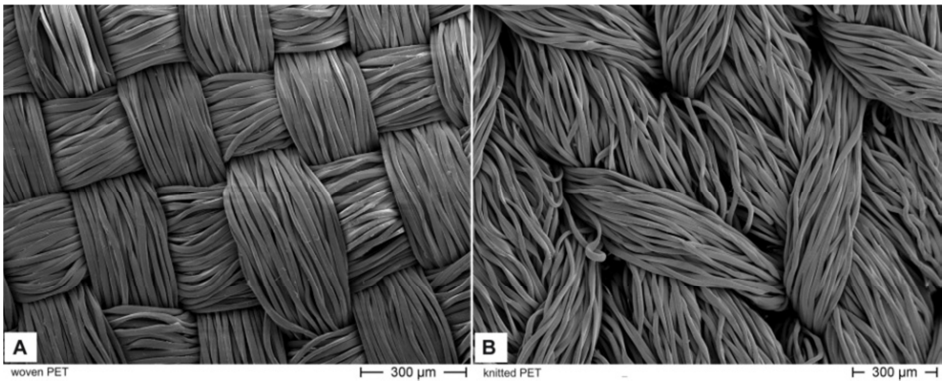

Figure 1. SEM micrographs of unmodified woven (A) and knitted (B) forms of crimped PET grafts. The multifilament PET threads in woven grafts are fabricated in an over-and-under pattern, while PET threads in knitted grafts are looped.

Denier reduction was employed to selectively cleave the ester linkage within PET surface resulting in free carboxyl group as schematically shown in Figure 2. Consequently, heparin was covalently immobilized to the resulting carboxyl group by the end-point attachment technique to maintain its chemical stability and bioactivity after immobilization process. To improve the endothelialization of cardiovascular PET grafts, the potential effect of collagen co-immobilization was evaluated. The surface modified PET was characterized by Fourier transform infrared spectroscopy (FTIR) and X-ray photoelectron spectroscopy (XPS).The biocompatibility of modified crimped PET grafts was confirmed *in-vitro* by direct blood coagulation test and platelets deposition under continuous flow condition. In addition, mouse L929 fibroblast cell line was used as model to assess the host cell adhesion and growth on the modified grafts.

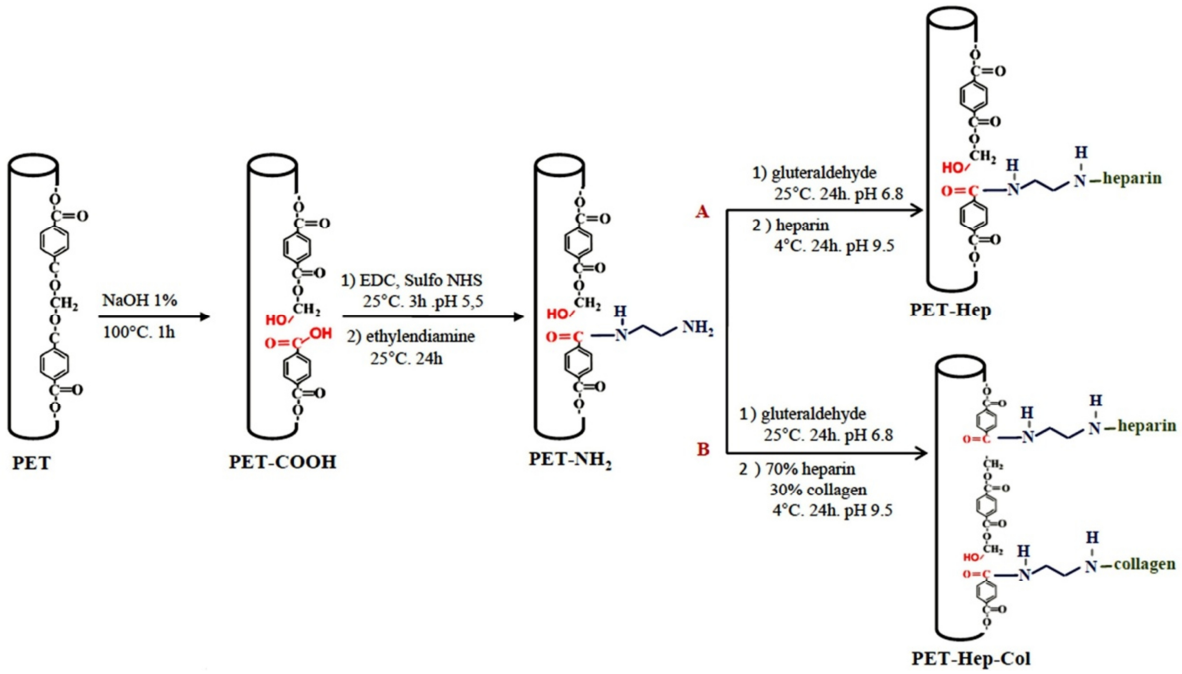

Figure 2. Schematic illustration of covalent immobilization of heparin (A), and co-immobilization of heparin/collagen (B) onto PET surface. The intrinsic ester linkage within the PET structure was cleaved by Denier reduction to produce functional carboxyl group on the surface (PET-COOH). Subsequently, the PET-NH_2 was obtained after grafting ethylenediamine on PET-COOH. The PET-Hep and PET-Hep-Col were obtained after immobilization of heparin or co-immobilization of heparin/collagen, respectively by the end point method.

2. Materials and methods

2.1. Materials

Woven and knitted forms of crimped Dacron®; polyethylene terephthalate PET grafts (14 mm internal diameter, 30 cm length and 12 filaments per yarn bundle) were kindly provided by Vascutek GmbH, Germany. Heparin sodium salt; 196 USP (U/mg), 1-ethyl-3-(3-dimethylamidopropyl) carbodiimide hydrochloride (EDC), N-hydroxysulfosuccinimide (Sulfo-NHS), glutaraldehyde, toluidine blue, and ethylenediamine were purchased from Sigma Aldrich, Germany. Sodium hydroxide was supplied by Carl Roth, Germany. Paraformaldehyde, Tris buffer, and Giemsa stain were bought from Merck, Germany. Water soluble collagen MW 80.000 and 2-N-morpholinoethanesulfonic acid (MES) were acquired from Serva, Germany. Mouse L929

fibroblasts cells line were obtained from DSMZ, Braunschweig, Germany. Dulbecco's Modified Eagle's Medium (DMEM), Earle's Balanced Salt Solution (EBSS), gamma irradiated Fetal Bovine Serum (FBS), trypsin, streptomycin, penicillin, and amphotericin B were purchased from PAA Laboratories GmbH, Germany. L-glutamine was bought from VWR, Germany. All other used chemicals were of analytical reagent grade.

2.2. Methods

2.2.1. Surface modification of crimped PET grafts

In the present study, two different forms of crimped PET cardiovascular grafts, woven and knitted as shown in Figure 1, were used for surface modification. All steps in the subsequent experiments were performed in triplicate for each form. Modified Denier reduction was used to introduce functional carboxyl groups on the surface of crimped PET grafts according to the method reported by Kissa [18] as schematically illustrated in Figure 2. Briefly, slices (2x2 cm^2) from woven and knitted forms of crimped PET grafts were immersed in 20 ml of an 50 % ethanol solution for 15minutes in an ultrasonic water bath (Sonorex RK 100H, Bandelin, Germany) to clean the surface. Subsequently, the grafts were rinsed several times with distilled water under stirring and then oven dried at 55°C for 2h. The cleaned grafts were dipped in 20 ml of 1% NaOH solution and incubated in a boiling water bath for 1h. The modified grafts were rinsed with distilled water and oven dried at 55°C for 2h. The obtained grafts are abbreviated as PET-COOH.

2.2.2.Grafting of ethylenediamine onto PET-COOH

Ethylenediamine was grafted onto previously produced carboxyl group using the adapted zero-length cross linker reaction known as carbodiimide plus sulfo-NHS as previously reported [19]. Crimped PET-COOH were immersed in 15 ml of MES buffer (0.1 M, pH 5.5) and hydrated for about

2h. Carboxyl group on the surface was activated by adding 0.1 M of EDC and 5 mM of sulfo-NHS and incubated under gentle stirring at 100 rpm/min (IKA C-MHGHS7, Germany) at room temperature for 3h. A solution of 50 mM of ethylenediamine was slowly added to the activated PET-COOH. The conjugation between one terminal amino group of ethylenediamine and one activated carboxyl group on the surface of PET-COOH was completed overnight at room temperature while stirring. Afterwards, grafts were rinsed with distilled water under sonication for 5 minutes and dried under dust free-airflow. The obtained grafts are abbreviated as PET-NH_2.

2.2.3. Immobilization of heparin onto PET-NH_2

Heparin was covalently immobilized onto PET-NH_2 using homobifunctional cross-linker glutaraldehyde as described elsewhere [20]. Briefly, PET-NH_2 (2x2 cm^2) were immersed in 10 ml sodium phosphate buffer (0.1 M, pH 6.8) containing 150 µl of 50 % glutaraldehyde and incubated overnight at room temperature under gentle stirring at 100 rpm/min. Afterwards, grafts were rinsed with distilled water under sonication for 5 minutes and dipped into 10 ml of heparin solution (1 mg/ml) in sodium carbonate buffer (0.5 M, pH 9.5) at 4°C. The excess aldehydes and the formed Schiff bases were reduced by adding 500 µl Tris buffer (0.2 M, pH 8.5) and incubated at 4°C for 1h. Finally, the grafts were washed with sodium phosphate buffer and rinsed with distilled water under sonication for 5 minutes and dried at room temperature under dust free-airflow. The obtained grafts are abbreviated as PET-Hep (Fig. 2A).

2.2.4. Co-immobilization of heparin and collagen onto PET-NH_2

Collagen was co-immobilized with heparin onto PET-NH_2 as previously described at concentration of 0.3 mg/ml and 0.7 mg/ml, respectively. The obtained grafts are abbreviated as PET-Hep-Col (Fig. 2B).

2.2.5.Surface characterization after modification

2.2.5.1. FTIR analysis

An FTIR (Alpha, Bruker, Germany) was utilized to detect the functional carboxyl group on the surface of modified PET-COOH compared to unmodified PET. The analysis was performed at 24 scans and at resolution of 4 cm^{-1}. Scanning was conducted in the mid-IR range from 400-4000 cm^{-1}. Three measurements were carried out for each graft.

2.2.5.2. XPS analysis

The chemical composition and survey spectra of modified and unmodified PET surfaces were investigated by XPS (PHI Versaprobe 5000, Physical Electronics). The XPS spectra of PET-Hep and PET-Hep-Col grafts were collected and compared with the corresponding native heparin, native collagen and unmodified PET. XPS spectra were acquired at a chamber pressure in range of 10^{-8} mbar using a monochromatized Al 1486.6 eV X-ray beam with an analytical spot size of 1400 µm x 200 µm. Two pass-energies were chosen; 187.75 eV for survey scans and 93.9 eV for higher resolution scans. The binding energy scale was calibrated by shifting the C1s aliphatic carbon peak to 284.8 eV. The XPS spectra were collected at the take-off angle 45° corresponding to a detection depth of about 4 nm for the relevant elements.

2.2.5.3. Determination of immobilized heparin concentration on PET-Hep

The concentration of covalently immobilized heparin on PET was determined using toluidine blue assay as previously reported [21]. Briefly, a dye reagent comprising from toluidine blue (5 mg) dissolved in 100 ml of 0.01 N hydrochloric acid containing 0.2 % NaCl was prepared. Two milliliters of various known concentrations of standard heparin in aqueous solution were added to 3 ml of the previously prepared dye reagent, and agitated using a vortex (Reax 2000, Heidolph, Germany).

The mixture was kept at room temperature for 10 minutes. Afterwards the formed toluidine blue-heparin complex in the mixture was extracted into organic layer of n-Hexane (3 ml). After separation, the absorbance of aqueous layer, which contained the non-extracted dye was measured within 30 minutes at 631 nm using spectrophotometer (Thermo Fischer 1510, Finland). The linear inverse relationship between absorbance at 631 nm caused by residual dye and the concentration of heparin in the aqueous layer was ascertained and used as a calibration curve to determine the concentration of immobilized heparin on PET-Hep.

Accordingly, slices (1x1 cm^2) of PET-Hep were immersed into a solution composed of 3 ml toluidine blue and 2 ml distilled water. The mixture was shaken well and incubated at room temperature for 30 minutes. Afterwards, 3 ml of n-hexane was added and mixed to ensure uniformity in treatment. The aqueous layer was separated and measured at 631 nm. The concentration of immobilized heparin was then calculated using the previously constructed calibration curve. Since only small amount of dye could be physically adsorbed onto dipped grafts, the separated grafts were rinsed again with 5 ml of 0.01 N hydrochloric acid and 0.2 % NaCl under sonication for 5 minutes, and the absorbance of the dye in washing solution was considered. For comparison, parallel experiment for PET-NH_2 was conducted.

2.2.6. *In-vitro* biocompatibility study

2.2.6.1. Platelets deposition on PET-Hep and PET-Hep-Col under continuous flow condition

Fresh whole blood from healthy human donator taking no therapy for at least 4 weeks was collected into anticoagulant sodium citrate at blood/citrate ratio 9:1 v/v. Platelets-Rich Plasma (PRP) was prepared by centrifuging the blood at 800 rpm for 13 minutes at 24°C. The PRP was separated and the platelets count was adjusted to 200 000 platelets /µl using saline.

Platelets deposition study was performed under continuous flow condition. Slices (0.5x0.5 cm^2) of unmodified PET, PET-Hep and PET-Hep-Col were held tightly onto an inner side of silicone tube. The silicone tube was connected to a pump (Pump drive 5001, Heidolph, Germany) using silicone rubber pump tube (strength 1.6, Carl Roth, Germany). The prepared platelets suspension and grafts attached-silicone tube were incubated in water bath at 37°C for 15 minutes to achieve temperature equilibration. The flow rate was then adjusted to 100 rpm/min. Flow was primed with saline at 37°C for 2 minutes then displaced by platelets suspension. After 30 minutes, the grafts were rinsed twice with saline and immersed in PBS containing 1% paraformaldehyde at pH 7.4 for 1h to fix the deposited platelets. After washing with distilled water, dehydration was performed by slow water replacement using series of ethanol solutions (50%, 70%, 80%, and 95%) for 90 minutes receiving final dehydration in absolute ethanol for 120 minutes. The grafts were then dried using a critical point dryer (Bal-Tec, CDP 030, Germany) followed by gold sputtering via Sputter coater (S150, Edwards, England) under vacuum using an inert argon dusting gas at 25 mA for 120 seconds before they were observed by scanning electron microscope. Silicone rubber tubes and pumping may lead to morphological changes to platelets due to flow rate. Hence, during the experiment, samples of platelets suspension were collected at 10 minutes intervals and the platelets aggregation or damage was investigated. However, no changes in platelets were observed during 30 minutes continuous flow study.

2.2.6.2. Counting of deposited Platelets on PET-Hep and PET-Hep-Col

The last procedure was repeated to count the deposited platelets on the examined grafts. After 30 minutes continuous flow, platelets deposited PET grafts were taken out, rinsed with saline and dipped in EBSS buffer solution without Ca^{+2}or Mg^{+2} at room temperature for 5 minutes. To remove the deposited platelets from the surface, grafts were incubated in 1ml trypsin solution (5 mg/ml)

at 37°C under gentle stirring 100 rpm/min for 15 minutes. The number of isolated platelets were immediately counted using Neubauer chamber.

2.2.6.3. Blood coagulation test on PET-Hep and PET-Hep-Col

Slices (1x1 cm^2) of unmodified PET, PET-Hep and PET-Hep-Col were wetted in saline and dipped into whole blood in water bath at 37°C for 10 minutes under gentle manual shaking. Afterwards, grafts were washed with saline and fixed with 1% paraformaldehyde at pH 7.4 for 1h. The grafts were rinsed with distilled water and dried as previously described before scanning electron microscopic observation.

2.2.6.4. L929 cells adhesion and growth on PET-Hep and PET-Hep-Col

L929 cell line was used as model to evaluate the biocompatibility of the PET-Hep and PET-Hep-Col with host tissue. Slices (0.5x0.5 cm^2) of unmodified PET, PET-Hep, and PET-Hep-Col were fixed onto sterile glass chip using inert, cell-nontoxic silicon glue and placed in a 12 well culture plate. L929 cells were seeded at a density of $1x10^5$ cells per well in 2 ml of DMEM medium, supplemented with 10 % FBS, 1 mM L-glutamine, penicillin (10.000 U/ml), streptomycin (10 µl/ml) and amphotericin B (25 µg/ml). The cultured grafts were incubated at 37°C and at 8.5 % CO_2. The medium was changed daily for 9 consecutive days, and a graft sample was taken out daily, rinsed twice with PBS at pH 7.4 and immersed in 1% paraformaldehyde for 1h to fix the adhered cells. Afterwards, the adhered cells after 24h culturing were stained by Giemsa stain (5 %) for 10h followed by color differentiation using 0.5 % acetic acid and dried at room temperature under dust free-airflow. The grafts were optically observed using microscope (Stemi 2000-C, Carl Zeiss, Germany) equipped with a camera (Canon G10, Japan). For scanning electron microscopy studies,

the cultured grafts were rinsed twice with PBS at pH 7.4 and fixed with 1% paraformaldehyde for 1h. The washing, drying, and sputter coating were conducted as previously described.

2.2.6.5. Counting of adhered L929 cells to PET-Hep and PET-Hep-Col

The number of adhered cells onto unmodified PET, PET-Hep, and PET-Hep-Col was performed 24h after cell culture. The medium was removed and the grafts were rinsed twice with sterile PBS at pH 7.4. The grafts were detached from glass chip and the adhered cells were removed using trypsin as described above. The number of isolated cells was immediately counted using Neubauer chamber.

2.2.7. Morphological observation using SEM

Scanning electron microscope SEM (Hitachi S-510, Japan) was used to observe the deposited platelets, blood clot, and L929 cells adherence and growth on unmodified PET, PET-Hep and PET-Hep-Col. The grafts were dehydrated using series of ethanol solutions, and dried by a critical point dryer as described above. Next, the grafts were mounted onto metal dish using double-sided adhesive tape and conductive carbonic cement. Gold sputter was conducted as described above. All images were taken at 25 kV under the same magnification for comparison study.

2.2.8.Statistically analysis

The data are expressed as means ± standard deviations of representative experiments. Statistical comparisons were made by analysis of T-distribution. The difference was considered to be significant at $p < 0.05$ for all statistical evaluations.

3. Results

3.1. FTIR surface characterization of functionalized PET-COOH

Woven and knitted forms of crimped PET grafts were surface modified using Denier reduction to produce functional carboxyl groups on their surfaces. The produced PET-COOH was activated using carbodiimide and sulfo-NHS and further used for grafting ethylendiamine as a spacer to yield PET-NH_2. Finally, PET-NH_2 was used for heparin immobilization or heparin/collagen co-immobilization to produce PET-Hep or PET-Hep-Col, respectively (Fig. 2).

FTIR was used to characterize PET-COOH after modification to detect the presence of the desirable functional group on the surface. FTIR spectra of unmodified PET and PET-COOH are depicted in Figure 3.

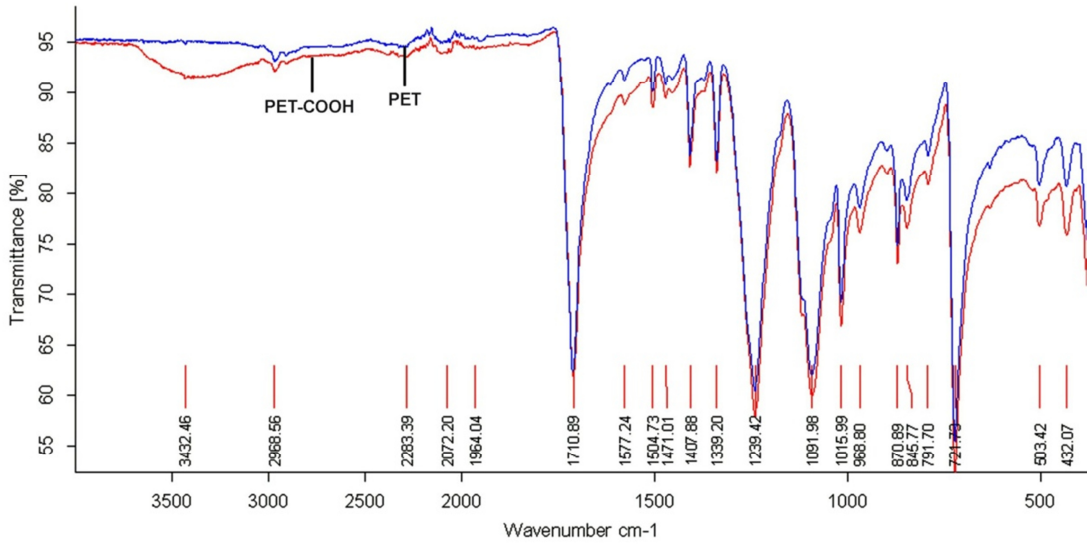

Figure 3. FTIR spectra of unmodified PET and PET-COOH. The selective absorption of light in the region of the hydroxyl group derived from the carboxyl group (3000-3500 cm^{-1}) in PET-COOH is illustrated.

The spectra of unmodified PET surface showed a substantial strong intensity of carbonyl bonds (C=O) indicated by the stretching vibration at 1711 cm^{-1}, and a medium intensity of aromatic (C=C), (=C-H) and (C-H) bonds detected by stretching vibrations at 1407, 870, 721 cm^{-1}, respectively. At the same time, alkane (C-H) showed a stretching vibration at 1339 cm^{-1}, and the

ester bond (C-O) was indicated by the presence of three strong stretching vibration bands at 1239, 1091 and 1015 cm^{-1}. The unmodified PET surface showed no peaks in the hydroxyl region of the carboxyl group (3000-3500 cm^{-1}), whereas a broad shoulder appeared in this region in the spectra of PET-COOH, indicating the presence of the desirable carboxyl group.

In addition, after grafting of ethylendiamine, the preliminary FTIR spectrum of PET-NH_2 was almost the same as that of the unmodified PET graft (data not shown). This is because the absorption frequencies of amide bonds based on (C=O) and (C-N) at (1650-1690 cm^{-1} and 1030-1220 cm^{-1}, respectively) overlap with that of the ester groups in unmodified PET itself. However, the grafted ethylendiamine, heparin, and collagen on the surface were confirmed using XPS.

3.2. XPS surface analysis of PET-NH_2, PET-Hep and PET-Hep-Col

The chemical compositions of native heparin, native collagen, unmodified PET, PET-NH_2, PET-Hep, and PET-Hep-Col were calculated from the XPS spectra as illustrated in Table 1. The results revealed a small amount of intrinsic silicon corresponding to the unmodified PET. The carbon component of the unmodified PET was decreased after alkaline treatment. In addition, nitrogen component was observed on the surface only after grafting of ethylendiamine and obviously increased in PET-Hep and PET-Hep-Col based on the amino groups of immobilized molecules. Notably, sulfur and sodium traces which were present in native heparin and native collagen were observed only on the surface of PET-Hep and PET-Hep-Col as a result of successful immobilization of heparin, and co-immobilization of heparin and collagen. Furthermore, the XPS detail spectra for all samples outlined two main peaks corresponding to carbon C-1s at 284.8 eV and oxygen O-1s at 532 eV. Two additional peaks from nitrogen N-1s at 399.6 eV and sodium Na-1s at 1071 eV were found in native heparin and collagen, and obviously observed on PET-Hep, whereas their corresponding elements in PET-Hep-Col spectra were more intense as shown in Figure 4.

Moreover, the peak of sulfur S-2p around 168 eV coincided with a satellite of strong silicon Si2p line at 153.3 eV of PET itself

Table1. XPS Study of PET after surface modification and heparin/collagen immobilization

PET Grafts	Atomic Compositions (%) for Modified/Unmodified Grafts					
	Carbon (C_1s)	Oxygen (O_1s)	Silicon (Si_2p)	Nitrogen (N_1s)	Sodium (Na_1s)	Sulfur (S_2p)
Native heparin	38.9	45.3	-	2.8	7.9	5.0
Native collagen	81.4	13.1	-	5.1	0.2	< 0.1
Unmodified PET	71.5	27.6	1.3	-	-	-
PET-COOH [a]	69.5	29.8	0.7	-	-	-
PET-NH_2 [b]	72.8	26.3	0.6	0.3	-	-
PET-Hep[c]	69.5	28.5	0.6	1.1	0.2	< 0.1
PET-Hep-Col[d]	70.4	24.6	0.7	3.6	0.6	< 0.1

[a] PET-COOH was obtained after Denier reduction of PET.
[b] PET-NH_2 was obtained by grafting of ethylendiamine onto PET-COOH.
[c] PET-Hep was obtained by immobilization of heparin onto PET-NH_2.
[d] PET-Hep-Col was obtained by co-immobilization of heparin and collagen onto PET-NH_2

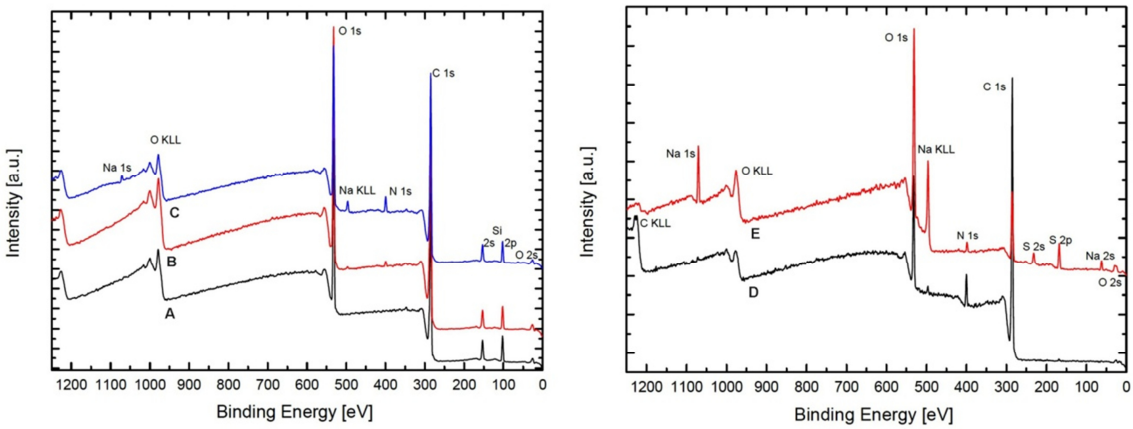

Figure 4. XPS survey scan spectra of unmodified PET graft (A), PET-Hep (B), and PET-Hep-Col (C). The XPS spectra of the native heparin (D) and collagen (E) are shown. Nitrogen (N 1s) and sodium (Na 1s) peaks were solitary appeared in the spectra of PET-Hep and PET-Hep-Col in accordance with the corresponding native compounds.

3.3. Efficiency of heparin immobilization on PET-Hep

The concentration of covalently immobilized heparin on PET surface was determined using toluidine blue assay. The blank assay was carried out using PET-NH_2 and the concentration of immobilized heparin was calculated from the prepared standard curve. However, the mean concentration of immobilized heparin per unit surface area of woven and knitted PET was appraised to be 1.31 µg/cm^2 based on three independent experiments.

3.4. In-vitro biocompatibility of PET-Hep and PET-Hep-Col grafts

3.4.1. Platelets deposition

The platelets deposition on PET-Hep and PET-Hep-Col was assessed using appropriate continuous flow condition and the number of adhered platelets was calculated per unite surface area of the studied graft. The SEM micrographs in Figure 5 demonstrated the platelets deposition on unmodified woven and knitted PET (A, B), PET-Hep (A1, B1), and PET-Hep-Col (A2, B2).

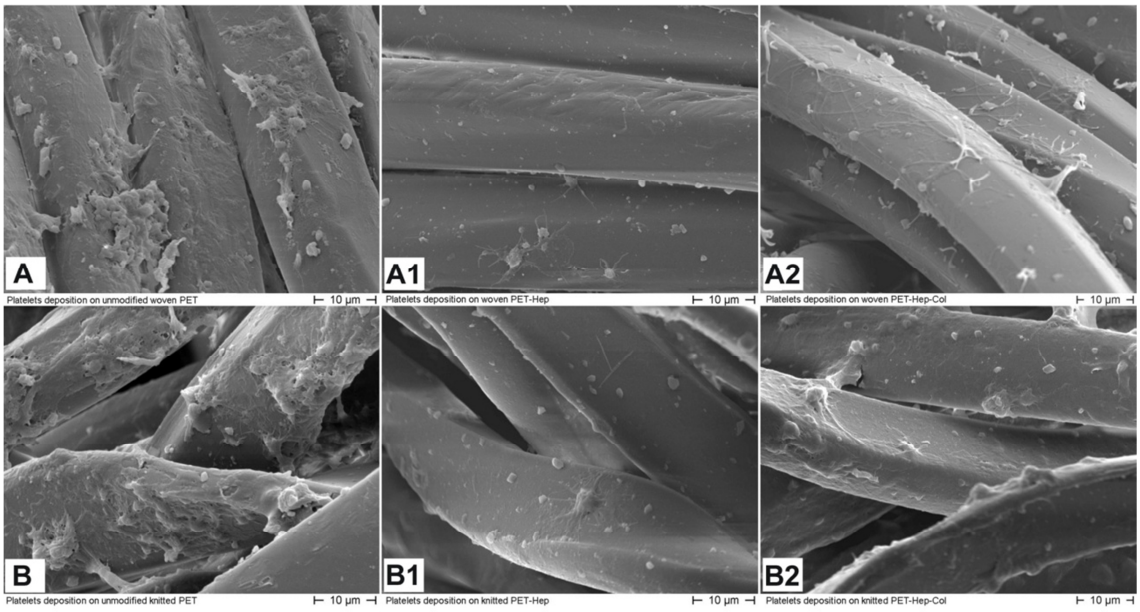

Figure 5. SEM micrographs of platelets deposited on PET grafts under flow condition. The platelets on unmodified woven (A) and knitted (B) PET grafts showed massive aggregation and demonstrated pseudopodia. The woven (A1) and Knitted (B1) PET-Hep, and woven (A2) and knitted (B2) PET-Hep-Col grafts showed obvious reduction in platelets deposition.

The platelets deposition was significantly reduced on PET-Hep and PET-Hep-Col. Specifically, the platelets deposited on woven and knitted PET-Hep and PET-Hep-Col exhibited fewest pseudopodia and aggregation compared to unmodified PET. From the statistical point of view, the number of deposited platelets on both woven and knitted PET-Hep decreased by 3 and 2.8 fold compared to unmodified PET at P=0.001. Lower platelets were deposited on PET-Hep-Col showed only 1.7 and 1.8 fold decrease in number per unite surface compared to unmodified PET at P = 0.01 (Fig. 6).

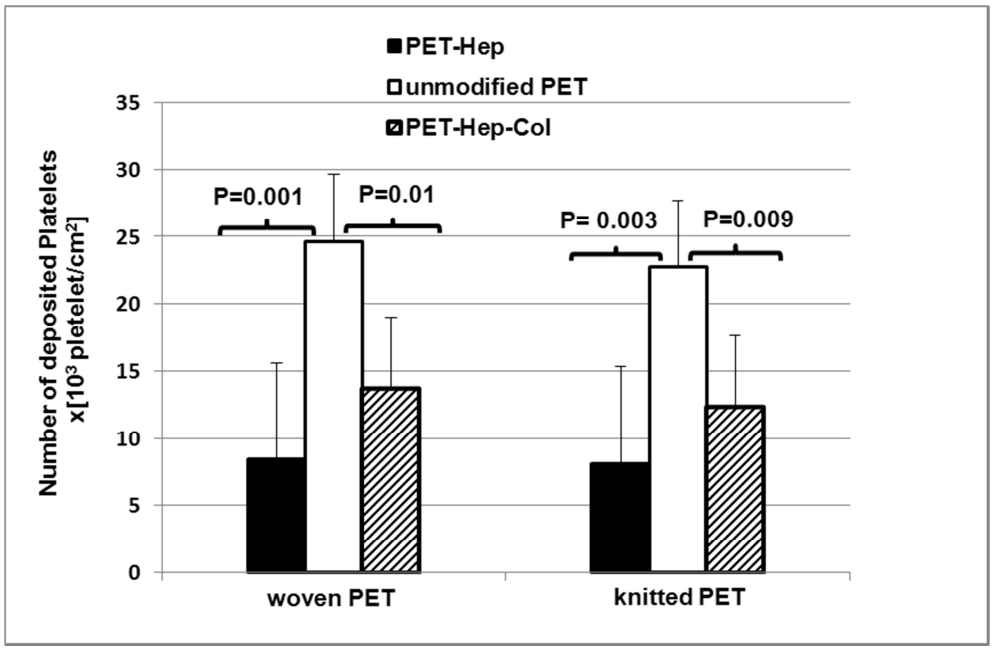

Figure 6. The number of platelets deposited on PET grafts under flow condition. The platelets number (x10^3 platelet/cm^2) was counted after isolation from woven and knitted forms of; unmodified PET (white bars), PET-Hep (black bars), and PET-Hep-Col (striped bars). Results are given as mean ± standard deviation of three independent experiments.

3.4.2. Blood coagulation test

Direct blood coagulation test was conducted on PET-Hep, PET-Hep-Col and unmodified PET in human-mimic conditions. Figure 7 shows SEM micrographs of formed clot and fibrin fibers on unmodified crimped woven PET (A), PET-Hep (B) and PET-Hep-Col (C). Similar results were detected for knitted grafts (data not shown). A wide clot was detected on unmodified PET

demonstrating intensive fibrin fibers on broad area of the graft surface, whereas, PET-Hep and PET-Hep-Col displayed a remarkable anti coagulation effect and only few fibrin fibers could be detected as shown in the corresponding magnified SEM micrographs (Fig. 7). Nevertheless, our results revealed that PET-Hep-Col supported more formation of fibrin fibers than PET-Hep.

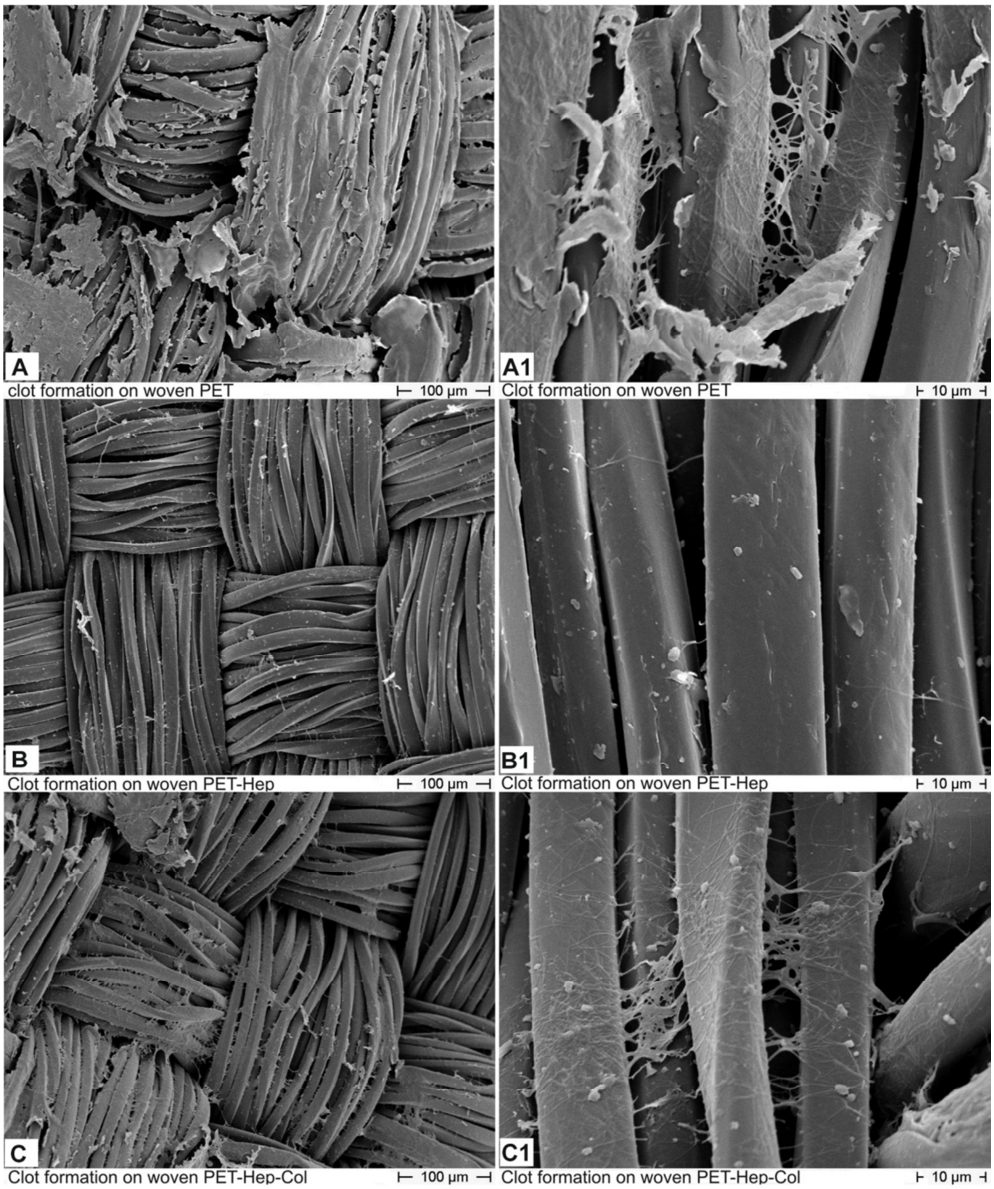

Figure 7. SEM micrographs of blood clot formed on woven PET grafts. Clot formed on unmodified PET (A), PET-Hep (B), and PET-Hep-Col (C) are shown. The magnified micrographs of unmodified PET (A1) showed well-formed enormous clots accompanied by intensive fibrin fibers, while PET-Hep (B1) and PET-Hep-Col (C1) illustrated clot resistance surface.

3.4.3. L929 cells adhesion and growth on PET-Hep and PET-Hep-Col grafts

The biocompatibility of modified PET grafts with host tissue was tested *in-vitro* using L929 cells as model. The cell adhesion and growth on woven and knitted PET-Hep and PET-Hep-Col were investigated and compared to unmodified PET. Our primary SEM micrographs confirmed the cell adhesion and growth on the investigated grafts (Fig. 8). PET-Hep demonstrated no significant effect on the cell behavior. Both unmodified PET and PET-Hep were first overgrown with confluent cellular monolayer after seven days. Furthermore, the potential effect of collagen on PET-Hep-Col to support cell adhesion and growth was obviously observed within 5 days compared to unmodified PET and PET-Hep.

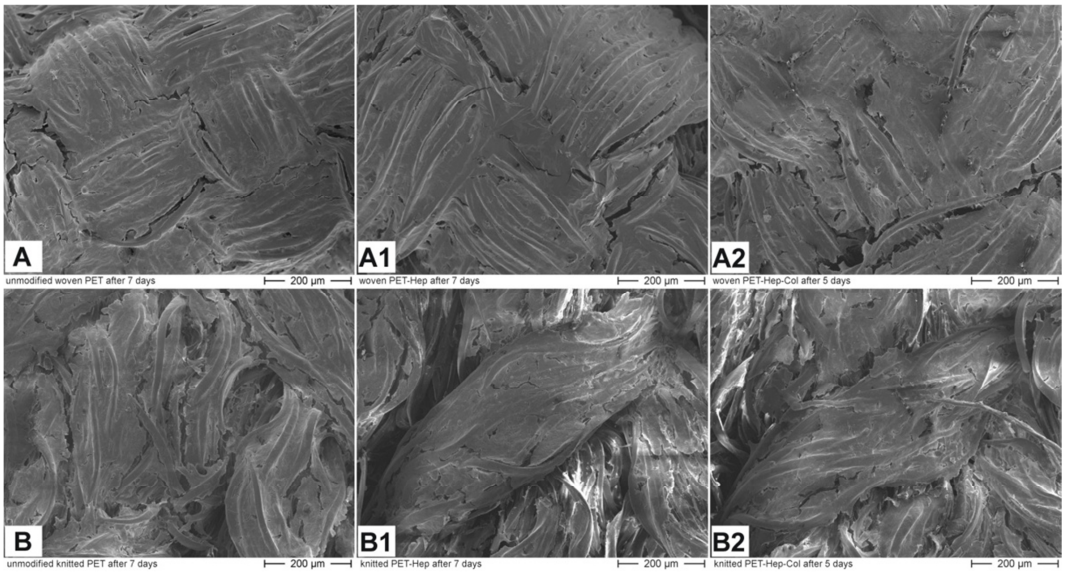

Figure 8. SEM micrographs of grown L929 cells on PET grafts. Confluent cell monolayers on unmodified woven (A) and knitted (B) PET, and on woven (A1) and knitted (B1) PET-Hep grafts were observed first after 7 days, while on woven (A2) and knitted (B2) PET-Hep-Col were early observed after 5 days.

An increase in the number of adhered cells on woven and knitted PET-Hep was barely observed compared to the corresponding unmodified PET with no statistical importance ($p>0.05$) (Fig. 9). Importantly, the number of adhered cells on woven and knitted PET-Hep-Col increased by 1.3 and

2 fold (P=0.02) compared to corresponding unmodified PET. This is in accordance with our data acquired from optical microscope after Giemsa stain shown in Figure 10. The adhered cells manifested the influence of collagen in promoting cell adhesion and growth on the modified grafts.

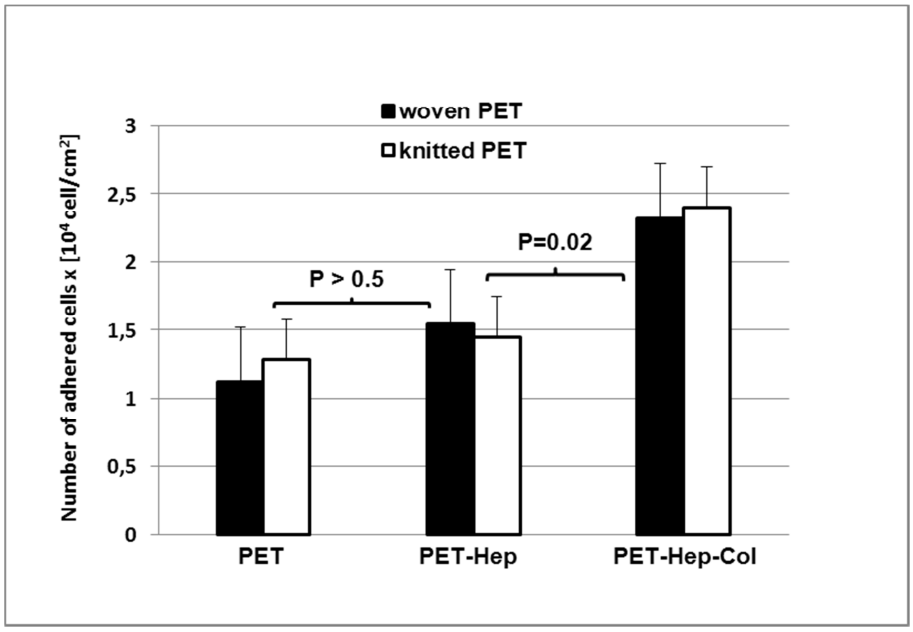

Figures 9. The number of adhered L929 cells to PET grafts after 24h cell culturing. The adhered cells were counted (x10^4 cell/cm^2) after isolation from woven (black bars) and knitted (white bars) forms of; unmodified PET, PET-Hep and PET-Hep-Col. Results are given as mean ± standard deviation of three independent experiments.

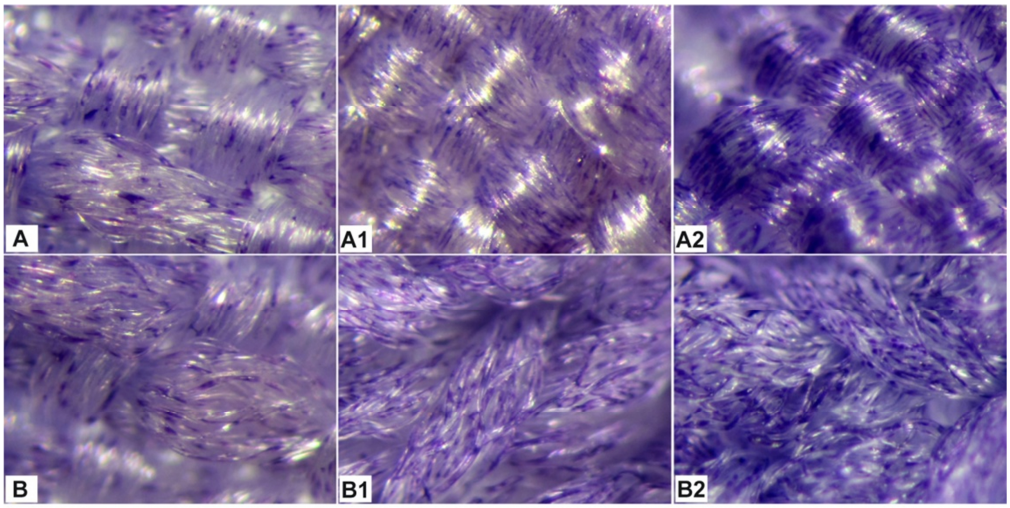

Figure 10. Micrographs of Giemsa stained adhered L929 cells on PET grafts after 24h cell culture. Woven (A2) and knitted (B2) PET-Hep-Col obviously enhanced cell adhesion, while the corresponding woven (A) and knitted (B) of unmodified PET and woven (A1) and knitted (B1) PET-Hep showed lesser cell adhesion.

4. Discussion

Long-term patency rates of woven and knitted forms of crimped PET cardiovascular grafts are limited mainly due to inadequate endothelialization and surface induced thrombosis. The thrombogenic property of PET, mostly initiated by the adsorption of plasma proteins and by the platelets activation, is the common mode of failure of cardiovascular grafts after implantation [1, 2, 3, 6].

Since the interactions that lead to thrombus formation occur at the graft-blood interface, the necessity of an appropriate surface modification is potential in improving the blood compatibility without altering the essential bulk properties of the graft for medical applications. One approach to reduce the surface thrombogenicity of the graft is to attach an anticoagulant molecule to the graft surface. In this study, we attempted to produce biocompatible graft by immobilization of heparin. Moreover, the combination of heparin and collagen presents synergic properties of thrombus resistance and cytocompatibility, therefore, the co-immobilization of heparin/collagen onto woven and knitted forms of crimped PET grafts was also investigated.

Heparin is the commonly used anticoagulant that forms a complex with anti-thrombin III. The heparin anti-thrombin III complex inactivates serine proteases, most importantly thrombin, which catalyzes the conversion of fibrinogen to fibrin in the final step of the coagulation cascade reaction [11]. In addition, collagen is the main component of the extracellular matrix on which the endothelial cells could adhere, proliferate, and differentiate [17]. However, the inert architecture of PET entails the functionalization of surface for immobilization purpose. Accordingly, to introduce carboxyl groups on the PET surface, the alkaline treatment of PET was utilized to cleavage the inherent ester linkages within the PET texture (Fig. 2) [18].

The presence of the desired functional group on PET-COOH was proven using FTIR based on the appearance of broad shoulder of the hydroxyl group originating from carboxyl group [22] (Fig.3). One terminal amino group of ethylendiamine was grafted to the generated functional group on PET-COOH via an amide bond to form PET-NH_2. The second amino group in ethylendiamine was further used as an anchor for heparin immobilization or heparin/collagen co-immobilization to produce PET-Hep or PET-Hep-Col, respectively.

To avoid the reaction between amino and carboxyl groups of heparin molecules, or between heparin and collagen, glutaraldehyde was used to activate the amino groups on the surface of PET-NH_2. This ensured that the reaction occurred only on the desired group by end-point method.

Quantitative analysis of atomic concentrations of studied grafts was calculated from XPS survey scan spectra (Table 1). The atomic concentration of carbon after modification was reduced due to the removal and loss of some molecules from the graft surface upon the alkaline treatment [18]. Furthermore, unlike unmodified PET, nitrogen and sulfur atoms were detected on PET-Hep and PET-Hep-Col confirming the successful co-immobilization of heparin and collagen. Similar results were obtained by comparing XPS spectra of native heparin and native collagen with PET, PET-Hep and PET-Hep-Col as shown in Figure 4. The XPS spectra of PET-Hep and PET-Hep-Col demonstrated

two peaks corresponding to nitrogen and sodium, while these peaks could not be detected in XPS spectra of unmodified PET thus, verifying the successful covalent co-immobilization of heparin and collagen. In accordance with XPS spectra of PET-Hep, the concentration of heparin on the surface as detected by toluidine blue assay indicated the effective immobilization of heparin on the surface.

Our approach to immobilize heparin by the end-point provided the needful flexibility for optimum surface passivation. This is in agreement with previous reports showed that the end-point attached of heparin completely inhibited thrombin activity and the subsequent thrombus formation on the graft surface during the massive blood flow [23].

Therefore, the biological activity of modified grafts was evaluated *in-vitro* under human-mimic conditions. The formation of clot on unmodified PET, PET-Hep and PET-Hep-Col was investigated by direct blood coagulation test. The results demonstrated intense clot after 10 minutes blood contact on unmodified PET surface. However, the fibrin deposition profile of unmodified PET presented wide net of fibrin fibers confirming highly thrombogenic characteristics at early time points as shown in the magnified images (Fig. 7). Unlike to unmodified graft, PET-Hep and PET-Hep-Col exhibited substantial resistance to clot and fibrin formation. This is attributed to the neutralization effect of heparin on thrombin formation. Moreover, the activated platelets can only adhere and aggregate if significant blood proteins adsorb on the graft surface [6,7,24], consequently, the inhibition of fibrin precipitation on the surface decreased the number of activated platelets and hence its deposition. Based on this, the stimulation of anti-thrombin III by heparin along with inhibition of factor Xa prevented the conversion of pro-thrombin to thrombin. Subsequently, the protein adsorption and platelets deposition on the surface were decreased (Fig. 5 and 6). Conversely, addition of collagen supported the protein adsorption to some extent on the PET surface and increased the number of deposited platelets. As a result, collagen restricts the

solitary use in the application for blood contacting biomaterials. Nevertheless, the co-immobilization of heparin and collagen showed synergic inhibition effect of platelets deposition after 30 minutes continuous flow condition to simulate the massive blood flow which defines the outcomes of cardiovascular graft patency [4].

Another potential strategy to limit short-term patency rate of cardiovascular grafts due to thrombus formation is by providing a rapid uniform and complete coverage with host cells [13, 16, 17]. The muco-polysaccharide structure of heparin is a natural component of arterial cell wall that decreases the surface hydrophobicity and encourages cell adhesion on the graft surface [8, 9, 10, 11]. This explained the insignificant increase in the number of the adhered cells on PET-Hep compared to unmodified PET (Fig. 9). Interestingly, collagen co-immobilization significantly enhanced the cell adhesion and growth by presenting a surface supplemented with natural connective component in endogenous extracellular matrix [17]. The beneficial effect of collagen on cell adhesion and growth was additionally confirmed by differential cell staining using Giemsa stain (Fig.10). This highly emphasized the enhancement of cell growth 5 days after cell culturing on PET-Hep-Col compared to either unmodified PET or PET-Hep (Fig.8). Notably, the cells displayed insignificant difference in growth pattern on woven and knitted forms of all tested grafts. The closed filaments in tightly woven and knitted forms enable the cells to bridge the distance between filaments. This confirmed the dependency of cell adhesion mainly on the surface properties [25, 26].

5. Conclusion

Co-immobilization of heparin and collagen on crimped PET grafts minimized the host response reactions on the graft surface and ensured a rapid coating of grafts with host cells. The reported anti-thrombus potential of the modified grafts highlights the utility of our strategy to treat the

common complications after implantation and to produce biocompatible crimped PET grafts for medical application.

6. Acknowledgements

The authors thank Prof. Dr. J. Janek, Institute of Physical Chemistry, Justus-Liebig-University, Giessen, Germany for his kind support of this research.

7. References

[1] S. Dimitrievska, M. Maire, GA.Diaz-Quijada, L. Robitaille, A. Ajji, L.Yahia, et al. Low thrombogenicity coating of nonwoven PET fiber structures for vascular grafts. Macromol Biosci. 11 (2011) 493.

[2] K. Kottke-Marchant, JM. Anderson, Y. Umemura, RE. Marchant. Effect of albumin coating on the in vitro blood compatibility of Dacron arterial prostheses. Biomaterials. 10 (1989) 147

[3] W. Jin, L. Jianxin, S. Liru, R. Ling, X. Zejin, Z. Ansha, et al. The biomedical properties of polyethylene terephthalate surface modified by silver ion implantation. Nucl Instrum Methods Phys Res B. 257 (2007) 141

[4] W. Oeveren, I. Tielliu, J. Hart. Comparison of modified chandler, roller pump and ball valve circulation models for in vitro testing in high blood flow conditions: application in thrombogenicity testing of different materials for vascular applications. Int J Biomater. 2012(2012)163

[5] P. Bracco, V. Brunella, L. Trossarelli, A. Coda, F. Botto-Micca. Comparison of polypropylene and polyethylene terephthalate (Dacron) meshes for abdominal wall hernia repair: a chemical and morphological study. Hernia. 9 (2005) 51

[6] H. Roald, R. Barstad, I. Bakken, B. Roald, T. Lyberg, K. Sakariassen. Initial interactions of platelets and plasma proteins in flowing non-anticoagulated blood with the artificial surfaces Dacron and PTFE. Blood Coagul Fibrinolysis. 5 (1994) 355

[7] L.Vroman. The life of an artificial device in contact with blood: initial events and their effect on its final state. Bull N Y Acad Med. 64 (1988) 352

[8] J. Leijon, F. Carlsson, J. Brännström, J. Sanchez, R. Larsson, B. Nilsson, et al. Attachment of flexible heparin chains to gelatin scaffolds improves endothelial cell infiltration. Tissue Eng Part A. 19 (2013) 1336

[9] J. Yu, A. Wang, Z. Tang, J. Henry, L. Ping, B. Lee, et al. The effect of stromal cell-derived factor-1α/heparin coating of biodegradable vascular grafts on the recruitment of both endothelial and smooth muscle progenitor cells for accelerated regeneration. Biomaterials. 33 (2012) 8062

[10] M. Yang,W. Lin. Surface modification and blood compatibility of polyacrylonitrile membrane with immobilized chitosan-heparin conjugate. J. Polym. Res. 9(2002) 201

[11] R. Linhardt, S. Claude. Hudson Award address in carbohydrate chemistry. Heparin: structure and activity. J. Med. Chem. 19 (2003) 2551

[12] Y. Kim, I. Kang, M. Huh, S. Yoon. Surface characterization and in vitro blood compatibility of poly (ethylene terephthalate) immobilized with insulin and/or heparin using plasma flow discharge. Biomaterials. 21(2000) 121

[13] O. Zouani, C. Chollet, B. Guillotin, M. Durrieu. Differentiation of pre-osteoblast cells on poly (ethylene terephthalate) grafted with RGD and/or BMPs mimetic peptides. Biomaterials. 31(2010) 8245

[14] Y. Lei, M. Remy, C. Labrugere, M. Durrieu. Peptide immobilization on polyethylene terephthalate surfaces to study specific endothelial cell adhesion, spreading and migration. J Mater Sci Mater Med. 23(2012) 2761

[15] M. Hiob, S. Wise, W. Kondyurin, A. Waterhouse, M. Bilek, Weiss A. et al. The use of plasma-activated covalent attachment of early domains of tropoelastin to enhance vascular compatibility of surfaces. Biomaterials. 34 (2013) 7584

[16] S. Manju, C. Muraleedharan, A. Rajeev, A. Jayakrishnan, R. Joseph. Evaluation of alginate dialdehyde cross-linked gelatin hydrogel as a biodegradable sealant for polyester vascular graft. J biomed Mater Res B Appl Biomater. 98 (2011) 139

[17] M. Burrows, V. Zamarion, F. Filippin-Monteiro, D. Schuck, H. Toma, A. Campa. et al. Hybrid scaffolds built from PET and collagen as a model for vascular graft architecture. Macromol Biosci. 12 (2012) 1660

[18] E. Kissa. Soil release finishes-Alkali treatment of polyester fibers. In: Lewin M. Sello S. editors. Handbook of fiber science and technology, New York: Marcel Dekker. 1984, p.265-89

[19] G. Hermanson. Bioconjugate reagents, Zero length cross linkers. In: G. Hermanson editor. Bioconjugate Techniques. 2thed. Elsevier. 1996, p.169-86

[20] G. Hermanson.Bioconjugate reagents, homobifunctional cross-linker glutaraldehyde. In: G. Hermanson editor. Bioconjugate Techniques. 2thed. Elsevier. 1996; p.470-72

[21] P. Smith, A. Mallia, G. Harmanson. Calorimetric method for the assay of heparin content in immobilized heparin preparations. Anal Biochem. 109 (1980) 466

[22] P. Griffiths, J. Hasseth. Fourier transform infrared spectroscopy. 2nd Wiley-Blackwell. 2007

[23] S. Murugesan, J. Xie, R. Linhardt. Immobilization of heparin: approaches and applications. Curr Top Med Chem. 8 (2008) 80

[24] K. Park, W. Kim. H. Jacobs , T. Okano , S. Kim . Blood compatibility of SPUU-PEO heparin graft-copolymers. J Biomed Mater Res. 26 (1992) 739

[25] F. Yu, F. Mücklich, P. Li, H. Shen, C. Lehr, U. Bakowsky. In vitro cell response to a polymer surface micropatterned by laser interference lithography. Biomacromolecules. 6 (2005) 1160
[26] P. Li, U. Bakowsky, F. Yu, C. Loehbach, F. Muecklich, C. Lehr. Laser ablation patterning by interference induces directional cell growth. IEEE Trans Nanobioscience. 2 (2003) 138

Chapter 6

Summary and Perspective

Summary discussion

Cardiovascular prostheses successfully restore the function of damaged vessels and cardiac valves [1,2,3]. Despite of the associated complications with polyethylene terephthalate (PET) grafts, the woven and knitted forms of crimped PET grafts are still the most effective employed biomaterials [1,2,3]. However, infections and the host response destruct the graft and damage the surrounding tissue which often necessitates graft removal upon surgical operation [4,5].In this study, we took priority over coating the crimped PET grafts with a newly synthesized SD-PHA-b-MPEO diblock co-polymer, utilizing its multifunctional advantages mainly negative charge, hydrophobicity, and the bactericidal effect of the sulfadimethoxine (SD) moiety. The structure of the employed polymer was proven and characterized using nuclear magnetic resonance (NMR), infrared (IR) and UV spectroscopy before use [6]. We intended to form a porous film to maintain the tensile ability of the grafts by evaporating the water-immiscible polymer solvent under saturated humid atmosphere [7]. The formed network architecture film displayed a local bactericidal effect while attaining suitable characteristics to PET surface in terms of cell adhesion and growth, which hold promise for sufficient coverage of the graft with host cell. This consideration is based on the fact that the adhesion and growth of the host cell on PET depend on surface hydrophobicity, porosity, electronegativity, mechanical properties, and in particular the distance between individual filaments in the yarn [8,9]. Accordingly, the hydrophobic block of the polymer and the negative charge on its surface hampered the cell adhesion to a small non-significant extent. In contrast, the formed network-structured coat provided a benefit to reduce the interval distance between the discrete filaments in the yarn. Additionally, the hydrophilic block of the polymer supported cell adhesion and growth and enabled the cells to bridge the filaments [8]. As a result, L929 cells readily overgrew the coated PET (PET-Net) and a cellular monolayer was observed after 7 days.

The *In-vitro* calculated anti-adhesion efficiency of PET-Net against three different bacterial strains, namely *S. epidermidis, S. aureus,* and *E. coli* representing the most common Gram-positive and Gram-negative pathogens indicated highly significant reduction on adhesion of all aforementioned strains compared to unmodified PET (P=0.003). Notably, we reinforced our results by using a violent pathogenic Gram-positive *S. epidermidis* strain previously isolated from a patient`s vein catheter. Indeed, bacteria tend to adhere on and colonize preferably neutral and hydrophilic rather than hydrophobic surfaces [4]. This is avoided in the presence of polyhexylene and sulfadimethoxine groups in the formed multifunctional coat which switch the surface into hydrophobic and render the graft surface negatively charged. Additionally, the bacterial cell-repelling characteristics of polyethylene oxide guided synergistic antibacterial effect of the sulfadimethoxine group that make the modified PET graft even more unsuitable for bacterial adhesion and colonization. Furthermore, bacterial adhesion could be influenced not only by electronegativity and hydrophobicity but also by surface porosity [10,11]. Therefore, the low porosity of the PET-Net makes it less favorable to bacterial adhesion.

In the second study: we modified PET grafts with the lysozyme to take advantage of its capacity to lyse β (1- 4) glucosidic bonds in the bacterial cell wall, resulting in an effective protection against bacterial adhesion and biofilm formation. The ligation of lysozyme on surfaces of woven and knitted forms of crimped PET cardiovascular grafts was confirmed by XPS spectra of native lysozyme and unmodified PET versus enzyme-immobilized PET (PET-Enz). Despite a minor reduction of the immobilized enzyme activity on woven and knitted PET grafts compared to free enzyme, we found obvious anti-adhesion efficiency of the immobilized enzyme against Gram-positive *S. aureus, S. epidermidis*, and Gram-negative *E. coli* bacterial strains.

The results demonstrated a better activity of PET-Enz grafts against Gram-positive than Gram-

negative bacteria. This attributed to that lysozyme, a glycoside hydrolase, cleaves the β (1- 4) glucosidic bond between N-acetylmuramic acid and N-acetyl-D-glucosamine residues in peptidoglycan of bacterial cell wall [12,13]. The targeted glucosidic β(1-4) bonds in a Gram-positive cell wall are uncovered and found in large quantities compared to the Gram-negative cell wall which contains an outer membrane [14]. Consequently, the enzyme on PET-Enz grafts can easily access these structures on Gram-positive bacteria, leading to pressure imbalance within the bacterial cell wall causing cell lysis and death, a finding that promises eradication of subsequent biofilm formation [13,14,15]. In contrast, in the outer membrane of Gram-negative bacteria, the β (1- 4) glucosidic bonds are hidden under a layer of lipoproteins and only few exist in the pili on the cell surface. Accordingly, the enzyme activity is limited mainly to the pili and the burdened bacterial adhesion without any effect on the wall structure [13,14,15]. Our PET-Enz grafts still retained activity against Gram-negative bacteria, may be explained by earlier findings stating that the irreversibly inactivated lysozyme showed antibacterial effects, suggesting that the antibacterial efficiency is not only attributable to its activity, but also to the alkaline nature of the enzyme [15]. In our study, woven grafts were more hospitable to bacterial adhesion than knitted grafts. Bacterial adhesion could, in theory, be influenced by factors other than lysozyme including graft porosity, surface tension, and electronegativity [16]. According to our results, the lower porosity of the woven PET may make it more favorable to bacteria adhesion. To ensure complete healing after graft implantation, coating of the graft by the natural host cells is critical. This process can be disturbed by successful bacterial adhesion and biofilm formation on the grafts surface. All PET grafts in our study were readily overgrown by L929 cells used as a model to evaluate the cell hosting. No significant difference in the number of attached cells after enzyme immobilization was observed. A trend towards an increased number of adhered cells on PET-Enz graft due to modulated surface hydrophobicity by lysozyme compared to unmodified grafts

showed no statistical significance. Altogether, these findings outline conformity of the modified grafts with the biocompatibility requirements for biomedical applications.

In the third study: we aimed to support the grafts patency by local delivery of hydrophilic drugs using PLGA nanoparticles as carrier and FITC-dextran (FD) as water soluble drug model. The nanoparticles (NPs) were covalently immobilized to PET and expanded polytetrafluoroethylene (ePTFE) grafts after surface functionalization. The functional amino group was directly produced on PET by aminolysis reaction using ethylendiamine to selectively cleavage of the ester bond within the PET surface [17]. Characterization of the aminolated graft by surface potential measurement demonstrated a negative potential over a wide pH range due to ionization of the surface amino group with an isoelectric point at around pH 7-8 conforming the successful amino functionalization [18]. While ePTFE was amino-functionalized by grafting 3-aminopropyl triethoxysilane to the previously produced hydroxyl groups using piranha solution [19]. The introducing of amino group on ePTFE was proven using FTIR corresponding to the definite band of amino group [20]. Afterwards, the produced amino groups on the surfaces were activated by glutaraldehyde and used further as anchor sites for covalent coupling to the carboxyl group in the PLGA nanoparticles. The nanoparticles were synthesized from biodegradable PLGA polymer for local, controlled release, taking advantages of the high capacity of hydrophilic drugs by *double emulsion-solvent evaporation* method and the stability of obtained particles [21].

Additionally, for immobilization purpose, the intrinsic carboxyl groups in the PLGA made it our first choice for nanoparticles syntheses along with Tween®80 as surfactant at suitable concentration to stabilize the nano suspension. The surfactant adsorb at the particles surface between the superficially COOH groups leaving them free and available for coupling [22]. The marked increase in the size of the obtained FD-loaded NPs in comparison to unloaded NPs is attributed to

expansion of polymeric matrix within FD encapsulation [22]. However, all particles seemed to possess the ideal surface charge suggesting that the surfactant and/or FITC-dextran have no masking effect on the superficial carboxylic groups [23].

However, the efficiency of nanoparticles coating for cardiovascular grafts entails the stability during the massive blood flow to secure the local controlled release of encapsulated drug. Therefore, the stability of immobilized NPs was evaluated *in-vitro* under human-mimic conditions. The surface visualization manifested permanence of monolayer coat on nano-immobilized grafts (PET-NPs and ePTFE-NPs) after 24h substantial continuous flow providing an appropriate carrier for controlled drug delivery over the tested time. Nonetheless, the ability of PET-NPs and ePTFE-NPs to support host cell adhesion and growth is decisive and displayed dependency on surface topography, hydrophobicity, and porosity [24,25]. Interestingly, the tested grafts were readily overgrown by L929 cells and shown no significant difference in the number of adhered cells on PET-NPs and ePTFE-NPs compared to unmodified grafts. Furthermore, the hosting ability of the modified grafts was additionally confirmed by differential cell staining using Giemsa stain. This highly emphasized the conformity of the nano-immobilized grafts with the biocompatibility requirements for biomedical applications.

In the fourth study: we attempted to produce biocompatible graft by immobilization of heparin. Moreover, the combination of heparin and collagen presents synergic properties of thrombus resistance and cytocompatibility, therefore, the co-immobilization of heparin/collagen onto woven and knitted forms of crimped PET grafts was also investigated. Heparin is the commonly used anticoagulant that forms a complex with anti-thrombin III. The heparin anti-thrombin III complex inactivates serine proteases, most importantly thrombin, which catalyzes the conversion of fibrinogen to fibrin in the final step of the coagulation cascade reaction [26]. In addition, collagen

is the main component of the extracellular matrix on which the endothelial cells could adhere, proliferate, and differentiate [27]. However, the inert architecture of PET entails the functionalization of surface for immobilization purpose. The successful covalent co-immobilization of heparin and collagen was confirmed by XPS spectra of heparin-immobilized PET (PET-Hep) and heparin/collagen co-immobilized PET (PET-Hep-Col). In accordance with XPS spectra of PET-Hep, the concentration of heparin on the surface as detected by toluidine blue assay indicated the effective immobilization of heparin on the surface. Therefore, the biological activity of modified grafts was evaluated *in-vitro* under human-mimic conditions.

The results demonstrated intense clot after 10 minutes blood contact on unmodified PET surface. However, the fibrin deposition profile of unmodified PET presented wide net of fibrin fibers confirming highly thrombogenic characteristics at early time points. Unlike to unmodified graft, PET-Hep and PET-Hep-Col exhibited substantial resistance to clot and fibrin formation. This is attributed to the neutralization effect of heparin on thrombin formation. Moreover, the activated platelets can only adhere and aggregate if significant blood proteins adsorb on the graft surface [5,28,29], consequently, the inhibition of fibrin precipitation on the surface decreased the number of activated platelets and hence its deposition. Based on this, the stimulation of anti-thrombin III by heparin along with inhibition of factor Xa prevented the conversion of pro-thrombin to thrombin. Subsequently, the protein adsorption and platelets deposition on the surface were decreased. Conversely, addition of collagen supported the protein adsorption to some extent on the PET surface and increased the number of deposited platelets. As a result, collagen restricts the solitary use in the application for blood contacting biomaterials. Nevertheless, the co-immobilization of heparin and collagen showed synergic inhibition effect of platelets deposition after 30 minutes continuous flow condition which defines the cardiovascular graft patency.

Otherwise, the mucopolysaccharide structure of heparin is a natural component of arterial cell

wall that decreases the surface hydrophobicity and encourages cell adhesion on the graft surface [27,30,31]. This explained the insignificant increase in the number of the adhered cells on PET-Hep compared to unmodified PET. Interestingly, collagen co-immobilization significantly enhanced the cell adhesion and growth by presenting a surface supplemented with natural connective component in endogenous extracellular matrix [28]. The beneficial effect of collagen on cell adhesion and growth was additionally confirmed by differential cell staining using Giemsa stain. This highly emphasized the enhancement of cell growth 5 days after cell culturing on PET-Hep-Col compared to either unmodified PET or PET-Hep. This confirmed the dependency of cell adhesion mainly on the surface properties.

Perspective

Prosthetic medical grafts, particularly, PET cardiovascular grafts have become an essential part of modern medicine and acquired an enlarged interests due to the significant improvement of patient's life quality after grafts implantation. However, development the quality and stability of implanted PET are still considered as the most challenges for prosthetic cardiovascular grafts. We attempted in this thesis to improve the biocompatibility and the resistance to infection of PET grafts in aim to increase the PET long-term patency. The employed strategies revealed an effective bacterial anti-adhesion efficiency by the network-structured polymer film coat, and to a higher extent, by lysozyme enzyme immobilization. The biocompatibility of the modified grafts was also established to offer anti-thrombotic PET grafts that ensure the rapid host healing. Furthermore, synergistic inhibition of platelets deposition and fibrin formation was accomplished by co-immobilization of heparin and collagen on the graft's surface. The heamocompatibility of the performed PET grafts showed fast natural host cell coverage. Interestingly, the coating of cardiovascular grafts with nanoparticles demonstrated advantageous model to load suitable drugs for treatment of the common complications after implantation.

Nevertheless, we are still encouraged for advanced studies proposed to evaluate the activity of immobilized nanoparticles in terms of local drug release, and finally, to investigate the proficiency of the described strategies *in-vivo*.

Zusammenfassende Diskussion

Kardiovaskuläre Prothesen stellen die Funktion beschädigter Gefäße und Herzklappen wieder her [1,2,3]. Solche Prothesen aus geknäueltem PET Gewebe sind, trotz der mit ihm verbundenen Komplikationen, das effektivste eingesetzte Biomaterial [1,2,3]. Infektionen und Reaktionen des Patienten beschädigen jedoch oft Implantat und umliegendes Gewebe, so dass ein Ersatz des Implantates nötig wird [4,5]. In der vorliegenden Arbeit wurden PET Implantate mit einem neu synthetisierten SD-PHA-b-MPEO-Diblock-Polymer beschichtet, dessen Vorteile seine negative Ladung, die Hydrophobizität und die antibakterielle Wirkung der Sulfadimethoxin (SD) Einheit sind. Die Struktur der eingesetzten Polymere wurde, vor ihrer Verwendung, durch Kernresonanzspektroskopie (NMR), sowie IR und UV Spektroskopie überprüft [6].

Wir beabsichtigten die Bildung eines porösen Filmes, durch welchen die mechanischen Eigenschaften des Implantates erhalten bleiben. Die Bildung des Filmes erfolgt durch Verdampfung einer wasserunlöslichen Polymerlösung in gesättigter Atmosphäre. Der gebildete Film besitzt antibakterielle Eigenschaften und verschafft dem PET-Implantat günstige Eigenschaften in Bezug auf Zelladhäsion und Wachstum. Dies ist vielversprechend für das Erreichen einer hohen Bedeckung des Implantates mit autologen Zellen. Die zugrundeliegenden Überlegungen basieren darauf, dass Adhäsion und Wachstum von Zellen auf einer PET-Oberfläche von mehreren Faktoren abhängen. Dies sind die Hydrophobizität, die Porosität, die Elektronegativität, die mechanische Eigenschafen und, im Besonderen, der Abstand zwischen den Fäden des Gewebes [8,9]. Der hydrophobe Anteil des Block-Polymers sowie die negativen Ladungen behindern die Zelladhäsion nur in geringem, nicht signifikantem, Ausmaß. Darüber hinaus hilft die gebildete Beschichtung, die Abstände innerhalb des Gewebes zu verkürzen. Das geht so nicht raus. Im Ergebnis überwucherten L929-Zellen das beschichtete PET (PET-Netz) und eine Monolage aus Zellen konnte nach 7 Tagen erreicht werden.

Die, In-Vitro bestimmte, antiadhäsive Wirkung des PET-Netzes gegen 3 verschiedene Bakterienstämme, S. epidermidis, S. aureus und E. Coli (Repräsentativ für die häufigsten Gram-positiven und Gram-negativen Pathogene) zeigte eine hochsignifikante Reduktion der Adhäsion aller voranstehend genannten Stämme, verglichen mit unmodifiziertem PET (P=0.003). Wir bestätigten unsere Ergebnisse durch Verwendung eines aggressiven pathogenen Stammes Gram-Positiver S. epidermidis, welcher aus dem Venenkatheter eines Patienten isoliert wurde. In der Tat tendieren Bakterien eher zur Anlagerung und Koloniebildung auf neutralen und hydrophilen als auf hydrophoben Oberflächen [4]. Dies wird durch das Vorhandensein von Polyhexylen und Sulfadimethoxin-Gruppen in der gebildeten Beschichtung verhindert, durch welche die Oberfläche Hydrophob und negativ geladen wird. Darüber hinaus unterstützt die Bakterien-abstoßende Wirkung des Polyethylen-Oxids die antibakterielle Wirkung der Sulfadimethoxin-Gruppen, wodurch die Oberfläche des Gewebes noch ungeeigneter für die Anhaftung von Bakterien wird. Darüber hinaus kann die Adhäsion von Bakterien nicht nur durch Elektronegativtät und Hydrophobizität, sondern auch durch Porosität der Oberfläche beeinflusst werden [10,11]. Die geringe Porosität des PET-Netzes ist für bakterielle Adhäsion weniger günstig.

In der zweiten Studie wurde PET-Gewebe mit Lysozym modifiziert, um die Eigenschaft des Lysozyms, ß(1-4)glykosidische Bindungen zu spalten, zu nutzen. Die Spaltung dieser Bindung in der bakteriellen Zellwand bewirkt einen effektiven Schutz gegen bakterielle Adhäsion und Biofilmbildung. Die Anbindung des Lysozym auf die Oberfläche des kardiovaskulären PET-Implantates wurde mittels XPS-Spektren von nativem Lysozym und unmodifiziertem PET im Vergleich mit PET-gebundenem Enzym überprüft. Trotz einer leicht verminderten enzymatischen Aktivität des gebundenen Enzyms, verglichen mit dem freien Enzym, wurden eine offensichtliche anti-adhäsive Wirkung des immobilisierten Enzyms gegen Gram-Positive S. aureus, S. epidermidis

und Gram-negative E.coli festgestellt. Die Ergebnisse zeigten eine besser Aktivität des PET-Enzym-Gewebes gegen Gram-positive als gegen Gram-Negative Bakterien. Dies ist darauf zurückzuführen, das Lysozym, eine Glykosid-Hydrolase, die ß(1-4)-glykosydische Bindung zwischen N-Acetylmuraminsäure und N-Acetyl-D-Glucosamin-Resten im Peptidoglycan der bakteriellen Zellwand spaltet [12,13]. Die anvisierten ß(1-4)-glykosydische Bindungen sind in gram-positiven Bakterien und in großer Zahl vorhanden, wohingegen sie bei Gram-Negativen Bakterien durch eine äußere Membran geschützt sind [14]. In Folge dessen haben die Enzyme auf dem PET-Gewebe leichten Zugang zu den Strukturen bei Gram-negativen Bakterien, was zum Abbau der bakteriellen Zellwand und somit auch zu Zell-Lyse und Tode der Bakterien führt. Diese Erkenntnis verspricht eine Verhinderung der Bakterien-Film-Bildung [13,14,15]. Im Gegensatz dazu sind die ß(1-4)-glykosydischen Bindungen in der Zellwand Gram-negativer Bakterien unter einer Schicht von Lipoproteinen verborgen, und nur wenige dieser Bindungen befinden sich in den Pili an der Oberfläche. Daher beschränkt sich in diesem Fall die enzymatische Wirkung auf die Pili und die bakterielle Adhäsion, jedoch ohne Effekt auf die Struktur der Zellwand [13,14,15]. Das neu hergestellte PET-Enzym-Gewebe trotzdem Wirkung gegen Gram-Negative Bakterien zeigt, könnte dadurch erklärt werden, das selbst irreversibel inaktiviertes Lysozym antibakterielle Wirksamkeit besitzt, was nahelegt, das die Wirkung nicht nur auf Enzymaktivität sondern auch auf dem basischen Charakter des Enzyms beruht [15].

In unserer Studie zeigte sich, dass gewebtes Implantat Material für die Anhaftung von Bakterien weitaus besser prädestiniert ist als gestricktes Material. Bakterielle Adhäsion könnte theoretisch auch durch andere Faktoren als Lysozym, wie zum Beispiel Porosität des Gewebes, Oberflächenspannung und Elektronegativität beeinflusst worden sein[16]. Nach unseren Ergebnissen macht die geringe Porosität des gewebten PET es geeigneter für die Anhaftung von Bakterien. Um ein vollständiges Einwachsen des Implantates zu gewährleisten, ist es wichtig, dass

das Implantat vollständig von den Zellen des Patienten bedeckt wird. Dieser Vorgang kann durch die Anlagerung von Bakterien und die Ausbildung eines Biofilmes gestört werden. Alle in dieser Studie genutzten PET-Gewebe wurden von L929-Zelle, welche als Modell genutzt wurden, zügig überwuchert. Nach Immobilisierung des Enzyms wurde kein signifikanter Unterschied in der Zahl der anhaftenden Zellen festgestellt. Ein Trend zu einer erhöhte Anzahl anhaftender Zellen auf PET-Enzym-Gewebe zeigte keine statistische Signifikanz. Zusammengefasst gesagt sind die Ergebnisse konforme mit den Biokompatibilitäts-Anforderungen an Gewebe für medizinische Anwendungen.

In der dritten Studie konzentrierten wir uns auf Erhöhung der Durchlässigkeit des Gewebes durch lokales Einbringen hydrophiler Substanzen mittels bioabbaubarer PLGA-Nanopartikel als Träger und mit FITC-Dextran (FD) als wasserlösliches Drug-Model. Die Nanopartikel wurden kovalent auf PET-Gewebe und auf ePTFE (expanded PTFE)-Gewebe, nach Oberflächenfunktionalisierung, immobilisiert. Die funktionellen Aminogruppen wurden direkt auf dem PET, durch Aminolyse-Reaktion unter Verwendung von Ethylendiamin zur selektiven Spaltung der Esterbindungen in der PET-Oberflächen [17]dargestellt. Die Charakterisierung des aminolierten Gewebes durch Messung des Oberflächenpotentials zeigte ein negatives Potential über einen weiten pH-Bereich, bedingt durch Ionisation der an der Oberfläche befindlichen Aminogruppen mit isoelektrischem Punkt um pH= 7-8, und bestätigte somit die erfolgreiche Funktionalisierung. ePTFE wurde durch Reaktion von 3-Aminopropyl Triethoxysilan, unter Zuhilfenahme von Piranha-Lösung, mit vorher dargestellten OH-Gruppen funktionalisiert. Der Erfolg der Einführung der Aminogruppe auf ePTFE konnte mittels FTIR gezeigt werden, wobei die charakteristische Amino-Bande darstellbar war [20]. Im Anschluss daran wurden die Aminogruppen auf der Oberfläche mittels Glutaraldehyd aktiviert und als Ankerstellen für die kovalente Anbindung von Carboxylgruppen der PGLA-Nanopartikel benutzt. Die Nanopartikel wurden aus bioabbaubarem PLGA-Polymer hergestellt.

Das Ziel war eine lokale, kontrollierten Freisetzung der in den Partikeln enthaltenen hydrophilen Wirkstoffe sowie eine hohe Stabilität der erhaltenen Partikel. Die PLGA Nanopartikelsuspension wurde vor der Immobilisierung an der Implantat Oberfläche erstmals mit Tween 80 stabilisiert. Der Anstieg in der Größe der FD-beladenen Nanopartikel im Vergleich mit unbeladenem Nanopartikeln ist durch Erweiterung der Polymermatrix bei FD-Einbau bedingt [22]. Alle Partikel besitzen eine ideale Oberflächenladung, was darauf hindeutet, dass das Tensid und\oder FD-Dextran keine maskierenden Einfluss auf die Carboxylgruppen an der Oberfläche ausüben [23].

Die Effektivität der Bedeckung kardiovaskulärer Implantate mit Nanopartikeln hängt auch davon ab, ob bei starkem Blutfluss eine lokale, kontrollierte Freisetzung der eingeschlossenen Wirkstoffe erreicht wird. Deshalb wurde die Stabilität der Nanopartikel in vitro, unter Bedingungen, die denen im Menschen vergleichbar sind, getestet. Die gezeigte Stabilität der Monolayer-Oberflächenbeschichtung auf Nano-Immobilisierten Implantaten (PET-NPs und ePTFE-NPs) nach 24 Stunden starkem, kontinuierlichem Fluss zeigt, dass diese ein geeigneter Träger für kontrollierten Wirkstofftransport über den Testzeitraum sind. Nichtsdestotrotz ist die Fähigkeit von PET-NPs und ePTFE-NPs zur Unterstützung der Anhaftung von Wirtszellen entscheidend und abhängig von der Oberflächentopographie, Hydrophobizität und Porosität [24,25]. Interessanterweise wurde die getesteten Implantate von den L929-Zellen zügig überwachsen und es trat keine signifikanter Unterschied in der Zahl anhaftender Zellen zwischen PET-NPs und ePTFE-NPs, verglichen mit unmodifizierten Transplantaten, auf. Dies unterstreicht deutlich, dass die Nano-immobilisierten Implantate mit den Biokompatibilitäts-Anforderungen für biomedizinische Anwendung konform gehen.

In der vierten Studie versuchten wir, biokompatible Transplantate durch Immobilisierung von Heparin herzustellen. Die Kombination aus Heparin und Kollagen besitzt synergistische Eigenschaften bei Thrombus-Resistenz und Zellverträglichkeit, daher wurde die Co-Immobilisation von Heparin und Collagen auf Transplantaten aus gewebtem und geknäueltem PET untersucht. Heparin ist das am häufigsten verwendete Antikoagulanz und bildet einen Komplex mit Antithrombin III. Der Heparin-Antithrombin III-Komplex inaktiviert Serinproteasen (hauptsächlich Thrombin) welche die Umwandlung von Fibrinogen in Fibrin im letzten Schritt der Gerinnungskaskade katalysiert [26]. Zusätzlich ist Kollagen die Hauptkomponente der extrazellulären Matrix, auf welcher die Endothelzellen anhaften, proliferieren und differenzieren können [27]. Die inerte Struktur der PET-Oberfläche macht eine Funktionalisierung für Immobilisierungen erforderlich. Der Erfolg der Co-Immobilisation von Heparin und Collagen wurde durch XPS-Spektren von PET mit immobilisiertem Heparin (PET-Hep) und PET mit co-immobilisiertem Heparin\Collagen (PET-Hep-Col) bestätigt. In Übereinstimmung mit den XPS-Spektren von PET-Hep, bestätigte die durch Toluidin-Blau-Anfärbung bestimmte Oberflächenkonzentration die effektive Immobilisierung von Heparin an der Oberfläche. Deshalb wurde die biologische Aktivität der modifizierten Transplantate in Vitro unter Menschen-Ähnlichen Bedingungen bestimmt.

Die Ergebnisse zeigen eine starke Thrombusformation auf unmodifizierter PET-Oberfläche nach ca. 10 Minuten. Das Verteilungsmuster von Fibrin auf unmodifiziertem PET zeigt ein weites Netz von Fibrins-Faser, was auf hohe thrombogene Eigenschaften schon zu frühem Zeitpunkt hinweist. Anders als bei unmodifizierten Implantaten, zeigten PET-Hep und PET-Hep-Col eine merkliche Resistenz gegen Thrombusbildung und Fibrinadhäsion. Die wird auf den hemmenden Effekt des Heparins auf die Thrombin-Bildung zurückgeführt. Darüber hinaus, können die aktivierten Plättchen sich nur dann anlagern und aggregieren, wenn signifikante Blutproteine sich auf der

Oberfläche anlagern [5,28,29]. Demzufolge senkt die Inhibierung der Fibrin Adhäsion die Anzahl und Ablagerung aktivierter Plättchen. Darauf basierend, verhinderte die Stimulation von Anti-Thrombin III durch Heparin, zusammen mit der Inhibierung von Faktor Xa, die Umwandlung von pro-Thrombin in Thrombin. Infolge dessen wurden die Proteinabsorption und die Plättchen-Ablagerung auf der Oberfläche vermindert. Im Gegensatz dazu wirkte das Hinzufügen von Collagen zur PET-Oberfläche zu einem gewissen Grads unterstützend auf die Proteinadsorption und erhöhte die Zahl der angelagerten Plättchen. Das Ergebnis hiervon ist, das Collagen als alleinige Oberflächenbeschichtung von Biomaterialien, die Kontakt mit Blut haben, ungeeignet ist. Dennoch zeigt die Co-Immobilisierung von Heparin und Collagen einen synergetischen inhibierenden Effekt auf die Anlagerung von Plättchen nach 30 Minuten kontinuierlichem Fluss, was die Durchgängigkeit des kardiovaskulären Implantates ausmacht.

Die Polysacharidstruktur des Heparins ist ein natürlicher Bestandteil der arteriellen Zellwand, welcher die Hydrophobizität senkt und Zelladhäsion auf der Oberfläche des Transplantates erleichtert [27,30,31]. Dies erklärt den insignifikanten Anstieg der Zahl anhaftender Zellen auf PET-Hep im Vergleich mit unmodifiziertem PET. Interessanterweise erhöhte Collagen-Co-Immobilisierung die Zelladhäsion und Wachstum signifikant, indem eine Oberfläche mit einem Anbindungspunkt, welcher auf in der endogen zellulären Matrix vorkommt, geschafften wird [28]. Der begünstigende Einfluss des Kollagens auf Zellanhaftung und Wachstum wurde durch Giemsa-Färbung zusätzlich bestätigt. Durch die Verbesserung des Zellwachstums nach 5 Tagen aus PET-Hep-Col im Vergleich mit unmodifiziertem PET und PET-Hep wird dies unterstrichen. Es bestätigt sich, dass die Zelladhäsion vor allem von den Eigenschaften der Oberfläche abhängt.

Ausblick

Künstliche medizinische Implantate, insbesondere Herz-Kreislauf Implantate aus PET, sind zu einem wesentlichen Bestandteil der modernen Medizin geworden und erlangen ein stetig vergrößertes Interesse aufgrund der deutlichen Verbesserung der Lebensqualität des Patienten nach Implantation. Allerdings gelten die Verbesserung der Qualität und der Stabilität von PET Implantaten immer als Herausforderungen im Bereich der künstlichen Herz-Kreislauf Implantate. In dieser Arbeit konnten wir die Biokompatibilität und das Infektionsrisiko von PET Implantate verbessern, mit dem Ziel, die langfristige Verträglichkeit zu steigen. Die eingesetzten Strategien zeigten einen wirksamen antiadhäsiven Effekt auf Bakterien durch den netzwerkartigen multifunktionalen Oberflächenüberzug und zu einem höheren Grad durch Lysozym Immobilisierung. Die Biokompatibilität der modifizierten Transplantate zeigte auch einen antithrombotischen Effekt der PET Implantate, der eine schnelle Heilung gewährleistete. Weiterhin wurde die Thrombozyten- und Fibrinanlagerung durch synergistische Co-Immobilisierung von Heparin und Kollagen auf der Implantatoberfläche vermindert. Die Blutverträglichkeit der hergestellten PET Implantate führte zu einer schnellen Besiedelung mit Zellen des Zielgewebes. Interessanterweise erwies sich die Beschichtung von kardiovaskulären Implantaten mit Nanopartikeln als eine geeignete Methode Arzneistoffe zur Behandlung der häufigsten Komplikationen nach der Implantation freizusetzten. Dennoch sind immer noch weiterführenden Studien nötig, um die Freisetzungseigenschaften der immobilisierten Nanopartikel für die lokalen Wirkstoffabgabe zu untersuchen und letztendlich die beschriebenen Modelle *in vivo* zu testen.

References

[1] Desai M, Seifalian A, Hamilton G. Role of prosthetic conduits in coronary artery bypass grafting. Eur J Cardiothorac Sur. 2011;40: 394-98

[2] Butany J, Collins J. Analysis of prosthetic cardiac devices: a guide for the practising pathologist. J ClinPathol. 2005;58:113-24

[3] William F. The williams dictionary of biomaterials, Liverpool university press, Liverpool. 1999

[4] Sabe M, Shrestha N, Menon V. Contemporary drug treatment of infective endocarditis. Am J Cardiovasc Drugs. 2013;13:251-8

[5] Vroman L. The life of an artificial device in contact with blood: initial events and their effect on its final state. Bull NY Acad Med.1988;64:352-57

[6] Assem Y, Greiner A. Biodegradable amphiphilic block copolymers: synthesis, characterization and properties evaluation. Philipps university. Marburg. 2011

[7] Xiong X, Lin M, Zou W, Liu X. Kinetic control of preparing honeycomb patterned porous film by the method of breath figure. Reactfuncpolym. 2011;71:964-71

[8] Eskin S, Trevino L, Chimoskey J. Endothelial cell culture on Dacron fabrics of different configurations. J Biomed Mater Res. 1978;12:517-24

[9] Oloffs A, Grosse-Siestrup C, Bisson S, Rinck M, Rudolph R, Gross U. Biocompatibility of silver-coated polyurethane catheters and silver-coated Dacron material. Biomaterials. 1994;15:753-55

[10] Friedlander R, Vlamakis H, Kim P, Khan M, Kolter R, Aizenberg J. Bacterial flagella explore microscale hummocks and hollows to increase adhesion.PNAS.2013;110:5624-9

[11] Katsikogianni M, Syndrevelis C, Amanatides E, Mataras D, Missirlis Y. Plasma treated and C:H coated PET performance in inhibiting bacterial adhesion. Plasma Process. Polym. 2007;4:1046-51

[12] Pellegrini A, Thomas U, Fellenberg R, Wild P. Bactericidal activities of lysozyme and aprotinin against Gram-negative and Gram-positive bacteria related to their basic character. J Appl Micro.1992;72:180-7

[13] Chaignon P, Sadovskaya I, Ragunah C, et.al. Susceptibility of staphylococcal biofilms to enzymatic treatments depends on their chemical composition. Appl Microbiol Biotechnol. 2007;75:125-32

[14] Rodrigues L. Inhibition of bacterial adhesion on medical devices. In: Rodrigues L editor “Bacterial Adhesion”. Goldman. 2010;351-67

[15] Qiu Y, Zhang N, An Y, Wen X. Biomaterial strategies to reduce implant-associated infections. Int J Artif Organs. 2007;30:828-41

[16] Abbott A, Rutter P. The influence of ionic strength, pH and a protein layer on the interactions between Streptococcus mutans and glass surfaces. J Gen Microbiol. 1983; 129:439-45

[17] Muthuvijayan V, Gu J, Lewis R. Analysis of functionalized polyethylene terephthalate with immobilized NTPDase and cysteine. ActaBiomaterialia. 2009;5:3382-93

[18] Butterworth M, Corrad R, Johal J, Lascelles F, Maeda S, Armes P. Zeta potential measurements on conducting polymer-inorganic oxide nanocomposite particles. J. Coll&interfac. 1995;174:510-17

[19] Löhbach C, Bakowsky U, Kneuer C, Jahn D, Graeter T, Schäfers HJ, Lehr CM. Wet chemical modification of PTFE implant surfaces with a specific cell adhesion molecule. Chem. Commun. 2002;2568-69

[20] Griffiths P, Hasseth J. Fourier transform infrared spectroscopy.2nd Wiley-Blackwell. 2007

[21] Mao S, Xu J, Cai C, Germershaus O, Schaper A, Kissel T. Effect of WOW process parameters on morphology and burst release of FITC-dextran loaded PLGA microspheres. Int. J. Pharm. 2007;334:137-48

[22] Giannavola C, Bucolo C, Maltese A, Paolino D, Vandelli MA, Puglisi G, et.al. Influence of preparation conditions on acyclovirloadedpoly-d,l-lactic acid nanospheres and effect of PEG coating on ocular drug bioavailability. Pharm. Res. 2003;20:584-90

[23] Muller RH. Charge determinations. In: Muller RH editor, Colloidal carriers for controlled drug delivery and targeting modification, characterization and in vivo. CRC, Baca Raton.1991

[24] Lei Y, Remy M, Labrugere C, Durrieu M. Peptide immobilization on polyethylene terephthalate surfaces to study specific endothelial cell adhesion, spreading and migration. J Mater Sci Mater Med. 2012;23:2761

[25] Yu F, Mücklich F, Li P, Shen H, Lehr C, Bakowsky U. In vitro cell response to a polymer surface micropatterned by laser interference lithography. Biomacromolecules. 2005;6:1160

[26] Linhardt R, Claude S. Hudson Award address in carbohydrate chemistry. Heparin: structure and activity. J. Med. Chem. 2003;19: 2551

[27] Burrows M, Zamarion V, Filippin-Monteiro F, Schuck D, Toma H, Campa A, et al. Hybrid scaffolds built from PET and collagen as a model for vascular graft architecture. Macromol Biosci. 2012;12: 1660

[28] Roald H., Barstad R, Bakken I, Roald B, Lyberg T, Sakariassen K. Initial interactions of platelets and plasma proteins in flowing non-anticoagulated blood with the artificial surfaces Dacron and PTFE. Blood Coagul Fibrinolysis. 1994;5: 355

[29] Park K, Kim W, Jacobs H, Okano T, Kim S. Blood compatibility of SPUU-PEO heparin graft-copolymers. J Biomed Mater Res. 1992;26: 739

[30] Leijon J, Carlsson F, Brännström J, Sanchez J, Larsson R, Nilsson B, et al. Attachment of flexible heparin chains to gelatin scaffolds improves endothelial cell infiltration. Tissue Eng Part A. 2013; 19: 1336

[31] Yu J, Wang A, Tang Z, Henry J, Ping L, Lee B, et al. The effect of stromal cell-derived factor-1α/heparin coating of biodegradable vascular grafts on the recruitment of both endothelial and smooth muscle progenitor cells for accelerated regeneration. Biomaterials. 2012;33:8062

Summary

In chapter 1: Polyethylene terephthalate (PET) is considered as the gold standard cardiovascular graft to restore the function of damaged vessels and heart valves. However, the post implantation complications essentially distract the long-term patency of PET grafts resulting in prolonged hospitalization, graft failure, and patient death. Most of the prominent shortcomings of PET are the substantial thrombogenic property and the associated infections as well as the biocompatibility issues. Therefore, in this thesis, the improvement of the biocompatibility and the infection-resistance properties of PET grafts were our foremost perspective. We fundamentally minimized the bacterial adhesion and enhanced the biocompatibility of woven and knitted forms of crimped PET cardiovascular grafts. Our results proved an effective strategy for graft surface modification in terms of biocompatible and infection-resistant.

In chapter 2: the initial bacterial adhesion was minimized by a multifunctional network-structured film coat using a newly synthesized amphiphilic SD-PHA-b-MPEO diblock copolymer. A versatile coating technique was described based on the repulsion forces between the surface and the used polymer to preserve the flexibility and tensile ability of crimped PET grafts. The surface modified graft was confirmed by Fourier transform infrared spectroscopy (FTIR) and by scanning electron microscope (SEM). The employed polymer manifested suitable biocompatibility to host cell as established using mouse L929 fibroblast cell line. Importantly, the negative charge and the hydrophobic properties of the polymer augmented the bactericidal effect of the sulfadimethoxine moiety as reported by the significant bacterial anti-adhesion efficiency for Gram-positive *S. aureus* and Gram-negative *E. coli* bacteria, and for the previously vein isolated Gram-positive *S. epidermidis.*

In chapter 3: Unlike previous studies, the bacterial adhesion was enzymatically inhibited using a bacterial lytic enzyme, lysozyme. Accordingly, graft with broad-spectrum bacteria-resistant was developed. The lysozyme enzyme was covalently immobilized on PET graft by end-point method and proved by FTIR and X-ray photoelectron spectroscopy (XPS). The activity of immobilized enzyme against *M. lysodeikticus* cells displayed a significant reduction as compared to the free enzyme. However, the remaining activity remarkably decreased the adhesion of Gram-positive *S. epidermidis* and *S. aureus* bacteria and to less extent of Gram-negative *E.coli*. The anti-adhesion efficiency showed bacterial cells specificity while, showed no significant effect on L929 cells adhesion and growth. This indicated the utility of the employed strategy to modulate the initial bacteria adhesion to inhibit the graft-associated infection.

In chapter 4: FITC-dextran loaded Poly lactic-glycolic acid (PLGA) nanoparticles were covalently immobilized onto two different cardiovascular prostheses namely; woven crimped PET and expanded polytetrafluoroethylene (ePTFE, Teflon®). The grafts surface was modified by introduction of amino groups on the surface. The surface modified graft was characterized by electro kinetic analyzer, and FTIR before the covalent coupling to the carboxyl group of PLGA Nanoparticles was performed. The prepared model manifested homogenous monolayer of nanoparticles on grafts surface and displayed a satisfactory stability under appropriate human-mimic continuous flow conditions for 24h. Additionally, the established biocompatibility of nano-coated grafts highlighted the utility of the immobilized nanoparticles on the graft's surface as an attractive strategy for local drug delivery to treat the common complications after graft's implantation, and hence increasing the grafts long-term patency.

In chapter 5: A thrombus-resistant graft was developed by covalent immobilization of heparin. Additionally, the host cell compatibility of PET grafts was enhanced by co-immobilization of collagen. Heparin and collagen were immobilized by end-point method into previously functionalized PET grafts and characterized using FTIR and XPS. The modified grafts manifested a significant biological activity *in-vitro* under human-mimic conditions mainly, substantial resistance of the graft to clot and fibrin formation. Importantly, the co-immobilization of heparin and collagen supported the host cell adhesion and growth, and showed synergistic inhibition effect of platelets deposition after continuous flow for 30 minutes to simulate the massive blood flow conditions. Consequently, this approach minimized the inherent thrombogenicity of the PET grafts and the corresponding host response, hence ensuring a rapid coating of grafts with host cells required for the grafts biocompatibility.

Zusammenfassung

Im Kapitel 1 Polyethylenterephthalat (PET) wird als der Goldstandard in der Therapie mit kardiovaskulären Implantaten wie z.B. künstlichen Herzklappen oder Gefäßen angesehen. Trotzdem gibt es Komplikationen nach der Implantation, die erhebliche Probleme in der Langzeit-Anwendung verursachen, wie z.B. Krankenhausaufenthalte, undichte Implantate oder sogar Tod des Patienten. Hierbei sind die am häufigsten auftretenden Probleme von PET die Biokompatibilität, die hohe thrombotische Aktivität und das damit verbundene Infektionsrisiko. Aus diesem Grund wurde in der vorliegenden Arbeit neben der Verbesserung der Biokompatibilität besonderer Wert auf die Reduzierung von Infektionen bei PET Implantaten gelegt. Wir konnten die Anhaftung von Bakterien deutlich reduzieren, und die Biokompatibilität von gekräuselten kardiovaskulären Implantaten aus gewebtem und gestricktem PET verbessern. Unsere Ergebnisse zeigen eine effiziente Möglichkeit durch Oberflächenmodifikation von Implantaten die Biokompatibilität dieser zu verbessern und ihre Resistenz gegen Infektionen zu erhöhen.

Im Kapitel 2 konnte die primäre bakteriellen Adhäsion bei Infektionen durch einen netzwerkartigen multifunktionalen Oberflächenüberzug aus einem neu synthetisierten amphiphilen SD-PHA-b-MPEO Diblockcopolymer minimiert werden. Das beschriebene vielseitig anwendbare Beschichtungsverfahren basiert hierbei auf den Abstoßungskräfte zwischen der Oberfläche und dem verwendeten Polymer, um die Flexibilität und Reißfähigkeit des gekräuselten PET Transplantates zu erhalten. Das oberflächenmodifizierte Implantat wurde mittels Fourier-Transformations-Infrarot-Spektroskopie (FTIR) und dem Rasterelektronenmikroskop (SEM) charakterisiert. Das eingesetzte Polymer manifestierte geeignete Biokompatibilität gegenüber dem Zielgewebe, was mit L929 Mausfibroblasten nachgewiesen werden konnte. Wichtig ist, dass

die negative Ladung und die hydrophoben Eigenschaften des Polymers die bakterizide Wirkung der Sulfadimethoxin-Einheit verstärkte. Diese wurde schon als signifikanter bakterieller Anti-Adhäsionseffekt für grampositive *S. aureus*, gramnegativen *E. coli* Bakterien, sowie für die zuvor aus einer Vene isolierten grampositiven *S. epidermidis* berichtet.

Im Gegensatz zu früheren Studien konnte **im Kapitel 3** die bakterielle Adhäsion enzymatisch mit Hilfe des bakteriellen lytischen Enzyms Lysozym verhindert werden. Somit konnte ein Implantat mit einer Breitspektrumresistentz gegen Bakterien entwickelt werden. Das Enzym Lysozym wurde kovalent auf dem PET Implantat durch die „end-point" Methode immobilisiert und mittels FTIR- und Röntgenphotoelektronenspektroskopie (XPS) nachgewiesen werden. Die Aktivität des immobilisierten Lysozyms gegen *M. lysodeikticus* zeigte eine signifikante Reduktion im Vergleich zum freien Enzym. Allerdings reichte die Restaktivität aus, um die Adhäsion von grampositiven *S. epidermidis* und *S. aureus* Bakterien und in geringerem Maße von gramnegativen *E. coli* zu verringern. Der antiadhäsive Effekt war Bakterienzellen spezifisch, während keine signifikante Wirkung auf Adhäsion und Wachstum von L929 Zellen sichtbar war. Dies zeigte den Nutzen der verwendeten Strategie, um die anfängliche Adhäsion der Bakterien zu modulieren und die Implantat-assoziierte Infektion zu behindern.

In Kapitel 4 wurden FITC-Dextran beladenen Poly-Milchsäure-Glykolsäure (PLGA)-Nanopartikel kovalent an zwei verschiedenen Herz-Kreislauf-Prothesen, nämlich gewebt gekräuselten PET und expandiertem Polytetrafluorethylen (ePTFE, Teflon ®), immobilisiert. Vor der Immobilisierung wurde die Implantate Oberfläche durch Einführung einer Aminogruppe an der Oberfläche aktiviert. Die so oberflächenmodifizierten Implantate wurden vor der kovalenten Bindung der PLGA-Nanopartikel über ihre Carboxylgruppe durch einen elektrokinetische Analysator und FTIR

charakterisiert. Das so hergestellte Modell wies eine homogene Monoschicht aus Nanopartikeln auf der Implantatoberfläche auf und zeigte eine zufriedenstellende Stabilität unter geeigneten menschenähnlichen kontinuierlichen Fließbedingungen innerhalb von 24 Stunden. Die erreichte Biokompatibilität der nanostrukturierte Implantatoberfläche ermöglicht bei Verwendung immobilisierter Nanopartikel an der Oberfläche einen vielversprechenden Therapieansatz für die lokale Arzneimittelabgabe, um die häufigsten Komplikationen nach dem Einsetzen des Implantates zu behandeln, und damit die Verträglichkeit langfristig zu verbessern.

In Kapitel 5 wurde die thrombotische Aktivität eine Implantat durch die kovalente Immobilisierung von Heparin reduziert. Zusätzlich wurde die Verträglichkeit der PET Implantate gegenüber dem Zielgewebe durch Co-Immobilisierung von Kollagen verbessert. Heparin und Kollagen wurden mittels „end-point“ Methode an die vorher funktionalisierten PET Implantate immobilisiert und mittels FTIR und XPS charakterisiert. Die modifizierten Implantate zeigten eine signifikante biologische Aktivität *in vitro* unter menschenähnlichen Bedingungen, insbesondere die Verminderung der Thrombus- und Fibrinbildung. Die Co-Immobilisierung von Heparin und Kollagen ist entscheidend für die Adhäsion und das Wachstum der Zielgewebezellen. Zusätzlich konnte ein synergistischer Effekt zur Verminderung der Thrombozytenanlagerung nach 30 min unter kontinuierlichen Fließbedingungen, die einen starken Blutfluss simulierten, gezeigt werden. Folglich minimiert dieser Ansatz die thrombotische Aktivität der PET Implantate und die entsprechende Reaktion des Zielgewebes, wodurch eine rasche Besiedelung der Implantate mit Zellen des Zielgewebes erreicht wird, was für die Biokompatibilität erforderlich ist.

Appendices

Abbreviation list

AT III	Anti-thrombin enzyme
DMEM	Dulbecco`s modified Eagle´s medium
EBSS	Earle`s balanced salt solution
E. coli	Escherichia coli
EDC	1-Ethyl-3-(3-dimethyl amidopropyl) carbodiimide hydrochloride
ePTFE	expanded Polytetrafluoroethylene
ePTFE-OH	expanded Polytetrafluoroethylene functionalized with hydroxyl group
ePTFE-NH_2	expanded Polytetrafluoroethylene functionalized with amino group
ePTFE-NPs	Nano immobilized polytetrafluoroethylene
FBS	Fetal bovine serum
FD	Fluorescein isothiocyanate labeled dextran
FTIR	Fourier transform infrared spectroscopy
MES	2-(N-morpholino) ethanesulfonic acid
M. lysodeikticus	Micrococcus lysodeikticus cells
NPs	Nanoparticles
PBS	Phosphate buffered saline
PDI	Poly dispersity index
PET	Polyethylene terephthalate
PET-COOH	Polyethylene terephthalate functionalized with carboxyl group
PET-Enz	Lysozyme immobilized polyethylene terephthalate
PET-Hep	Heparin immobilized polyethylene terephthalate
PET-Hep-Col	Heparin/collagen Co-immobilized polyethylene terephthalate
PLGA	Poly lactic-glycolic acid

PET-Net	Network-structured coated Polyethylene terephthalate
PET-NH_2	Polyethylene terephthalate functionalized with amino group
PET-NPs	Nano immobilized polyethylene terephthalate
PRP	Platelets-rich plasma
PVE	Prosthetic valve endocarditis
PVGI	Prosthetic vascular graft infection
S. aureus	Staphylococcus aureus
SD	Sulfadimethoxine
SD-PHA-b-MPEO	Sulfadimethoxine polyhexylene adipate-b-methoxy polyethylene oxide
SEM	Scanning electron microscope
S. epidermidis	Staphylococcus epidermidis
Sulfo-NHS	N-hydroxysulfosuccinimide,
W1/O/W2	Double emulsion water/oil/water
XPS	X-ray photoelectron spectroscopy
Z-Ave	Particle mean diameter
ζ potential	Average potential value

List of Publications

1) Al Meslmani. B, Mahmoud. G, Lohoff. M, Bakowsky. U. Multifunctional Network-structured Film Coating for Woven and Knitted Polyethylene Terephthalate against Cardiovascular Graft-associated Infections. (Prepared to be submitted to biomaterials)

2) Al Meslmani. B, Mahmoud. G, Leichtweiß. T, Strehlow. B, Sommer. F, Lohoff. M, Bakowsky. U. Covalent Immobilization of Lysozyme onto Woven and Knitted Crimped Polyethylene Terephthalate Grafts to Minimize the Adhesion of Broad Spectrum Pathogens. (submitted to Biomacromolecules Journal)

3) Al Meslmani. B, Mahmoud. G, Bakowsky. U. Immobilization of Hydrophilic PLGA Nanoparticles Model onto Polyethylene Terephthalate and Polytetrafluoroethylene Cardiovascular Grafts. (Prepared to be submitted to Tissue Engineering Journal)

4) Al Meslmani. B, Strehlow. B, Mohr. E, Mahmoud. G, Leichtweiß. T, Bakowsky. U. Development of Thrombus-resistant and Cell Compatible Crimped Polyethylene Terephthalate Cardiovascular Grafts Using Surface Co-immobilized Heparin and Collagen. (submitted to Colloid and Interfaces Journal)

5) Al Meslmani. B, Mahmoud. G, Bakowsky. Nano Coating for Cardiovascular Grafts. ThGOT Thementage Grenz- und Oberflächentechnik. September 3-5th (2013), Zeulenroda, Germany. (**Poster**)

This seit has a personal data

Danksagung

Mein besonderer Dank gilt Prof. Dr. Udo Bakowsky für die Betreuung meiner Doktorarbeit und für seine große Unterstützung während der gesamten Promotion.

Ich möchte mich herzlich bedanken bei:

Prof. Dr. Michael Lohoff, Institut für Medizinische Mikrobiologie und Krankenhaushygiene, Philipps-Universität Marburg, für die enge Zusammenarbeit bei den Bakterienversuchen sowie für die stete Unterstützung.

Prof. Dr. Jürgen Janek und Dr. Thomas Leichtweiß, Physikalisch-Chemisches Institut, Justus-Liebig-Universität Gießen, für die Unterstützung bei den XPS Aufnahmen.

Dr. Gihan Mahmoud, Institut für Pharmazeutische Technologie und Pharmazeutische Industrie, Helwan-Universität Kairo, Ägypten, für die Zusammenarbeit sowie für die Hilfe bei der englischen Sprache.

Prof. Dr. Andreas Greiner und Dr. Yasser Assem, Institut für Makromolekulare Chemie, Philipps-Universität Marburg/Universität Bayreuth, für die Abgabe von Polymeren.

Boris Strehlow für die Hilfe bei der Mikroskopie.

Eva Mohr für die Hilfe bei der Zellkultur.

sowie meinen Kollegen aus dem Arbeitskreis: Dr. Jens Schäfer, Anett Sommerwerk, Thomas Betz, Dr. Eyas Dayyoub, Dr. Jana Brüßler, Dr. Elena Marxer, Dr. Jarmila Jedelska, Dr. Olga Samsonova, Dr. Irina Levacheva, Dr. Leonie Baginski, Dr. Aybike Hemetsberger, Boris Strehlow, Eric Sasko, Elias Baghdan, Konrad Engelhardt, Shashank Pinnapireddy, Matthias Wojcik, Julia Michaelis, Eva Mohr, Susanne Lüttebrandt sowie auch den Kollegen aus den Arbeitskreisen Prof. Dr. Kissel und Prof. Dr. Schneider für die gemeinsamen Stunden am Institut.